AD-A154 107 PHYSIOLOGICAL INFLUENCES ON TISSUE ELECTRICAL PROPERTIES IN SITU(U) GEORGIA INST OF TECH ATLANTA E C BURDETTE ET AL. SEP 82 DAMD17-78-C-8044 1/2

UNCLASSIFIED F/G 6/16 NL

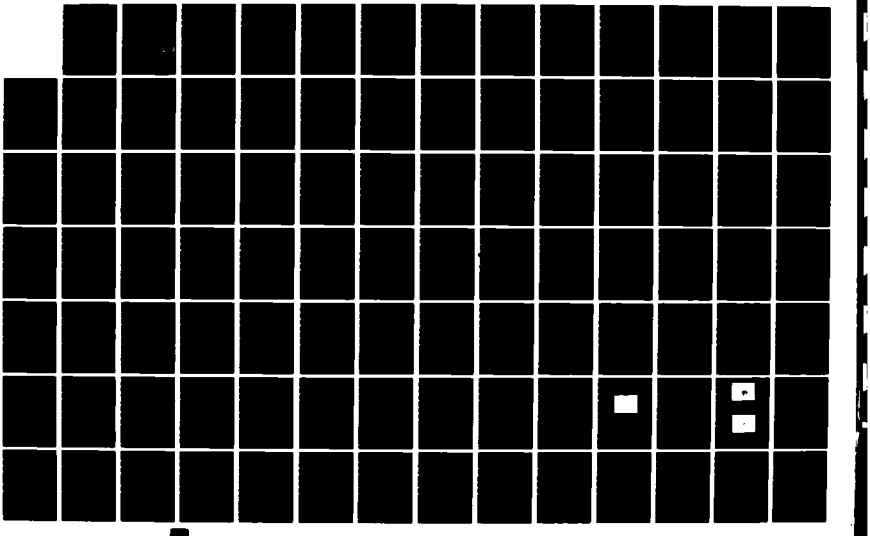

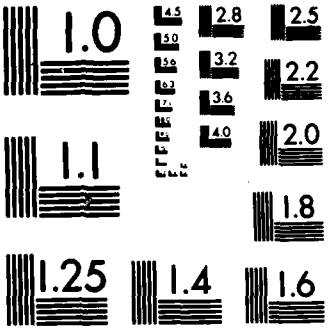

MICROCOPY RESOLUTION TEST CHART
NATIONAL BUREAU OF STANDARDS-1963-A

AD_____

(1)

AD-A154 107

Physiological Influences on Tissue Electrical Properties In Situ

Annual Report

E. C. Burdette
P.G. Friederich
S. R. Crowgey

September 1982

Supported by

U.S. ARMY MEDICAL RESEARCH AND DEVELOPMENT COMMAND
Fort Detrick, Frederick, Maryland 21701-5012

Contract No. DAMD17-78-C-8044

Georgia Institute of Technology
Georgia Tech Research Institute
Atlanta, Georgia 30332

DOD DISTRIBUTION STATEMENT

Approved for public release; distribution unlimited

The findings in this report are not to be construed as an official Department of the Army position unless so designated by other authorized documents

UNCLASSIFIED

SECURITY CLASSIFICATION OF THIS PAGE (When Data Entered)

REPORT DOCUMENTATION PAGE		READ INSTRUCTIONS BEFORE COMPLETING FORM
1. REPORT NUMBER	2. GOVT ACCESSION NO. AD-A154107	3. RECIPIENT'S CATALOG NUMBER
4. TITLE (and Subtitle) Physiological Influences on Tissue Electrical Properties In Situ		5. TYPE OF REPORT & PERIOD COVERED Annual Report (1 Sept. 81 - 30 Sept. 82)
		6. PERFORMING ORG. REPORT NUMBER A-2171
7. AUTHOR(s) E. C. Burdette, S. R. Crowgey and P. G. Friederich		8. CONTRACT OR GRANT NUMBER(s) DAMD17-78-C-8044
9. PERFORMING ORGANIZATION NAME AND ADDRESS Georgia Institute of Technology Georgia Tech Research Institute Atlanta, Georgia 30332		10. PROGRAM ELEMENT, PROJECT, TASK AREA & WORK UNIT NUMBERS 62777A.3E162777A878.BB.013
11. CONTROLLING OFFICE NAME AND ADDRESS U.S. Army Medical Research and Development Command Fort Detrick, Frederick, Maryland 21701-5012		12. REPORT DATE September 1982
		13. NUMBER OF PAGES 108
14. MONITORING AGENCY NAME & ADDRESS(if different from Controlling Office)		15. SECURITY CLASS. (of this report) Unclassified
		15a. DECLASSIFICATION/DOWNGRADING SCHEDULE

16. DISTRIBUTION STATEMENT (of this Report)

Approved for public release; distribution unlimited

17. DISTRIBUTION STATEMENT (of the abstract entered in Block 20, if different from Report)

18. SUPPLEMENTARY NOTES

19. KEY WORDS (Continue on reverse side if necessary and identify by block number)

In-Vivo probe
Dielectric properties
In-Situ tissues
Autoregulation
Renal blood flow
Electromagnetic energy
Radioactive tracers

20. ABSTRACT (Continue on reverse side if necessary and identify by block number)

The overall objectives of this research investigation are to further develop and extend the capabilities of the recently-developed in-situ probe measurement technique and to use this technique to study the possible effects of induced physiological changes on tissue dielectric properties. During the fourth year of the program, the research investigations performed included (1) dielectric measurements of renal tissue under controlled perfusion conditions, (2) investigations of different artificial perfusate solutions -continued-

DD FORM 1 JAN 73 1473 EDITION OF 1 NOV 65 IS OBSOLETE

UNCLASSIFIED

SECURITY CLASSIFICATION OF THIS PAGE (When Data Entered)

to develop a solution which best preserved renal function, (3) characterization of renal pressure flow relationships using both in-line flow measurement and radioactive tracer techniques, (4) design and development of software for a fully automated data acquisition and processing system , (5) development of a controlled contact force multiple probe holder, and (6) comparison of radioactive tracer and dielectric probe measurement results.

Results of the in-vitro renal studies consistently showed a proportional relationship between renal flow and relative permittivity and conductivity. For both tissue types, autoregulation of renal flow was observed and the dielectric properties followed the same relationship. Cortex and medulla tissues exhibited dielectric changes in the same direction, although cortical changes were generally greater.

The upgraded data acquisition and logging system includes 15 channels of signal-conditioning buffer amplifiers and a 10-position event marker, from which the output signals are routed through a multiplexing A/D converter capable of a 20 kHz sampling rate and to a Zenith/Heath WH-89 microcomputer having 300 kbytes disk storage. Software was developed during the fourth year research efforts to allow the WH-89 microcomputer to control the network analyzer system and overall data acquisition and to provide initial processing of measured data. New software was also written for multiplexing dielectric measurements data from up to five probes to permit simultaneous data recording at different measurement sites.

Programs developed on the Cyber 70/74 computer system were used to perform most data processing functions, including baseline subtraction, averaging, and computation of linear correlation coefficients and correlation probabilities for pairs of variable. These programs were used for the analysis of the measured renal physiological and dielectric property data.

AD_____

Physiological Influences on Tissue Electrical Properties In Situ

Annual Report

E. C. Burdette
P.G. Friederich
S. R. Crowgey

September 1982

Supported by

U.S. ARMY MEDICAL RESEARCH AND DEVELOPMENT COMMAND
Fort Detrick, Frederick, Maryland 21701-5012

Contract No. DAMD17-78-C-8044

Georgia Institute of Technology
Georgia Tech Research Institute
Atlanta, Georgia 30332

DOD DISTRIBUTION STATEMENT

Approved for public release; distribution unlimited

The findings in this report are not to be construed as an official Department of the Army position unless so designated by other authorized documents

FOREWORD

Research during the fourth year of this program was conducted by personnel of the Biomedical Research Division of the Electronics and Computer Systems Laboratory of the Engineering Experiment Station at the Georgia Institute of Technology, Atlanta, Georgia 30332. Mr. E. C. Burdette served as the Principal Investigator. The program, which is sponsored by the U.S. Army Medical Research and Development Command, Fort Detrick, Frederick, Maryland 21701, under Contract No. DAMD17-78-C-8044, is designated by Georgia Tech as Project A-2171.

This Annual Technical Report covers work performed from 1 September 1981 through 30 September 1982. This work was made possible through the combined efforts of many people at the Walter Reed Army Institute of Research (WRAIR), at the Emory University School of Medicine, and at the Georgia Institute of Technology. The authors would especially like to thank Dr. L. E. Larsen and J. H. Jacobi at WRAIR and Drs. V. P. Popovic and R. M. Sarper at the Emory University School of Medicine, all of whom contributed significantly to this research program.

In conducting the research described in this report, the investigator(s) adhered to the "Guide for the Care and Use of Laboratory Animals," prepared by the Committee on Care and Use of Laboratory Animals of the Institute of Laboratory Animal Resources, National Research Council (DHEW Publication No. (NIH) 78-23, Revised 1978).

SUMMARY

The overall objectives of this research investigation are to further develop and extend the capabilities of the recently-developed in-vivo probe measurement technique and to use this technique to study the possible effects of induced physiological changes on tissue dielectric properties.

During the fourth year of this program, research investigations included (1) dielectric measurement of renal tissue under controlled perfusion conditions in-vitro, (2) investigations of different artificial perfusate solutions to develop a solution which best preserved renal function, (3) characterization of renal pressure/flow relationships using both in-line flow measurement and radioactive tracer techniques, (4) design and development of software for a fully automated data acquisition and processing system, (5) development of a controlled contact force multiple probe holder and fabrication of smaller (1 mm diameter) probes, and (6) comparison of radioactive tracer and dielectric probe measurement results.

Results of the in-vitro renal studies consistently showed a proportional relationship between renal flow and relative permittivity and conductivity. For both tissue types, autoregulation of renal flow was observed and the dielectric properties followed the same relationship. Cortex and medulla tissues exhibited dielectric changes in the same direction, although cortical changes were generally greater.

The upgraded data acquisition and logging system includes 15 channels of signal-conditioning buffer amplifiers and a 10-position event marker, from which the output signals are routed through a multiplexing A/D converter capable of a 20 kHz sampling rate and to a Zenith/Heath WH-89 microcomputer having 300 kbytes disk storage. Software was developed during the fourth year research efforts to allow the WH-89 microcomputer to control the network analyzer system and overall data acquisition and to provide initial processing of measured data. New software was also written for multiplexing data from up to five probes to permit simultaneous dielectric data recording at different measurement sites.

Programs developed on the Cyber 70/74 computer system were used to perform most data processing functions, including baseline subtraction, averaging, and computation of linear correlation coefficients and correlation probabilities for pairs of variables. These programs were used for the analysis of the measured renal physiological and dielectric property data.

TABLE OF CONTENTS

LIST OF FIGURES

LIST OF FIGURES

Continued

LIST OF FIGURES

Continued

LIST OF FIGURES

Concluded

SECTION I
INTRODUCTION

The electrical properties of a biological system largely determine the interaction between that system and an applied electromagnetic (EM) field. Accurate knowledge of in-situ tissue electrical property information would be of significant benefit in many ways. Real-time in-situ measurement of living tissues could be used for the detection of patho-physiologic conditions in tissues, for measuring changes in normal physiological processes (such as changes in local perfusion), for differentiating between normal and diseased tissues, and for elucidating pharmaco-physiological effects due to the administration of polar drugs. Also, it is important to note that tissue electrical properties play a key role in electromagnetic imaging, whether dosimetric or diagnostic in nature. Specific differences or changes in in-situ electrical properties within a single tissue type or among tissues are reflective of the ability of EM imaging methods to discern the existence of patho-physiological conditions in intact tissues, organs, or organisms. Differences between in-situ living tissue properties and in-vitro properties are of key importance in dosimetry determinations (in both magnitude and distribution) via EM imagery [1-4]. In dosimetry determinations with respect to potential EM radiation hazards and in treatment planning for cancer patients using hyperthermia induced by electromagnetic fields, an accurate knowledge of the respective in-situ tissue electrical properties is essential to an accurate determination of absorbed power [5-7].

A. Research Objectives

The overall objectives of this research program are to further develop the capabilities of the existing in-situ probe measurement technique and to use this technique to study the possible effects of induced physiological changes on tissue dielectric properties. A detailed account of the past accomplishments is given in Annual Technical Report Nos. 1, 2, and 3 [8-10]. Minor modifications to the goals for the current program period (fourth year) were made following a meeting between the Contracting Officer's Technical Representative (COTR) and the Principal Investigator held in late February 1982 at the Walter Reed Army Institute of Research. The revised goals for the current year's research effort are (1) to develop a microcomputer-controlled

multiplexing system to permit simultaneous recording of dielectric property data from multiple probes located at different measurement sites, (2) to develop a smaller-diameter (~1 mm) probe for measuring medullary perfusion/flow changes, (3) to develop improved methods for controlling probe/tissue contact force during renal tissue dielectric measurements, (4) to evaluate different perfusate solutions with respect to functional and autoregulatory preservation during isolated kidney studies, (5) to perform studies of renal flow distribution as a function of perfusion pressure using radiographic methods, and (6) to correlate renal electrical properties with changes in renal flow and perfusion pressure. Each of these goals was achieved during this reporting period.

B. Summary of Research Performed

During the present program, under Army Medical Research and Development Command support, the measurement capabilities of the in-situ dielectric probe have been significantly improved. The versatility of the probe was increased through the use of a high-quality flexible probe cable, and systemic and cable/connector measurement errors were accounted for through the development and application of a data correction and processing program which corrects the impedance data measured by the probe for those errors. Methods were developed to eliminate fluid accumulation at the tip of the measurement probe, and an investigation to determine the minimum sample volume necessary for accurate dielectric measurement results was performed. Techniques for rapid data acquisition and processing were studied and developed, and a new controlled-contact-force multiple probe holder which maintains the probe contact pressure on the tissue being measured at a nearly constant value was developed and tested. In-situ measurements of different locations within dog brain were performed which yielded information about the existence of significantly different electrical properties for the various types of brain matter, which in turn impacts EM-hazards dosimetry determination. Studies of antemortem/postmortem dielectric characteristics of the pial surface of dog brain, investigation of renal dielectric properties under conditions of altered renal blood flow, and initial studies of acoustical stimulation effects on auditory cortex dielectric properties were performed.

The first year of the present 4-year effort was largely devoted to refinement of the in-situ probe measurement technique. Under previous research

efforts [8,11], it was determined that probe positioning was a critical factor in the performance of accurate in-vivo dielectric measurements. Further, it was determined that positioning of the probe needed to be made more compatible with measurement conditions associated with animals larger than mice or rats, which were positioned beneath a fixed measurement probe. Several alternative methods involving the use of semi-rigid or flexible coaxial cable attached to the in-vivo measurement probe were evaluated. The technical requirements of a suitable cable for use with the probe were the following: a length adequate to allow the probe to be positioned on a large experimental animal (dog) and still permit convenient location of the network analyzer, adequate cable flexibility for ease in repositioning, introduction of minimal phase variations due to cable movement, low attenuation and VSWR, and the ability to withstand sterilization. Following an examination of cables from nearly a dozen manufacturers, it was determined that the best-suited cable was the Gore-Tex flexible cable. A three-foot length cable, including connectors, was tested and found to perform satisfactorily over the frequency range examined (2-4 GHz).

An investigation of the accuracy of the results obtained from measurements of standard dielectric materials indicated a need to evaluate the residual systemic errors associated with the network analyzer measurement system [8,12]. An existing model [13] for reduction of microwave measurement errors (directivity, source match, frequency tracking) associated with the network analyzer, reflectometer, and interconnecting cables was further developed to include multiple-load data in the determination of the directivity error. Also, the systemic error correction model was incorporated in a microprocessor-based data acquisition/data processing system. The error correction is performed through measurements of terminations (short circuits, open circuit, and a sliding matched load) for which the reflection coefficients are known. From these measurements, the error terms are computed using the error correction model and the measured tissue sample data are corrected to account for the systemic measurement errors.

The semi-automated microprocessor-based dielectric property data acquisition system was upgraded during the first year of the program [8]. Specifically, a digital frequency locking capability was added to the system, an external keyboard/printer was interfaced, and the computer algorithm was rewritten to increase system flexibility and to accommodate additional system hardware.

Reflection coefficient data from test samples measured by the probe are automatically collected and processed, and corrected dielectric property information outputted. The software was written such that measurements may be made either over swept frequency bands between 0.11 GHz and 10 GHz or as a function of time at a single frequency.

Effort was also directed toward the evaluation of the effects of fluid accumulation in the vicinity of the probe. Excessive fluid accumulation affects both the accuracy of the dielectric measurements and the repeatability of the measurements. It was determined that fluid accumulation around the probe did not appreciably effect the results of dielectric measurements of high-loss tissues (muscle, kidney). However, significant effects of fluid accumulation were observed in the results of measurements on relatively low-loss tissues (fat). After investigating several methods of preventing the fluid accumulation, a simple approach using a "wick" to absorb excess fluids was developed which yielded accurate and consistent results.

Preliminary in-situ measurements of living and non-living brain and of in-vivo dielectric properties of brain under conditions of induced physiological change were also performed as a part of the first-year efforts. All measurements were performed at a frequency of 2450 MHz using a probe having a diameter comparable to that of a 16-gauge hypodermic needle. In-situ dielectric measurements of both living and non-living canine brain were performed on the dura, on the pia, and in gray and white matter. Measurements of dielectric properties as a function of time after death were performed both in brain and on the pial surface in separate experiments.

During studies of antemortem/postmortem dielectric changes in dog brain, it was determined that probe contact pressure on the tissue was also a factor in the accuracy and repeatability of measured results. Following cessation of blood flow, the brain receded slightly into the skull, resulting in a change in probe contact pressure and a concomitant change in measured dielectric properties. A six percent maximum change in dielectric constant was measured between the conditions of initial probe contact with the pia and an applied pressure producing a 0.4-cm depression of the pia using a 2.1-mm diameter probe. An approximate change of four to five percent in conductivity was also observed under the above stated probe contact conditions. To minimize these effects of probe contact pressure on measured tissue dielectric characteristics, in the second year of the program a mechanical "spring-loaded

in-situ probe holder" was designed to maintain the probe contact on the tissue at a constant or nearly constant pressure. The contact force and therefore, contact pressure of the probe with the tissue was determined by the spring constant. Springs were selected which provided sufficient tension for maintaining constant uniform probe/tissue contact over a probe travel distance of one inch. Using the spring-loaded probe holder, the probe contact-induced variations in measured in-situ dielectric properties were on the order of one percent. During the third year's efforts, the spring-loaded probe holder design was modified to permit the use of a single spring. The ability to follow tissue movements either pushing against or moving away from the in-situ probe was maintained.

Methods for further reducing systemic measurement errors associated with the microwave network analyzer were investigated during the second year [9]. Following implementation of the vector measurement error correction model during the first year of the program, the only remaining systemic measurement error source of significance was noise present in the measurement of the phase angle of small-magnitude reflection coefficients. Two approaches to the solution of this problem were examined. The first approach involved the use of an active filter to remove high frequency noise from the phase signal. However, filtering of noise in this manner both added complexity to the measurement system and reduced the maximum data sampling rate. The second approach utilized a software filtering technique in which the reflection coefficient phase data were multiply sampled at each frequency of interest and the statistical mean computed. Thus, sampling rate was not affected and no additional hardware was required. The software filter greatly reduced the noise present in the phase measurement of small complex reflection coefficients.

The Commodore PET microcomputer initially used with the probe dielectric measurement system for control and data acquisition purposes lacked sufficient memory to permit storage of computed dielectric property data for the duration of an experiment. Several possible solutions to the need for an increased data storage capability were examined, and the necessity for time-locking data sampling to the respiratory cycle of the animal was evaluated. The primary question concerned selection of a digital sampling frequency high enough to record the rapid dielectric and physiological changes which occurred immediately upon terminating the animal. However, it was also noted that throughout most of the period during which experimental data were recorded,

those changes took place very slowly. Although the optimal solution would be the use of a digital recording system which automatically increased sampling frequency at the onset of a physiological change, it was determined that by recording the dielectric property data in both analog and digital form, it was possible to record the more rapid dielectric property changes in analog form, permitting the use of a slower digital sampling rate. Two modifications to the recording methodology were incorporated. The Commodore PET microcomputer (8 kBytes memory) was replaced by a Hewlett-Packard 9835A Desktop Computer (48 kBytes memory). The additional memory in the HP-9835A provided adequate data storage for sampling dielectric property data at a rate of one point per minute during a ninety-minute experiment. Simultaneous with digital recording of dielectric property data, the amplitude and phase of the complex reflection coefficient and various physiological parameters were also recorded in analog form. Recording data in this manner permitted both on-line digital dielectric property computations and continuous monitoring of dielectric parameters during periods of rapid physiological change. Further, it was not necessary to time-lock the digital sampling of dielectric data to the respiratory cycle of the animal because of the correlated continuous analog recording of dielectric property data.

The method described above for acquiring and storing data involved recording the physiological signals on a strip chart recorder and recording the measured dielectric property information in digital form using a Hewlett-Packard semi-automated network analyzer system. In order to analyze the data and correlate the different signals, data had to be tabulated on a point-by-point basis and then transcribed to data cards for a computer analysis. This manual method of data logging was found to be both time consuming and tedious, and thus formed a practical limitation to the extent of the actual analysis of the data (and to the number of experiments which could be performed and analyzed).

Improvements to the data acquisition and logging system investigated during the third and fourth years of the program involved the implementation of a microcomputer-controlled multiplexing A/D system and storage of the data on magnetic disks. The system has sixteen (16) data channels capable of being sampled at a variable, computer-controlled rate. These 16 analog signals along with a time frame marker are recorded on magnetic disk. The data stored on disk are in the proper form for detailed correlation analyses

by the microcomputer or, if necessary, for transfer to a large mainframe computer where a more detailed analysis may be undertaken. An additional feature incorporated within this system was an IEEE-STD-488 interface to allow control of the network analyzer used for acquiring dielectric data.

The primary constraints on the system were (1) the ability to sample data at rates up to 20 kHz, (2) data storage for the duration of one experiment (300 kBytes disk storage), (3) enough computing power to implement some real-time data reduction, and (4) the funds limitation under the present contract. The final system configuration is discussed in Section II.

In order to meet the expense constraint, three systems in the prospective price range were considered; the PET, APPLE II, and Zenith Heathkit WH-89 microcomputers. In addition, an existing Intecolor 8052 microcomputer previously purchased with internal funds, and which could be shared with other projects, was considered.

Among the microcomputers considered, the Zenith/Heathkit WH-89 appeared to be the best choice. Its advantages included two Z-80 microprocessors (as opposed to a single MCS-6502 in the PET and APPLE and an 8080A in the Intecolor computer). One of the Z-80s in the WH-89 is used as the CPU, the other is used as the controller for a "smart" terminal. In addition, the WH-89 has the most versatility for input/output functions. However, the PET and APPLE computers do have commerically available IEEE interfaces, whereas the Heathkit WH-89 and Intecolor do not. During the latter portion of the third year of this research program, internal funds were made available for purchasing the Zenith/Heathkit WH-89 microcomputer system. Funds for this program were used to purchase external dual floppy disk drives for use with the microcomputer system. During the fourth year, this computer system was interfaced to the network analyzer system and to the 16-channel data acquisition system.

Studies of antemortem/postmortem dielectric property changes in dog brain were conducted during the second year, and a limited investigation of vascular effects on measured in-situ tissue impedance was performed. Each of the antemortem/postmortem experiments involved measurement of the in-situ dielectric properties of dog brain with the dura mater and arachnoid removed and the probe placed directly on the pia mater over the ectosylvian gyrus. All dielectric measurements were performed as a function of time at a frequency of 2450 MHz using a 2.1-mm diameter probe.

In-situ dielectric measurements were performed over a two-hour period. Both dielectric property data and physiological data were recorded for 30 minutes prior to sacrificing the animal. This ensured physiological stability of the animal and permitted recording in-situ dielectric data under conditions of homeostasis. Sacrifice was performed by injecting a 30 cc bolus of saturated KCl or $CaCl_2$ into the femoral vein. All dielectric and cardiovascular physiological parameters were monitored for 90 minutes postmortem, with death being defined to be the time at which all systemic pressures were zero. A comparison of results obtained with KCl sacrifice to those obtained with $CaCl_2$ sacrifice can be found in Tables II and III in Section III of Annual Technical Report No. 2 [9]. The overall trend in both groups is similar. Both conductivity and dielectric constant gradually decrease as a function of time postmortem. However, in cases of $CaCl_2$ sacrifice, the values peak immediately upon intravenous injection and change more than in the KCl cases. While nominal values for the dielectric constant are about 57 in both cases, the $CaCl_2$ sacrifice results in an increase to about 67.3, or a change of approximately 17%. This peak occurs from 6-10 seconds before systemic pressures reach zero. This indicates that the $CaCl_2$ injection causes a stronger and more abrupt change in blood flow to the brain, as would be expected from the different mechanisms by which the K^+ and Ca^{2+} ions cause death.

In a limited study of the effects of acoustical stimulation on dielectric properties of the auditory cortex in dogs, no correlation between acoustic stimuli and dielectric property changes was oberved. However, this lack of effect does not necessarily mean that no correlation exists because the cortical EEG recordings taken during auditory stimulation showed no change in the electrical activity of the auditory cortex. It is believed that the problem was due to the CNS depressant effects of anesthesia used (pentobarbital sodium in most trials) on higher cortical centers and to the use of non-optimal auditory stimulation, thus preventing a good cortical response to the sensory stimuli. The use of a different anesthetic agent (halothane gas anesthesia or α-chloralose plus ethane) and improved auditory stimulation (possibly loud clicks) should correct the problem, thus permitting evaluation of the effect of sensory stimulation on the dielectric properties of canine cortex.

It was previously reported that an increase in total renal flow produced a decrease in both the relative permittivity and conductivity, and vice

versa [10]. During this reporting period (fourth year), renal tissue measurements were performed in an isolated, perfused kidney preparation. The dielectric properties were measured under varying controlled conditions of flow rate and arterial pressure. Measured renal dielectric changes were usually in the same direction in both the cortex and medulla, with the greater change being observed in the cortex.

The inverse dielectric property/flow relationship observed during our in-vitro measurements of dog kidneys during the third year seemed contrary to what one would expect from simple bulk water effects. That is, if increased renal flow caused an increased presence of bulk water, one would expect a corresponding rise in the measured components (and in the computed dielectric properties) rather than the measured decrease. Thus, the third-year results obtained using the probe measurement technique seemed to suggest that the pressure-flow-volume relationship in the kidney is not a simple one, and that redistribution of flow within the renal vasculature likely influences local renal dielectric properties.

However, further studies of the renal dielectric property/flow relationship during this reporting period indicated that the measured dielectric data are very sensitive to probe contact force. Presumably, and later confirmed, this sensitivity was due to local tissue compression at the probe contact point which altered perfusion of the local tissue region being measured by partially obstructing or possibly completely blocking normal flow. Also, as expected, the effect was greater on cortex than on medulla. Results from additional experiments performed under controlled conditions of constant light probe contact force exhibited a direct relationship between dielectric property changes with controlled total renal flow changes. This result is in keeping with the expected result for bulk flow changes. Radioactive tracer studies using an Anger camera were used to confirm that dielectric changes closely followed regional renal flow rate changes, with little or no dielectric change being observed at perfusion pressures where flow autoregulation occurred. Further, regional flow changes in cortex and medulla were often similar, but not equal.

In the following sections of this report, the investigations performed during the period 1 September 1981 through 30 September 1982 are detailed. Section II describes the development of a microcomputer-controlled 16-channel data acquisition system and the associated software developed for data acquisition

and analysis. In Section III, the experimental methods used in the investigations are described and results therefrom are presented in Section IV. Conclusions from results and recommendations for future studies are presented in Section V.

SECTION II

DATA ACQUISITION AND ANALYSIS

During the third year of this research program, the tradeoffs between developing an analog computer for direct recording of dielectric property data or developing a 16-channel multiplexed data acquisition system having a programmable sampling rate were evaluated. Because of the limitations placed on data processing and analysis by the analog approach, the second approach was selected. During the present year (fourth) of the program, efforts were directed toward the implementation of a microcomputer-based data acquisition, storage, and processing system. The new system replaces the manual system used during all earlier studies (Years 1-2), in which physiological signals and complex reflection coefficient data were recorded on stripchart recorders and dielectric property information from the Hewlett-Packard semi-automated network analyzer was printed out. Using the older method, data had to be tabulated by hand on a point-by-point basis and transcribed to computer cards for further processing on the Georgia Tech CYBER 70/74 computer. The nature of this manual system made data storage and retrieval cumbersome and hence formed a practical limitation to the extent of the data analysis. A new microcomputer-based system for data acquisition and control was designed and implemented during the fourth-year studies.

A. Current Data Acquisition System Design

The current data acquisition and processing system consists of a signal conditioning system, a HP 6940B Multiprogrammer (16-channel multiplexer, high-speed A/D converter, I/O electronics, and power supplies), and a Zenith/-Heathkit WH-89 microcomputer system with three 5-1/4" floppy-disk drives and an IEEE-488 interface. The hardware included in the overall data acquisition and dielectric property measurements system was described in Annual Technical Report No. 3 [10]. The signal conditioning unit has 15 general-purpose buffered amplifier channels and an event marker switch for labeling up to eleven distinct experimental conditions, and inputs for direct connection of thermistors for temperature measurement and pressure transducers for pressure measurement. This system permits acquisition of not only probe dielectric measurement data (amplitude and phase of complex reflection

coefficient), but also signals which reflect various physiological data pertinent to the experimental investigations (systemic blood pressures, renal perfusion pressure, organ and systemic temperatures, flow rate, ECG, etc.).

Conditioning of the signals from the various transducers/instrumentation was required in order to keep all electrical input signals to the A/D converter within a single input voltage range (-5 to 5 volts), which can be digitized, stored, and later processed by the data analysis programs. The signal conditioning hardware consists of a 16-channel analog signal buffering/temperature measurement system. Three of the sixteen input channels may be connected through front-panel switches to temperature measurement circuits for use with conventional commercially-available plug-in thermistor probes. The probes may be plugged directly into the signal processing system without a requirement for any additional temperature measurement instrumentation. Temperature information from a thermistor sensor is converted to an analog voltage in the 0-5 volt range for digitizing by the A/D converter. One of the sixteen channels is reserved for an event marker which consists of a ten-position switch for selection of one of ten discrete DC voltage levels plus an "off" position for zero volts. Thus, eleven different measurement conditions may be distinctly labelled in each experiment.

The equipment in the data acquisition system is connected to an IEEE-488 standard interface bus. It can thus be controlled by any computing system with access to the bus. Several mini/micro-computer systems are now available which could perform the role of data-acquisition system controller (a Zenith WH-89 is available on a full-time basis, and a Hewlett-Packard 1000 E-series computer and 9835A desktop computer are available on a limited basis). The Zenith WH-89 is the computer most often used for this task and hence a complete software package was implemented on it first. The first major step toward this goal was the development and implementation of an I/O board to enable the WH-89 to communicate with the IEEE-488 bus. The software which was developed previously for the network analyzer system was modified for application to the new equipment with expanded capabilities. For instance, the old system included a separate relay actuator unit and an A/D converter unit. The new system incorporates a HP 6940B Multiprogrammer with appropriate plug-in cards to perform these functions. In addition, a high-speed analog data multiplexing card was installed in the HP 6940B

to enable switching between sixteen channels of input data. The new software has the capability for monitoring these sixteen different parameters via the Multiprogrammer, as well as controlling the collection of dielectric property data through the automated network analyzer system. The sixteen monitored parameters may include dielectric properties measured at several different spatial locations. Dielectric measurement probes at the various locations are multiplexed into the network analyzer setup with the use of a 5-pole PIN diode RF switch, which is also software controlled.

B. Data Acquisition Software

Computer algorithms for two major functions were coded. One algorithm interfaces the Zenith WH-89 desktop computer to devices on the IEEE-488 bus (using an IEEE-488 interface card developed under this program) through versatile assembly language subroutine programs which can be "called" from either BASIC or FORTRAN source programs. The other major algorithm consists of a series of BASIC application programs for data acquisition and calibration. Flow charts for the data acquisition program and for the physiological data and dielectric property measurements calibration programs are presented in Figures 1-3.

The data acquisition software used with the WH-89 system controller is modelled after that previously used with the HP9835A system controller. Expanded capabilities in the new system include the facility for use of up to five dielectric measurement probes simultaneously, and the collection of data from fifteen channels of general purpose amplifiers (including the channels containing dielectric property information).

The basic software is described by the flow charts in Figures 1-3. Once appropriate labeling information has been entered, the frequency at which measurements will be made is selected and the microwave source is frequency-locked. Next, each of the fifteen data channels being used is calibrated. The calibration procedure consists of measuring from two to five calibration standards for each data channel. The calibration results are displayed, along with the A/D output, for approval by the operator. If necessary, the channel may be recalibrated. When experimental data are inputted, they are evaluated against a calibration curve based on these standard measurements.

SINGLE FREQUENCY DATA ACQUISITION PROGRAM

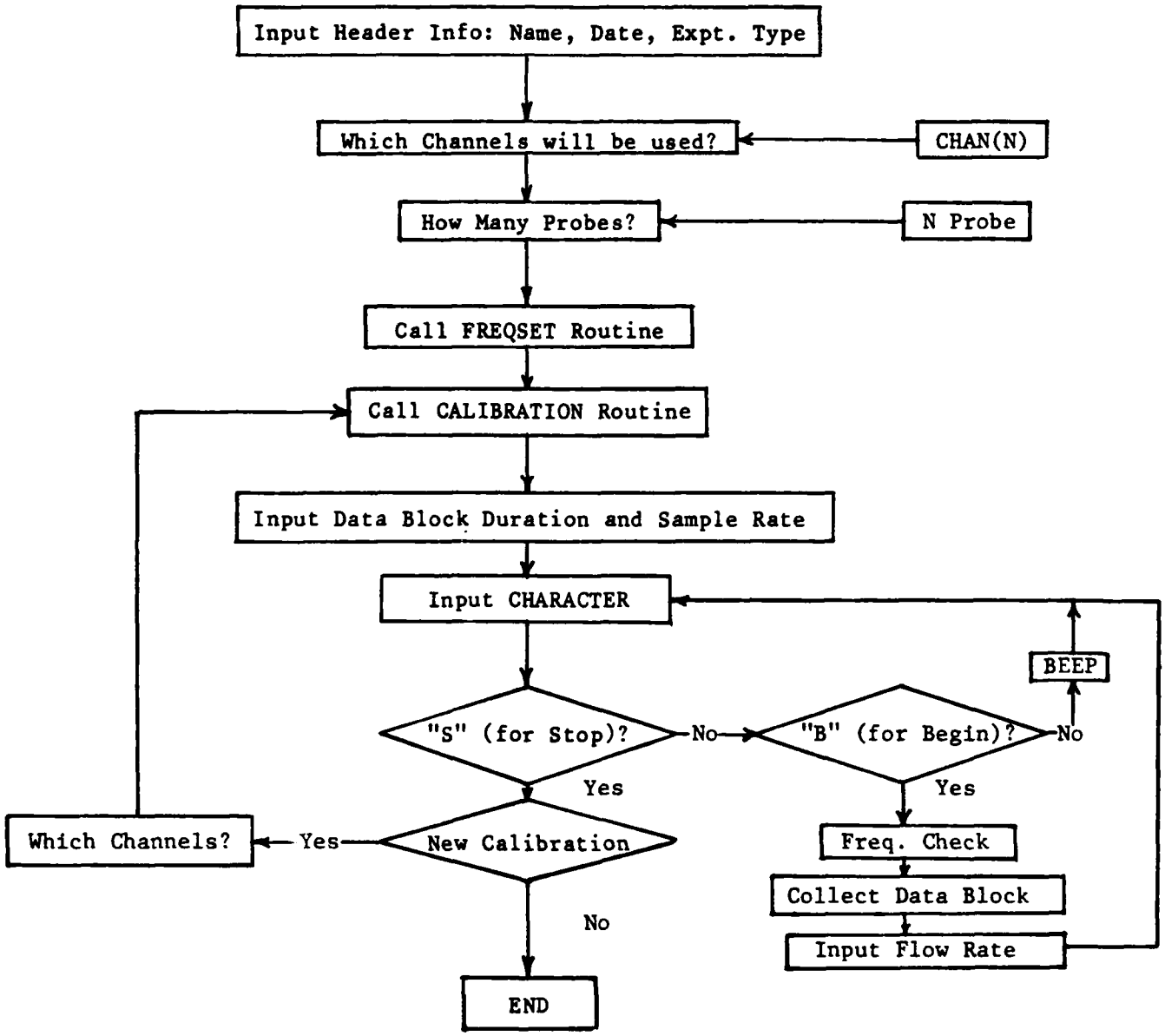

Figure 1. Flow chart of data acquisition algorithm for single frequency operation.

CALIBRATION ROUTINE

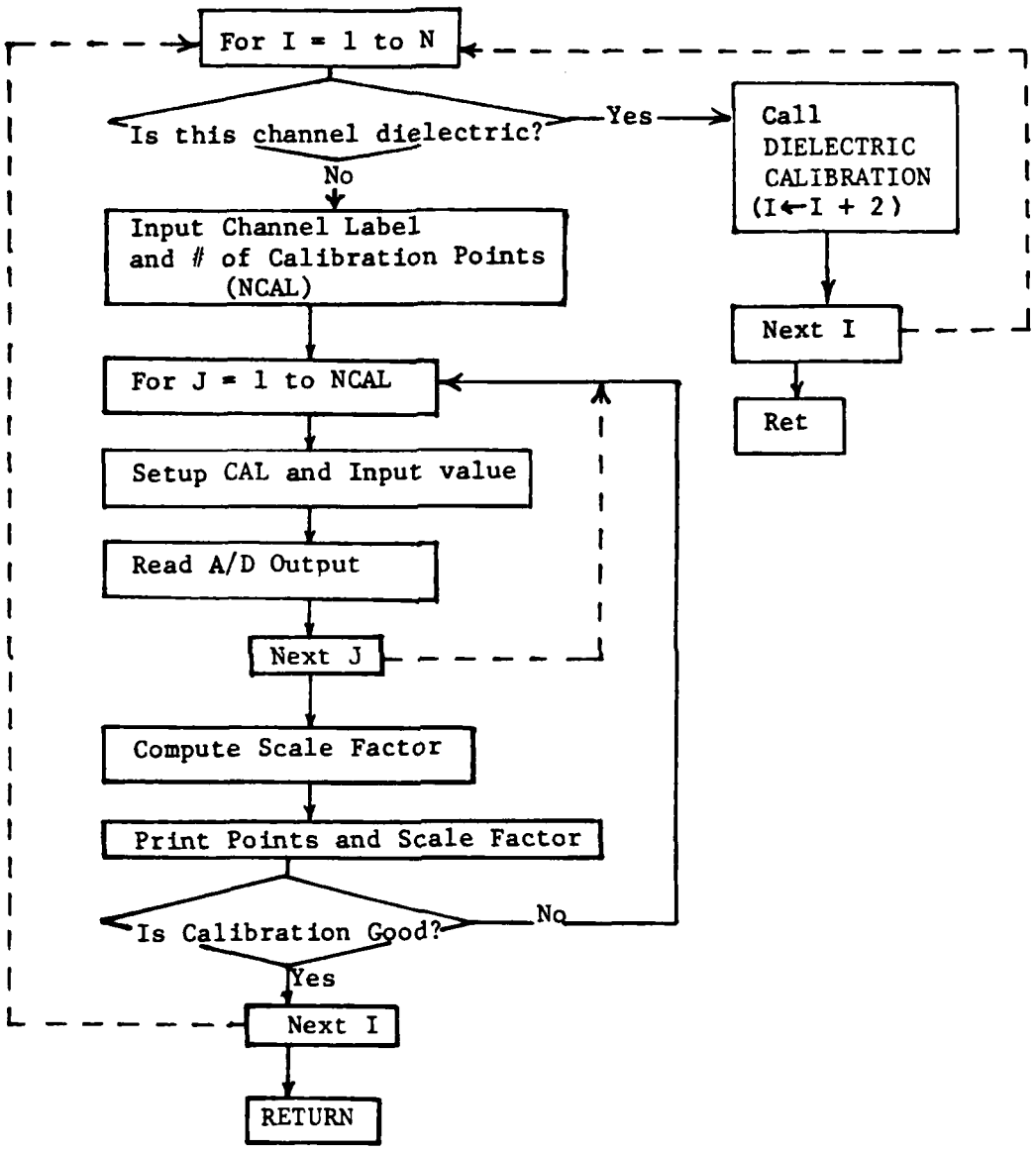

Figure 2. Flow chart of calibration routine for all input channels except those used for probe dielectric measurements.

DIELECTRIC CALIBRATION ROUTINE

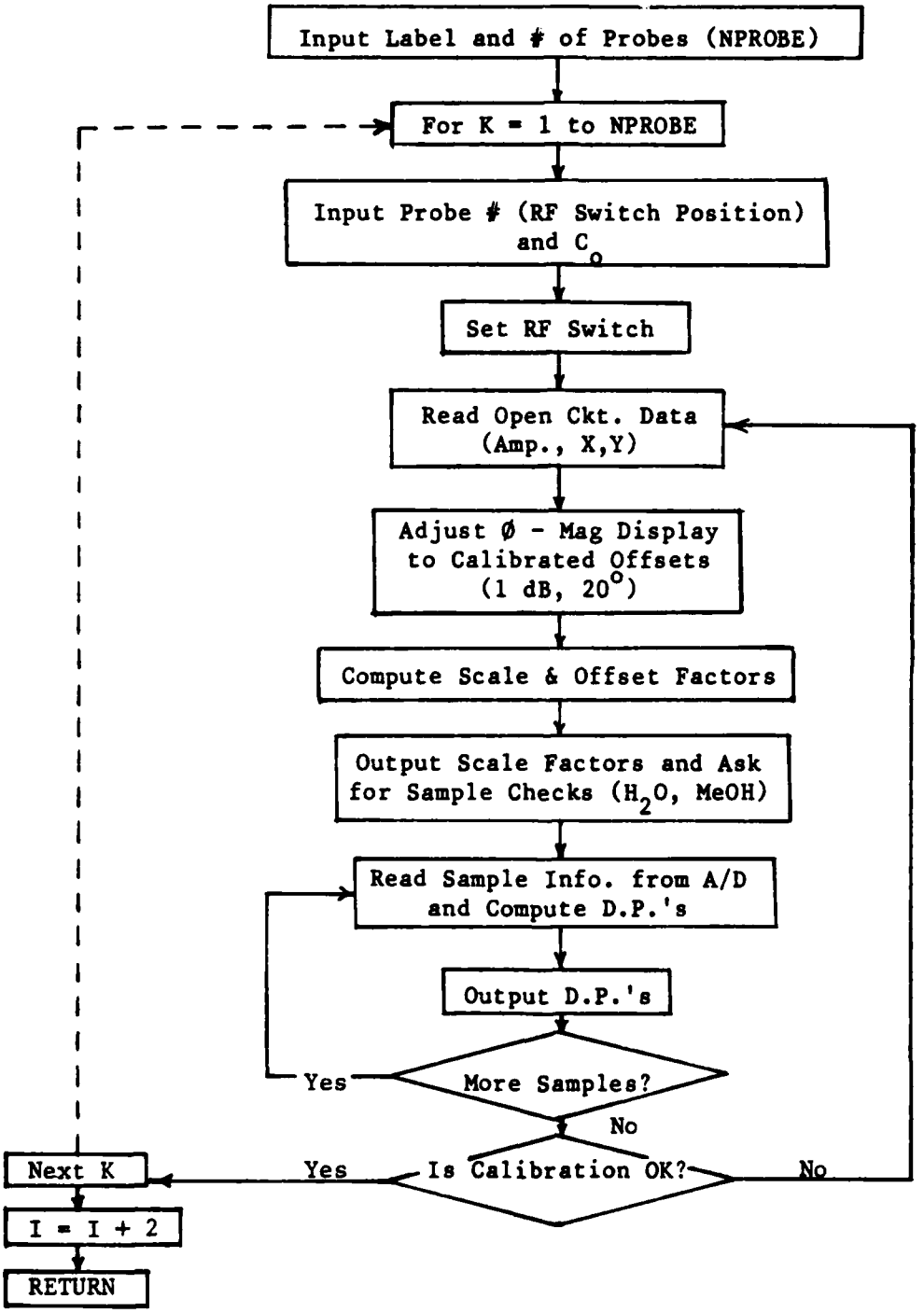

Figure 3. Flow chart of calibration routine used for probe dielectric measurements channels.

The three channels containing dielectric property information are calibrated in a separate routine. Open-circuited and standard sample measurements are taken with each probe, and the information for each probe is multiplexed in turn onto the three data channels with the PIN diode RF switch. Again, the calibration curve is subject to operator approval and recalibration if necessary. Once all the channels to be used have been calibrated, data collection is accomplished in blocks determined by the user. The operator enters the sample rate (which determines how often an acquisition is made) and the block duration (which determines how many times the channels are read within each data block). After each block has been collected, the user is prompted to either (1) initiate collection of another data block, (2) begin a new series of measurements with a new calibration run, or (3) end the data acquisition altogether. Thus the data acquisition system contains sufficient flexibility to be used for many different experimental investigations.

The development of the data acquisition system and associated software was somewhat more complex and involved than originally anticipated, and significant effort was expended "debugging" these programs, particularly the assembly language "call" subroutines for the IEEE-488 interface bus. As a result, the simultaneous multiple-probe dielectric property/radioactive tracer flow studies had to be postponed until interface software debugging was complete. The software was debugged in the final quarter of this reporting period and measurements were begun. Results of the combined dielectric measurement/radioactive tracer studies are detailed in Section IV of this report.

SECTION III
EXPERIMENTAL METHODS

This section summarizes the experimental methods used in the investigations of physiological influences on tissue dielectric properties and in the development and refinement of new devices and techniques and better physiological models for future investigations. The investigations consisted of (1) in-vitro renal flow/dielectric property studies, wherein isolated canine kidneys were placed on an external perfusion circuit and renal dielectric properties were measured under various controlled flow conditions; (2) in-vitro renal flow/pressure studies, wherein the flow/pressure characteristics of kidneys in response to different perfusates were measured on a modified external perfusion circuit; (3) in-vitro renal Radioactive Tracer studies using isolated canine kidneys both to confirm the correlation of the radioactive tracer flow measurement method with in-line flowmeter measurements and to provide a more accurate means of correlating the regional dielectric properties with the regional state of perfusion; and (4) combined renal flow/dielectric property studies and radioactive tracer studies, wherein dielectric property measurements and radioactive tracer measurements were performed simultaneously in an attempt to correlate all of our measurement techniques. The development of a new multiple-probe holder designed to control contact pressure will be described first followed by an outline of the surgical procedure and the experimental methods used for much of the four categories of investigations listed.

A. Multi-Probe Holder

During this year, a new device capable of holding and positioning multiple dielectric measurement probes was designed and fabricated. The multiple-probe holder positioned above an experimental subject is illustrated in Figure 4. The new holder permits simultaneous placement and positioning of five measurement probes, including three needle-probes and two surface-contact probes, within a 90-degree arc from vertical to horizontal orientation. In the case of renal dielectric measurements, the needle probes would be inserted at desired depths in the cortex or medulla and the surface probes

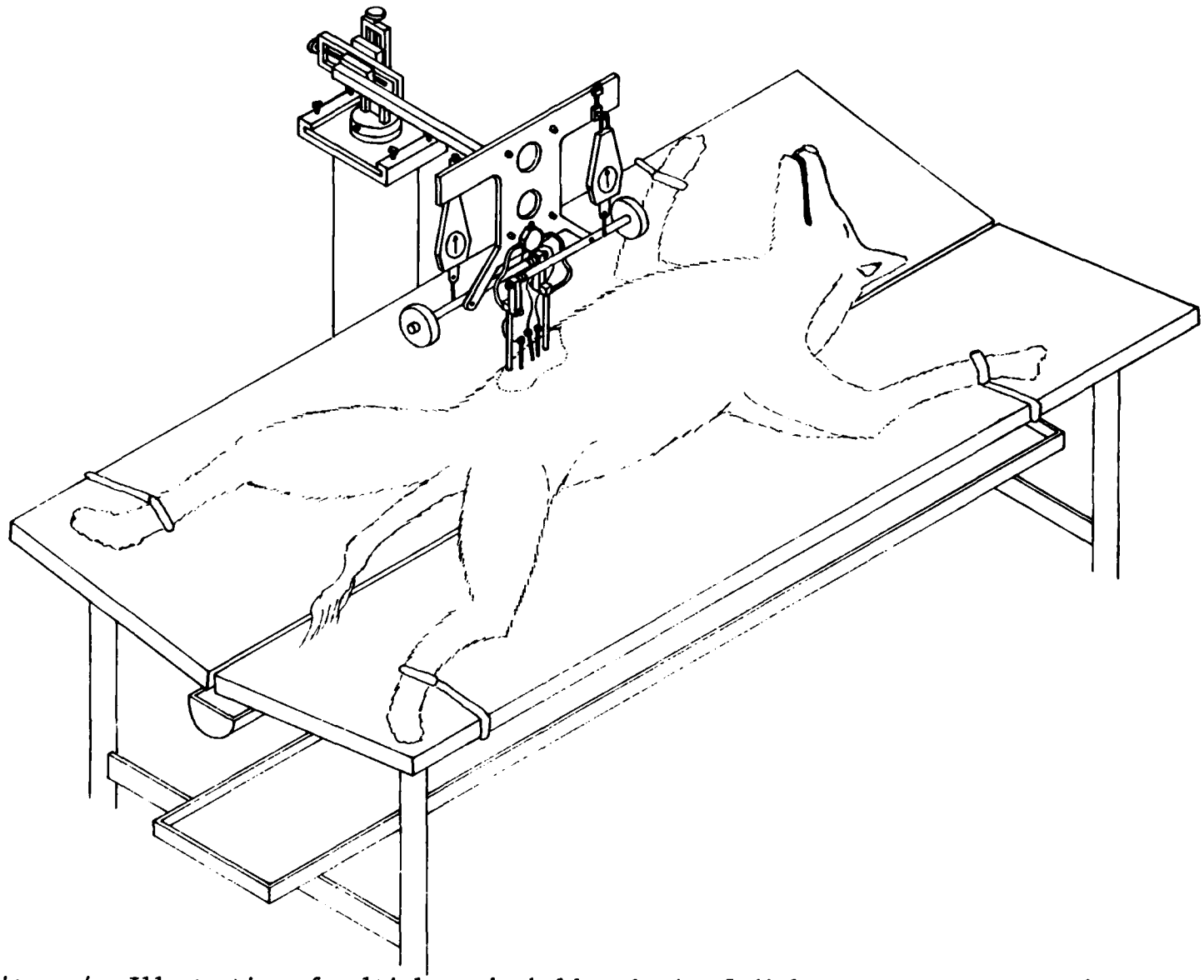

Figure 4. Illustration of multiple-probe holder showing 5 dielectric measurement probes and force-measurement strain gauges.

would be placed in contact with the outer cortex. The needle-like probes are identical to the larger 2.16 mm diameter probes except that they were fabricated from 1.1 mm diameter semi-rigid coaxial cable. Measured signals from the five probes are multiplexed via computer-control of a 5-position PIN diode switch mounted on the probe-holder support frame. The PIN diode switch used operates over the 1-18 GHz frequency range with a VSWR of less than 1.7 for the "on" position, a minimum isolation of 50 dB between positions, and a switching time of 100 ns. Probe/tissue contact force for the two surface probes is both controlled and monitored in the new multiple-probe holder design. The two surface probes are supported by cap bearings to provide near-frictionless movement of the probes, and are cabled so as to minimize the connecting cable's effect on probe/tissue contact force. Contact force is maintained as a constant value between 1 gm and 15 gm which is preset by adjusting the counterweight on each surface probe lever-arm support. Contact force is read directly from the strain scales mounted on the support frame. Contact force adjustment is repeatable to within $\pm$ 0.3 gm.

B. Surgical Procedure

Dogs were used as the experimental subjects for the renal dielectric studies. Surgical procedures used were similar to those reported in Annual Technical Report No. 2 [9]. These are reviewed and changes noted below. Subject dogs weighing 15-20 kg were obtained from Emory University Department of Physiology, and surgical and measurement procedures were performed in the animal surgery laboratory at Georgia Tech for the initial dielectric property experiments, and later in the animal surgery laboratories at Emory University in the Physiology and Nuclear Medicine departments for the radioactive tracer studies and kidney model studies. Each dog was anesthetized initially with 30 mg/kg body weight of pentobarbital sodium (Nembutal) intravenously (IV) and maintained at Geudel's Stage III, Level 3 of anesthesia with supplemental doses of 30-60 mg administered as needed.

With the dog in a supine position, the right femoral triangle and both left and right sides of the abdomen were shaved and scrubbed. The right femoral vessels were cannulated to provide a site for IV injections (femoral vein) and a site for continuous monitoring of systemic pressure (femoral artery). The cannulae were filled with heparinized saline to prevent clotting.

Following the femoral cannulation, the surgical procedure for isolating the kidney was begun. The left kidney (as viewed dorsally) was always approached

first since it lies lower in the abdomen than the right and is less difficult to surgically expose. An electrosurgical unit was used to make the initial incision (8-10 cm in length) just below the last rib on the left side. In the experiments at Emory University, a scalpel was used for the initial incision since the electrosurgical unit was not available. The subdermal fascia and fatty tissue were separated by blunt dissection, using hemostats. In a similar manner, the several layers of abdominal wall muscle were each separated until the peritoneal cavity was opened. Then the left kidney was located and the surrounding fascia and fatty tissue were separated from the kidney. The renal blood vessels and ureter were isolated and the renal artery traced from the renal pelvis to its junction with the aorta. Ligatures were tied loosely around the vessels and the ureter was severed. The renal artery was next tied, cannulated distal (with respect to the heart) to the tie, and cut between the tie and the cannula. Next, the renal vein was tied and cut distal to the tie, at which point the kidney was free to be removed from the animal and placed on the external perfusion circuit illustrated in Figure 5. The period between the time at which arterial flow was first cut off and the time when perfusion on the external circuit was begun for each kidney was three to ten minutes. Similar surgical procedures were followed when isolating the right kidney. During this current reporting year, this surgical procedure was modified slightly in an attempt to shorten the time period between tying the renal artery and perfusing the isolated kidney. Some of these modifications included (1) clamping the vessels with large hemostats instead of tying them off, (2) connecting the renal artery cannulae to a heparinized saline IV infusion set-up with the ability to flush manually so that slow perfusion could be initiated while the cannulation was being secured, and (3) monitoring more closely the time between clamping of the artery, flushing after cannulation, and connecting to the perfusion circuit.

Once a kidney was isolated and cannulated it was then connected to the in-vitro perfusion circuit which has been described previously [10] and is illustrated in Figure 5. During this year, this perfusion circuit underwent several modifications which will be described in more detail in later sections. These modifications consisted of adding an in-line flowmeter and an in-line variable resistance. The kidney was then allowed to stabilize after connecting to the circuit. The organ chamber in which the kidney rested was placed on an electronic balance scale and tared to zero. Then

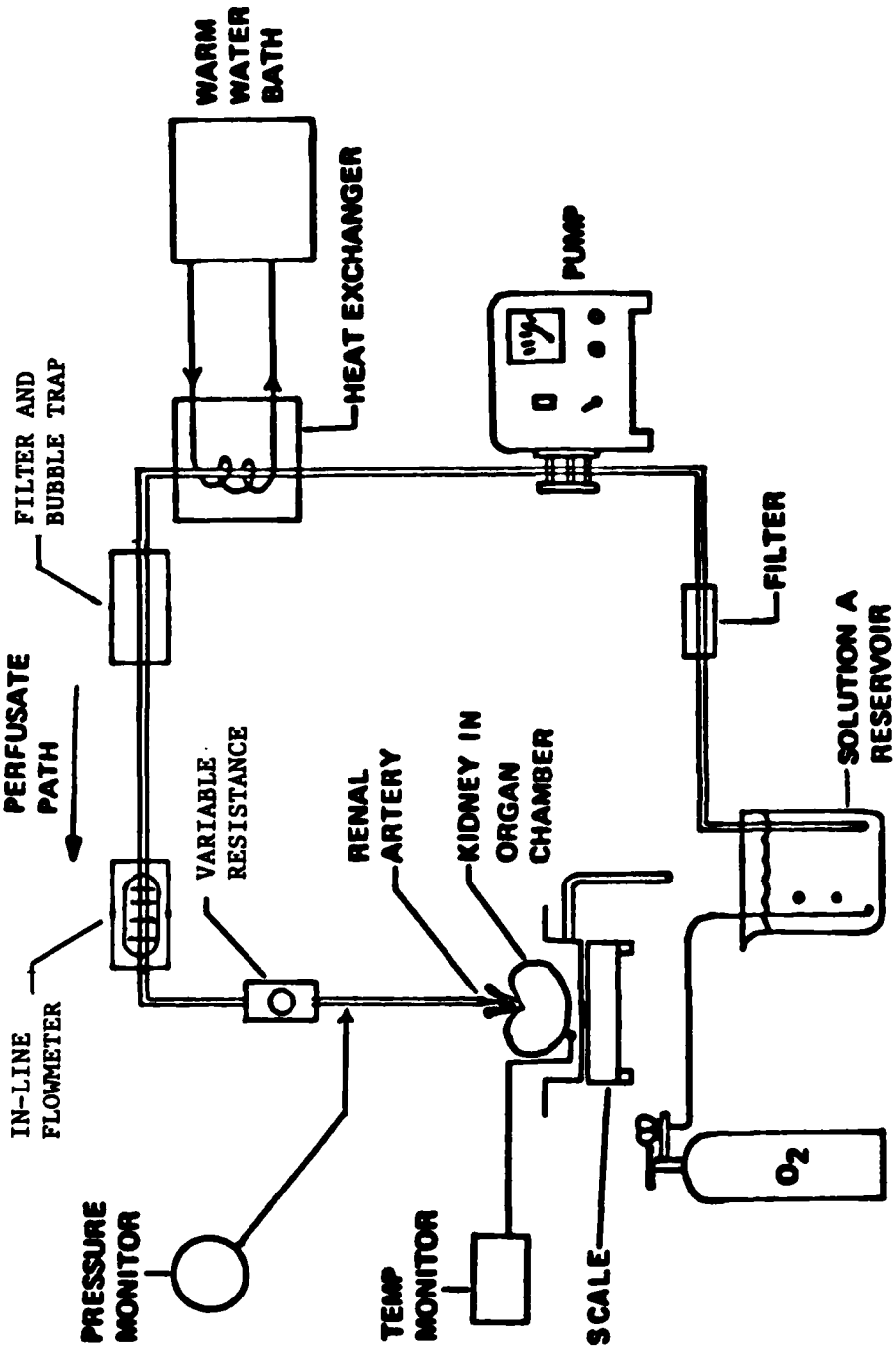

Figure 5. Diagrammatic illustration of experimental setup used for perfusion during *in-vitro* renal dielectric measurements.

the kidney was placed in the chamber and venous output was collected from the drain tube on the organ chamber.

C. Dielectric Property Studies

During this reporting period, dielectric measurement studies were performed on four kidneys (#7,8,9, and 10) which were not also studied as part of the renal autoregulatory or radioactive tracer flow studies. In each case, a kidney was placed on an in-vitro perfusion circuit and investigated to characterize the relationship between tissue dielectric properties and perfusion rates and pressures. The surgical procedure for isolating a kidney has already been described above. The perfusion circuit was configured the same as in previous experiments, with the addition of an in-line flowmeter with 10 ml/min calibration markings. During this period, the flowmeter was used in the investigation of kidneys #9 and 10, though perfusion rates of kidneys # 7 and 8 were still inferred by correlating pump speeds to previously measured flow rates. For each kidney measured, the total renal flow rate was plotted as a function of perfusion pressure (Figures 6, 16, 20; Section IV).

Once each kidney was removed from the dog and placed on the perfusion circuit, it was allowed to stabilize for thirty minutes to an hour. Then a series of dielectric property measurements with the in-situ probe was begun. Kidney #7 was measured according to the protocol established in previous experiments. A small section of the renal capsule was separated and cut away and the dielectric measurement probe was placed in contact with the renal cortex. Data were taken until the dielectric properties reached a steady state condition. Pump speed was varied to produce different perfusion rates. At each pump speed, the perfusion rate and pressure, kidney temperature, kidney weight, and dielectric properties (relative permittivity, K, conductivity, α, and loss tangent, tan δ) were recorded until they had reached a steady state. Information on probe contact force was unavailable for Kidney #7. Data for flow rates for 0.2 to 2.0 ml/g-min (milliliters per minute per gram kidney weight) were collected, first with the probe on the surface of cortex tissue, and then with the probe inserted into medulla tissue.

The same parameters were recorded for Kidney #8 with the addition of a measure of probe contact force. Three series of measurements were made on the cortex, and one in the medulla, all including flow rates from 0.8 -

1.5 ml/g-min kidney weight. The spring-loaded probe configuration, which performed well for brain dielectric property studies, proved to be too stiff for renal tissue measurements (particularly cortex measurements). Because of the probe configuration, contact force increased as the kidney became more turgid with increased flow. For this reason, the first series of cortex measurements were taken with probe contact force ranging from 11-30g. The second cortex series ranged from 0-19g of contact force. With the third series, an attempt was made to hold the probe contact force constant by making slight adjustments in the position of the probe holder. (These data are presented graphically in Figure 14). In the third cortex data set, probe/tissue contact force varied only from 21-27g. It was more difficult to maintain a constant contact force during medulla measurements since the probe was inserted into the organ. These measurements were made with a contact force of 35-50g.

Measurements made on kidneys #9 and 10 included the use of an in-line flowmeter, so perfusion rates were set with direct observation of the flowmeter, rather than by indirectly adjusting the flow condition according to pump speed. Only cortex mesurements were made for both kidneys, with perfusion rates ranging from 0.2 - 2.1 ml/g-min for the first kidney and from 0.4 - 3.9 ml/g-min for the second one studied. All measurements were made with probe/tissue contact force maintained between 5 and 10 grams.

D. Kidney Model Studies

The methods used in these experiments were virtually identical to those used during the dielectric measurements except for the addition of an in-line variable resistance above the site of pressure measurement. With this addition, the perfusion system was changed from one with flow as the forcing function to one with perfusion pressure as the forcing function. The surgical procedure used to isolate each kidney was identical to that of previous studies. For each kidney measured, the total renal flow was recorded as a function of perfusion pressure. The kidney model experiments were conducted in order to evaluate the effect of different perfusates on the flow-pressure curve. Different kidneys were perfused with a variety of perfusates and some were perfused with several different perfusates in series. Perfusate composition studies alone were performed using ten kidneys and combined kidney perfusion model/radioactive tracer studies were performed in eight additional animals.

Once each kidney was removed from the dog and placed on the perfusion circuit filled with the desired perfusate, it was allowed to stablize for approximately thirty minutes. Then, flow rate was increased until the maximum desired perfusion pressure of 250 mm Hg was reached after which perfusion pressure was gradually decreased by adjustments in the variable upstream resistance in increments of 25 mm Hg. When the minimum perfusion pressure of 25 mm Hg was reached, the variable resistance was gradually decreased, thus increasing the perfusion until a maximum value was reached (~250 mm Hg). In this manner, a pressure/flow curve was generated for each kidney on each perfusate. No dielectric measurements were made during these experiments.

When different perfusates were to be used on the same kidney, the system was first flushed with the next desired solution for a period of fifteen to thirty minutes prior to taking measurements. The different solutions evaluated as perfusates included Solution A, Solution A with 1.7 g/100cc of human albumin, Euro-Collins solution, and Krebs-Henseleit solution. The low concentration of albumin was necessary because of the expense of human albumin.

As a result of these kidney studies and a literature review (see Results in Section IV), it was decided to use a modified Krebs-Henseleit solution with 20 g/l Bovine Serum Albumin, Fraction V as the perfusate. Several further experiments using this perfusate verified that it was adequate to produce autoregulation and led to a further adaptation to our experimental protocol. We began setting a pressure of either 100 or 150 mm Hg as the baseline pressure which was monitored both before and after each measured pressure point in order to better characterize time-dependent pressure/flow changes evidenced by the kidneys. Further details of this protocol and its analysis are presented in Section IV. As an additional result of our literature review, we began limiting perfusion duration for each kidney to 2 hours, shortening the "settling down" period to 10-15 minutes, and shortening the period at each pressure setting to 1-5 minutes.

E. Radioactive Tracer Studies

The methods used in these experiments were virtually identical to those used in the kidney model studies and included the addition of both the in-line flowmeter and in-line variable resistance, as well as the use of the modified protocol to monitor a baseline pressure and the use of the new

perfusate, modified Krebs-Henseleit solution with 20 g/l of Bovine Serum Albumin, Fraction V. The surgical procedure was identical to that of previous studies. The purpose of the radioactive tracer experiments was to study both total renal flow and flow distribution by an independent means.

The radioactive tracer used in the Anger camera studies was free Technetium Tc 99m DTPA (New England Nuclear - Radiopharmaceutical Division) with a physical half-life of 6.02 hours and specific gamma ray constant of 0.8 R/millicurie-hr at 1 cm. A dose of 4mCi of Tc 99m was injected into the perfusate for each pressure-flow condition studied. The perfusion circuit was operated open-circuit so that each injected dose for a given pressure-flow condition could be completely cleared by the kidney before the next perfusion condition was set and tracer injected. Thus, it was possible to evaluate the total renal flow and renal flow distribution (using the Anger camera) for each pressure-flow perfusion condition.

Kidney perfusion data (uptake, distribution, and initial clearance) were recorded by the Anger gamma camera and stored on magnetic disk for 2-min intervals at the rate of 1 frame/2 sec. From these recorded data, kidney images and time/activity curves were generated for total kidney flow and for regional flow distribution in the cortex and medulla. Time/activity curves were generated for each perfusion pressure-flow condition. The total renal flow is proportional to the rate of uptake of free Technetium by the kidney. This rate of uptake is simply the slope of each curve during the period Technetium is entering the kidney through the arterial circulation until a steady-state condition between arterial and venous flow of the free Technetium is reached.

F. Combined Radioactive Tracer/Dielectric Property Studies

A key step in this year's efforts was the performance of experiments in which dielectric measurements and radioactive tracer measurements were made simultaneously on the same organ so that results could be compared to the measured pressure/flow data as well as compared to each other. We performed two such experiments in which dielectric measurement and pressure/flow measurement data were recorded continuously while the radioactive tracer measurements were made for 7-8 separate injections of Tc 99m. The methods used were essentially a combination of the methods already described in the sub-sections on dielectric property studies and radioactive tracer studies with the modifications described in the sub-section on kidney model studies.

SECTION IV

EXPERIMENTAL RESULTS

This section summarizes the experimental results of the investigations of physiological influences on tissue dielectric properties as well as the results of the studies performed to develop and refine both new techniques and better physiological models for future investigations. The investigations consisted of (1) in-vitro renal flow/dielectric property studies wherein the renal dielectric properties of isolated canine kidneys were measured under various controlled flow conditions; (2) in-vitro renal flow-pressure studies, wherein the flow/pressure characteristics of isolated kidneys were measured in response to different perfusates on a modified external perfusion circuit; (3) in-vitro renal flow/radioactive tracer studies, wherein similar isolated canine kidneys were used to confirm the correlation of the radioactive tracer flow measurement technique with in-line flow meter measurements and to provide independent regional flow distribution information; and (4) combined renal flow/dielectric property studies and radioactive tracer studies, wherein dielectric property measurements and radioactive tracer flow rate and distribution measurements were performed simultaneously on the isolated canine kidney preparation under various flow/pressure conditions in order to compare the results of all three techniques.

A. Renal Dielectric Property Studies

At the beginning of this reporting period, the dielectric properties of four isolated kidneys (#7, 8, 9, and 10) were measured using basically the same perfusion circuit and methods as described in previous reports [9,10]. Kidneys #7 and 8 were investigated using the same method of probe contact control as in previous studies and yielded similar results. Suitability of the spring-loaded probe holder used in the canine brain studies [9] for renal cortex measurements was dubious. This was tested using kidney #8 in an experiment to determine what the effects of various probe contact force were on measured renal dielectric properties. Kidneys #9 and 10 were then used to measure the dielectric properties when probe contact force was controlled.

The results of the probe dielectric measurements performed during in-vitro experiments on kidneys #7 and 8 without any control of probe contact force are presented graphically in Figures 6 through 13. These measurements were performed under the conditions and using the procedures described in Section III, B (Methods). Figures 6(a) and 6(b) present the flow/pressure curves for kidneys #7 and #8, respectively. Unfortunately, both kidneys were more hypertensive than desired and we were unable to produce demonstrable effects of autoregulation on the flow/pressure curves using the perfusate Solution A. It should be noted that all renal flows are normalized to kidney weight and expressed in terms of ml/g-min in order to permit normalization of flow rates for all kidneys studied. From Figure 6, we observe that kidney #8 is more hypertensive than kidney #7. The means of the data from these two flow/pressure curves are illustrated in Figure 6(c). The weight gain for these two kidneys measured as a function of flow rate is displayed graphically in Figures 7(a) and 7(b). In each case, the measurements were repeated three times, and as previously reported [2], the kidneys exhibited relatively small weight gains in proportion to changes in pressure and flow. In Figures 8 and 9, the measured changes in relative permittivity and conductivity from baseline values as a function of total renal flow rate are shown for kidneys #7 and 8, and in Figures 10 and 11 the same measured changes are shown as a function of perfusion pressure. Figures 12 and 13 display the mean measured changes in dielectric characteristics (with standard errors) for the two kidneys. It should be noted that the means and standard errors are calculated from four sets of measured data, i.e., two sets of data from each kidney, as opposed to the single sets of data obtained from previous kidneys. All six graphs show results very similar to previously reported data. The dielectric properties (relative permittivity and conductivity) exhibit a strong negative correlation with flow rate and renal perfusion pressure changes. The dielectric property differences between cortex and medulla are relatively small but measurable. As in previous experiments, measured changes in pressure and kidney weight with changing flow rate had a strong positive correlation, while the changes in dielectric properties had the opposite relation.

It should be noted that the dielectric properties of the medulla measured in kidney #8 differed greatly from the properties of the medulla in kidney #7. This is primarily a result of changes in local perfusion caused by

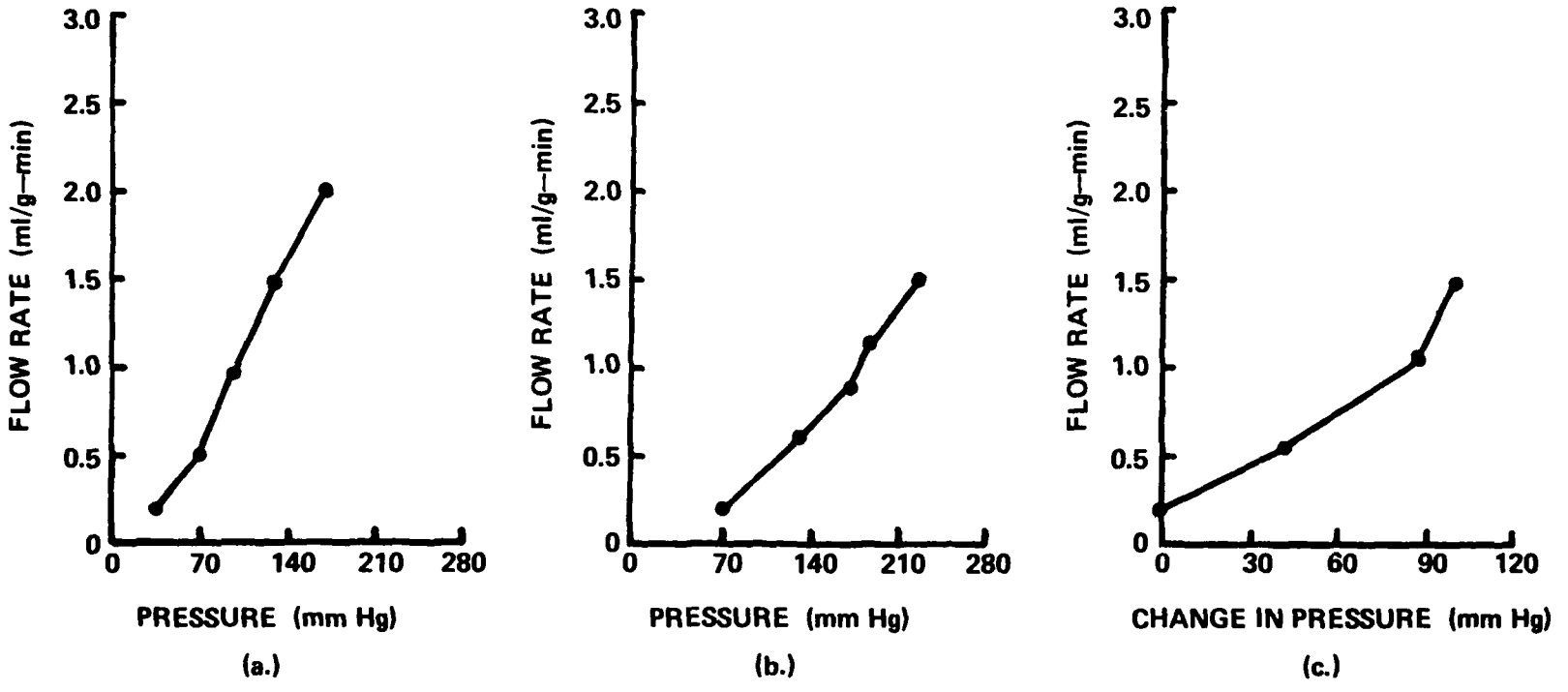

e 6. (a) Flow rate versus perfusion pressure for Kidney #7. (b) Flow rate vs. perfusion pressure for Kidney #8. (c) Mean changes in flow rate plotted as a function of perfusion pressure for Kidneys #7 and #8

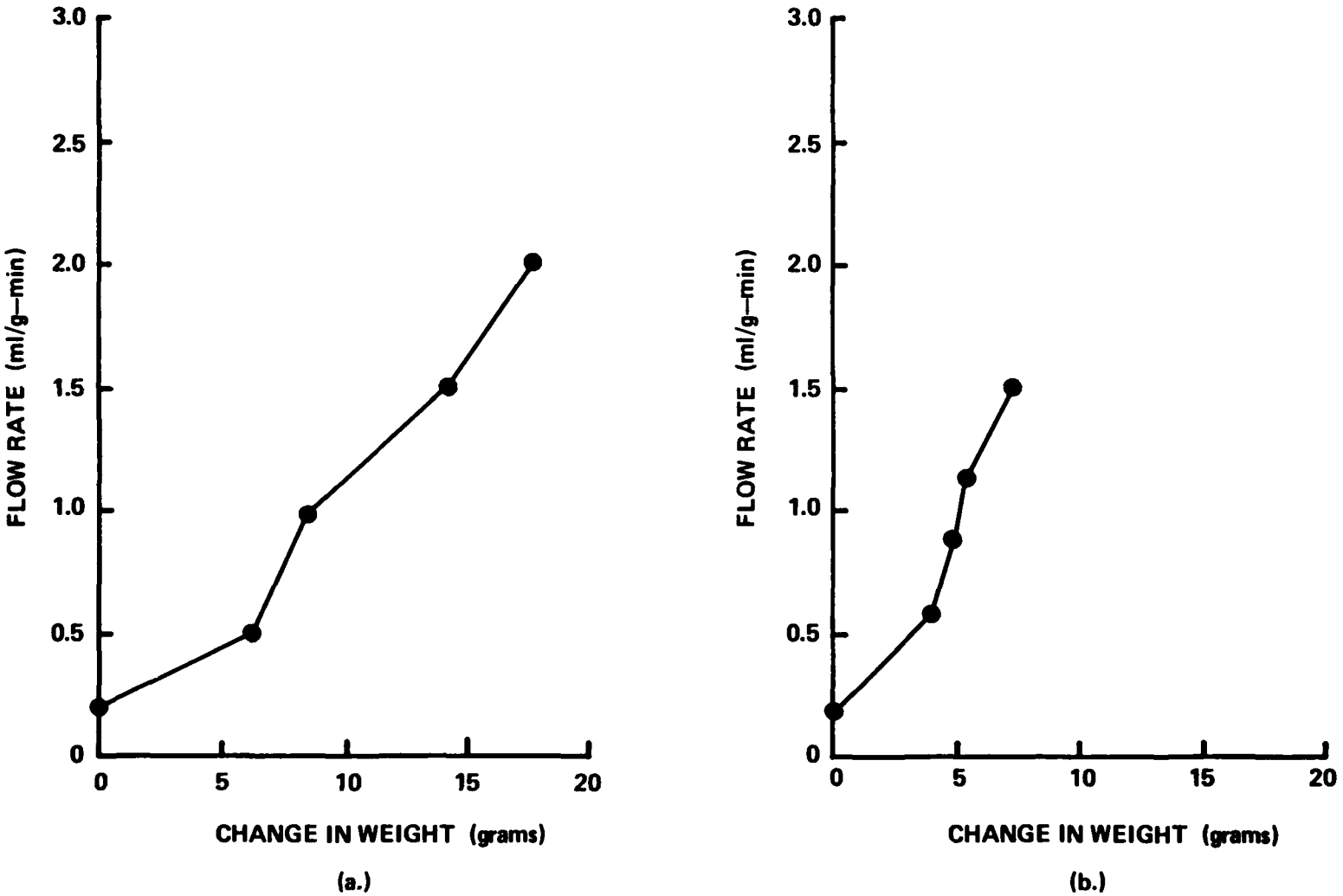

Figure 7. Relationship between changes in kidney weight and flow rate for Kidney #7 (7a.) and Kidney #8 (7b.).

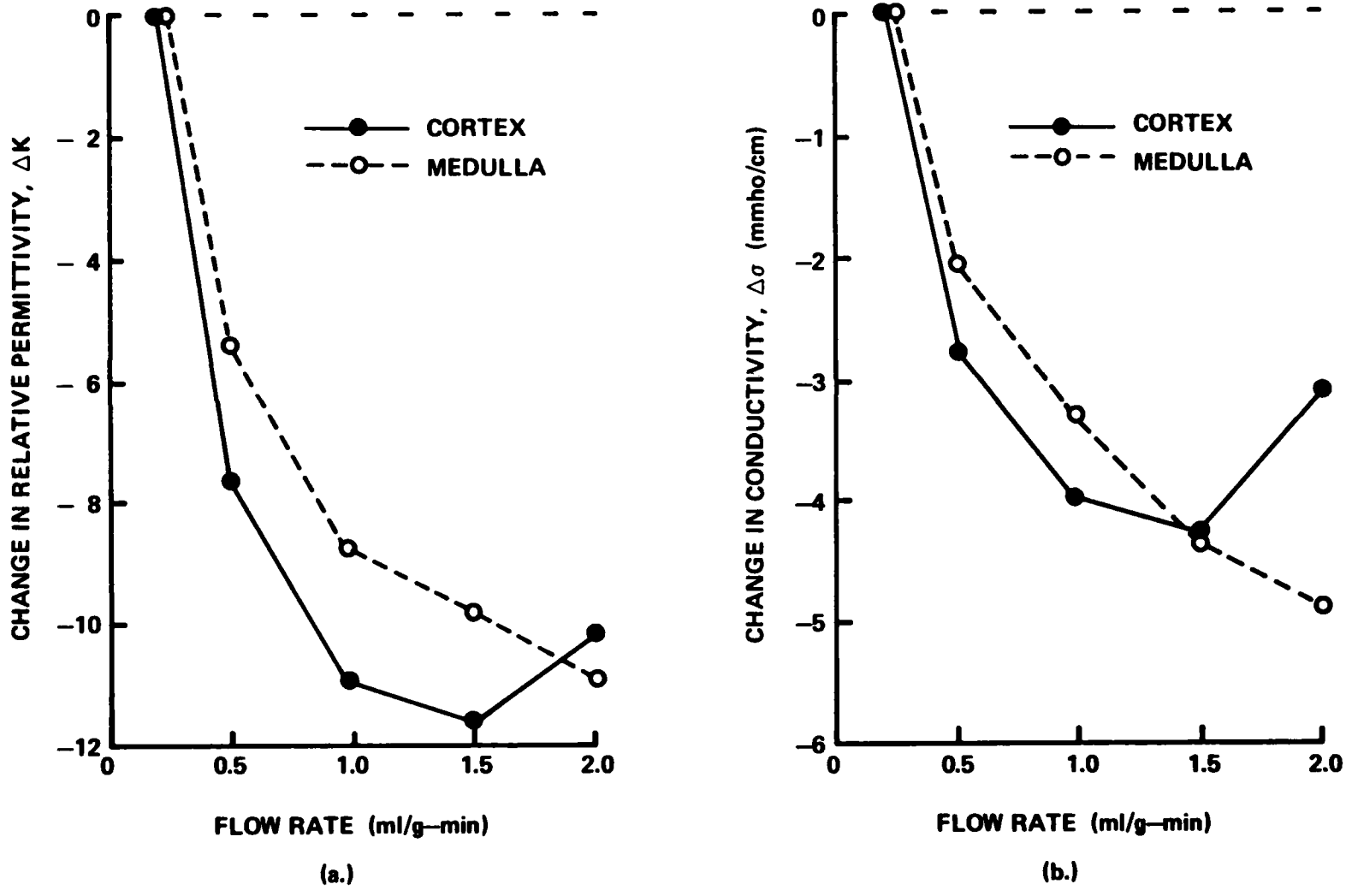

Figure 8. Baseline-subtracted dielectric properties (relative permittivity and conductivity) as a function of flow rate in Kidney #7.

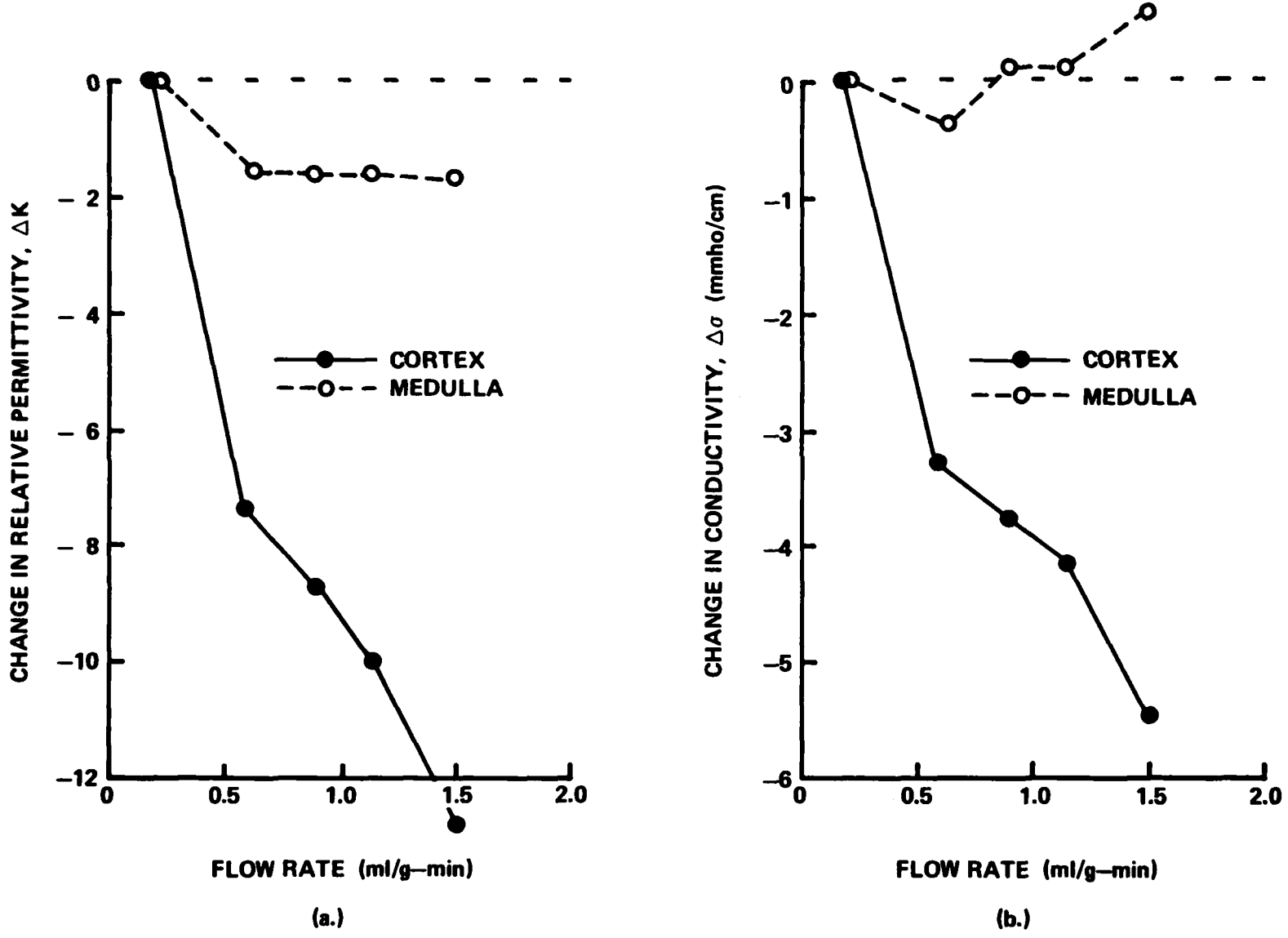

Figure 9. Baseline-subtracted dielectric properties as a function of flow rate in Kidney #8. Note the large difference in the dielectric properties of the medulla as compared to Kidney #7. This difference is interpreted to be secondary to increase probe contact force. Refer to text for additional information.

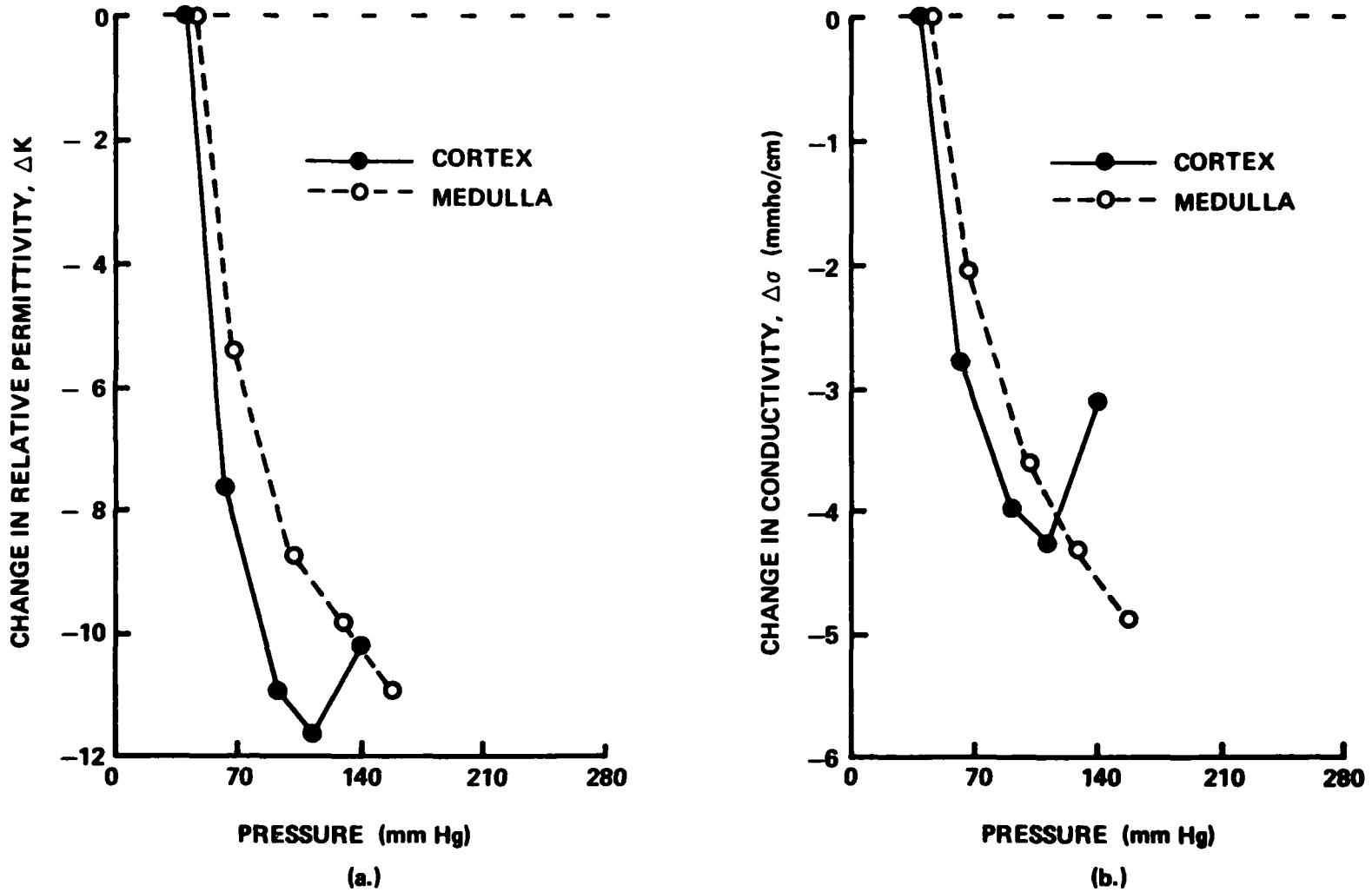

Figure 10. Baseline-subtracted dielectric properties as a function of pressure in Kidney #7.

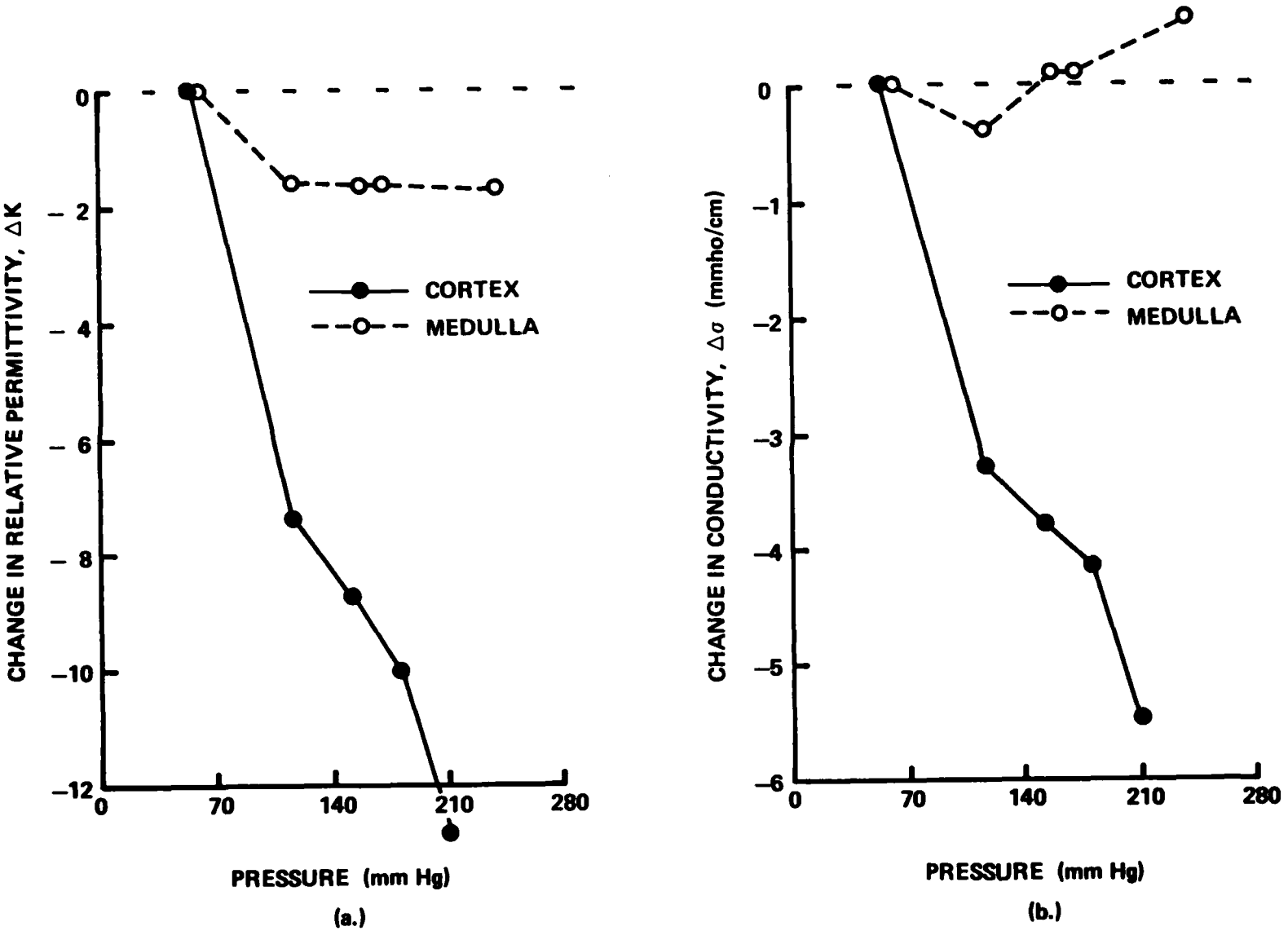

Figure 11. Baseline-subtracted dielectric properties as a function of pressure in Kidney #8. Note the large difference in the dielectric properties of the medulla as compared to Kidney #7. This difference is interpreted to be secondary to increased probe contact force. Refer to text for additional information.

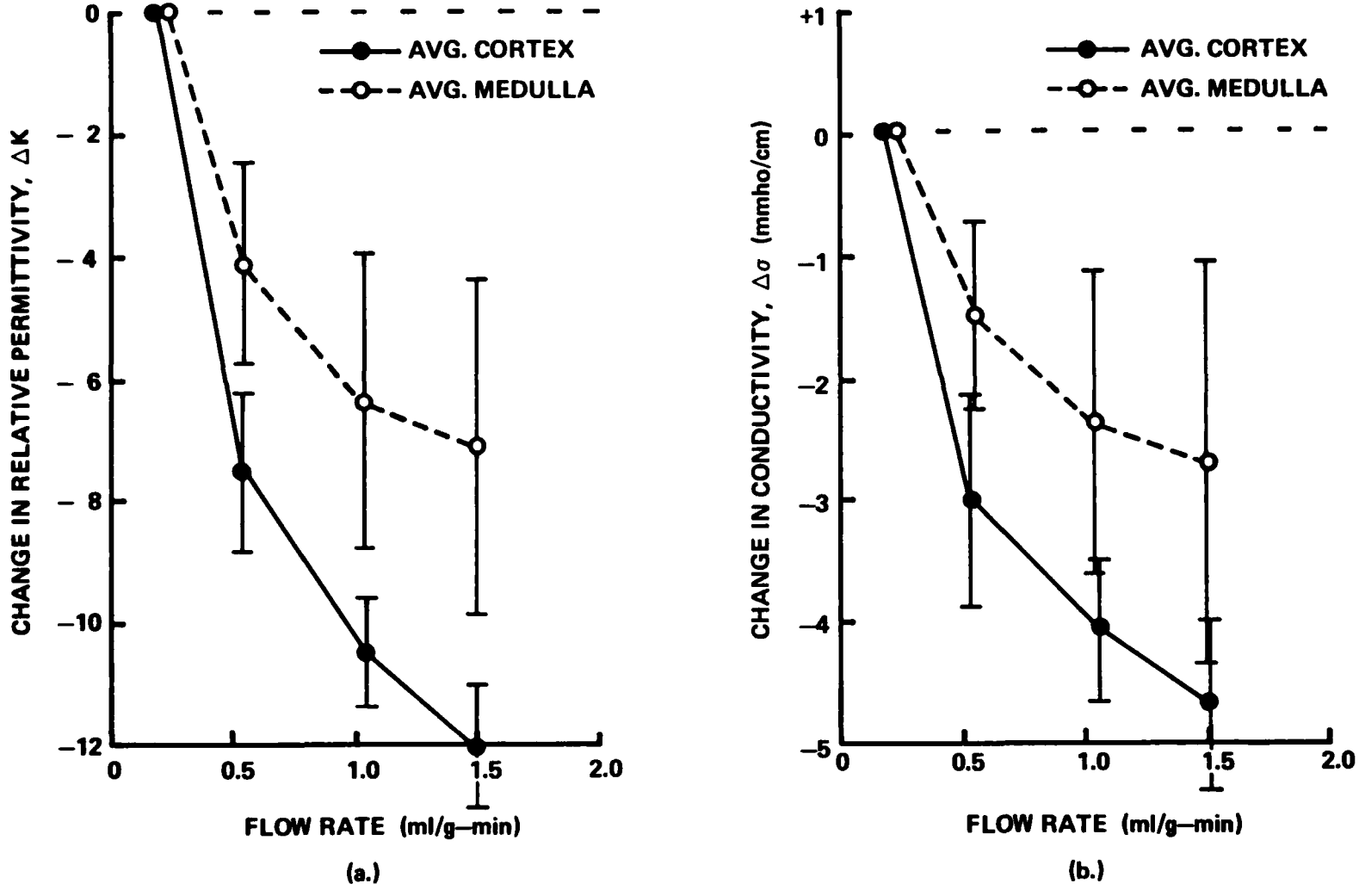

Figure 12. Averaged, baseline-subtracted dielectric properties and standard errors as a function of flow rate in Kidneys #7 and #8.

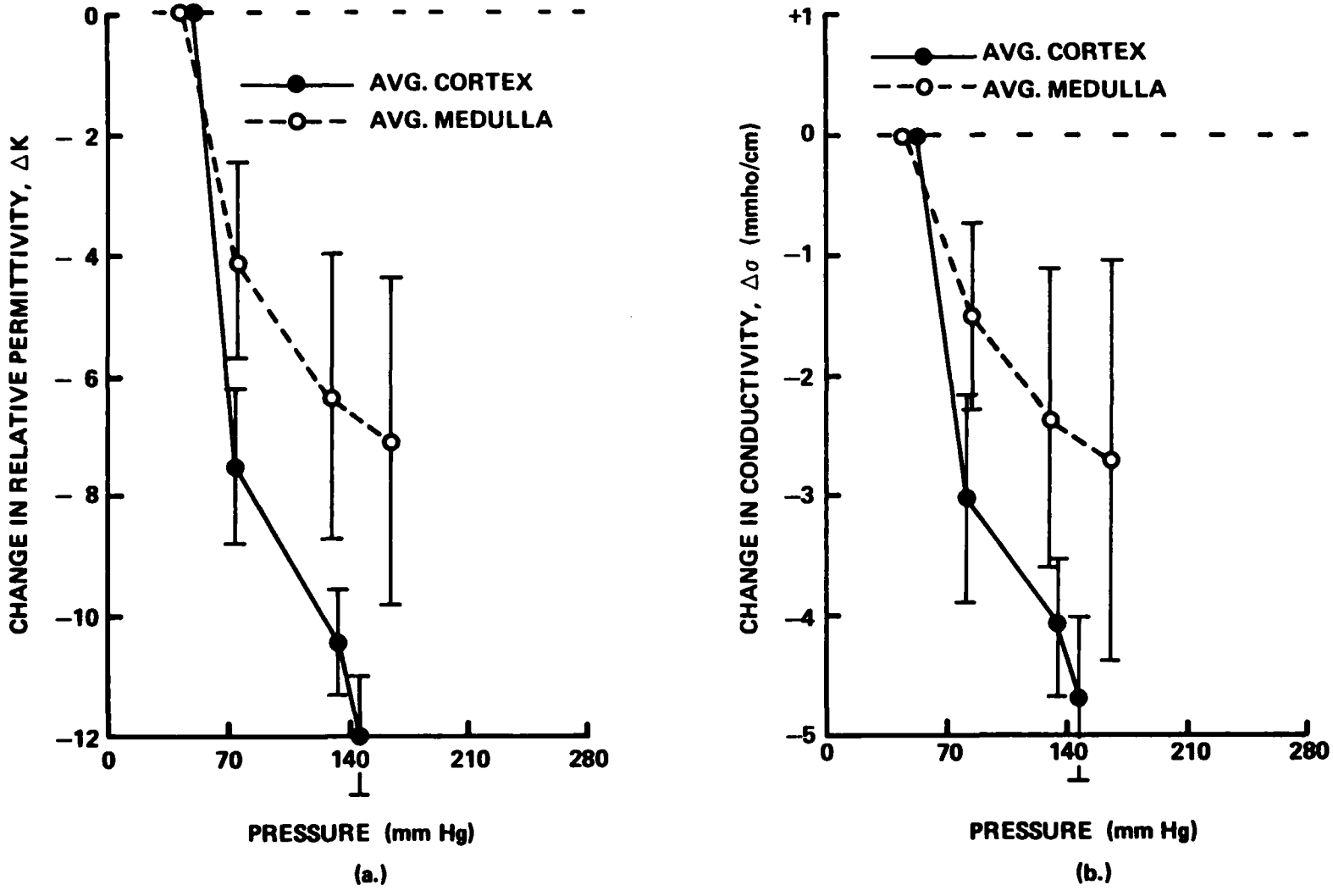

Figure 13. Averaged, baseline-subtracted dielectric properties and standard errors as a function of pressure in Kidneys #7 and #8.

a significant difference in probe contact force for these two measurement sets. In previous experiments, we have not taken into account the effect of changes in probe contact force on our dielectric data, but have used our probe contact force estimates only to correct measured kidney weight for different perfusion pressures. Since the previously described [9] spring-loaded probe holder was used for holding the dielectric measurement probe during tissue measurements, probe contact forces were not specifically monitored. It appears that the approach which worked so well for the brain dielectric studies by itself was not adequate for the renal studies. In measuring the cortex of kidney #8, we initially collected data very different in character from data obtained from previous renal perfusion experiments, and could only conclude that these changes were a result of increased probe contact force. On decreasing the probe contact force, we obtained measurements virtually identical to data from previous experiments. We then decided to hold probe contact force at a value constant to within preset limits and not permit it to vary (as allowed previously) when increased renal flow and perfusion pressure produced increases in kidney surface tension and resultant upward pushing against the spring-loaded probe. Results for three sets of renal cortex measurements performed under different conditions of probe contact force are shown in Figures 14 and 15. Figure 14 shows the contact forces used for each set of cortex dielectric measurements as a function of controlled total renal flow rate, while Figure 15 displays the changes in relative permittivity and conductivity with respect to the same flow rates. It is readily apparent from the data of Figure 15 that the differences in probe contact force produced marked differences in the measured dielectric properties.

We interpret these differences in measured dielectric properties to be the result of the probe tip compressing the kidney tissue locally and altering the flow present in the tissue volume being interrogated. Therefore, when probe contact force is great, perfusion of the region being measured may be partially obstructed or even blocked entirely, and there will be very little change seen in the measured dielectric properties. If this interpretation is true, then previously reported dielectric changes have been a function not only of increasing flow, but also of increasing probe contact force. As the kidney's surface tension increased with increasing flow, the kidney pushed upward against the probe with increasing force,

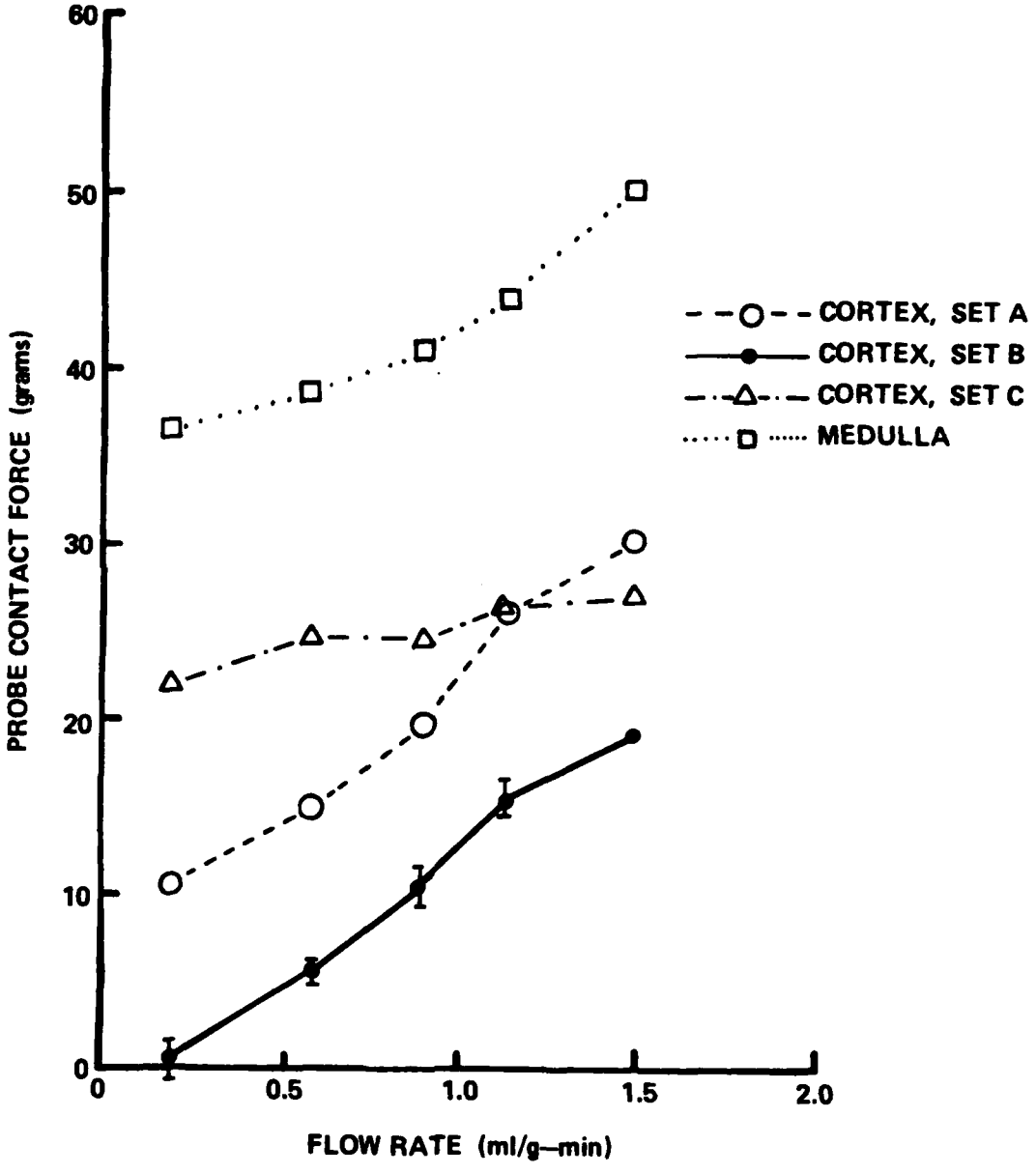

Figure 14. Probe contact force versus flow rate in Kidney #8. Three sets of data for cortex and one set for medulla. Cortex, Set A represents a heavy, variable contact force. Cortex, Set B represents a light, variable contact force. Cortex, Set C represents a heavy, constant contact force. The Medulla data were obtained using an even heavier contact force.

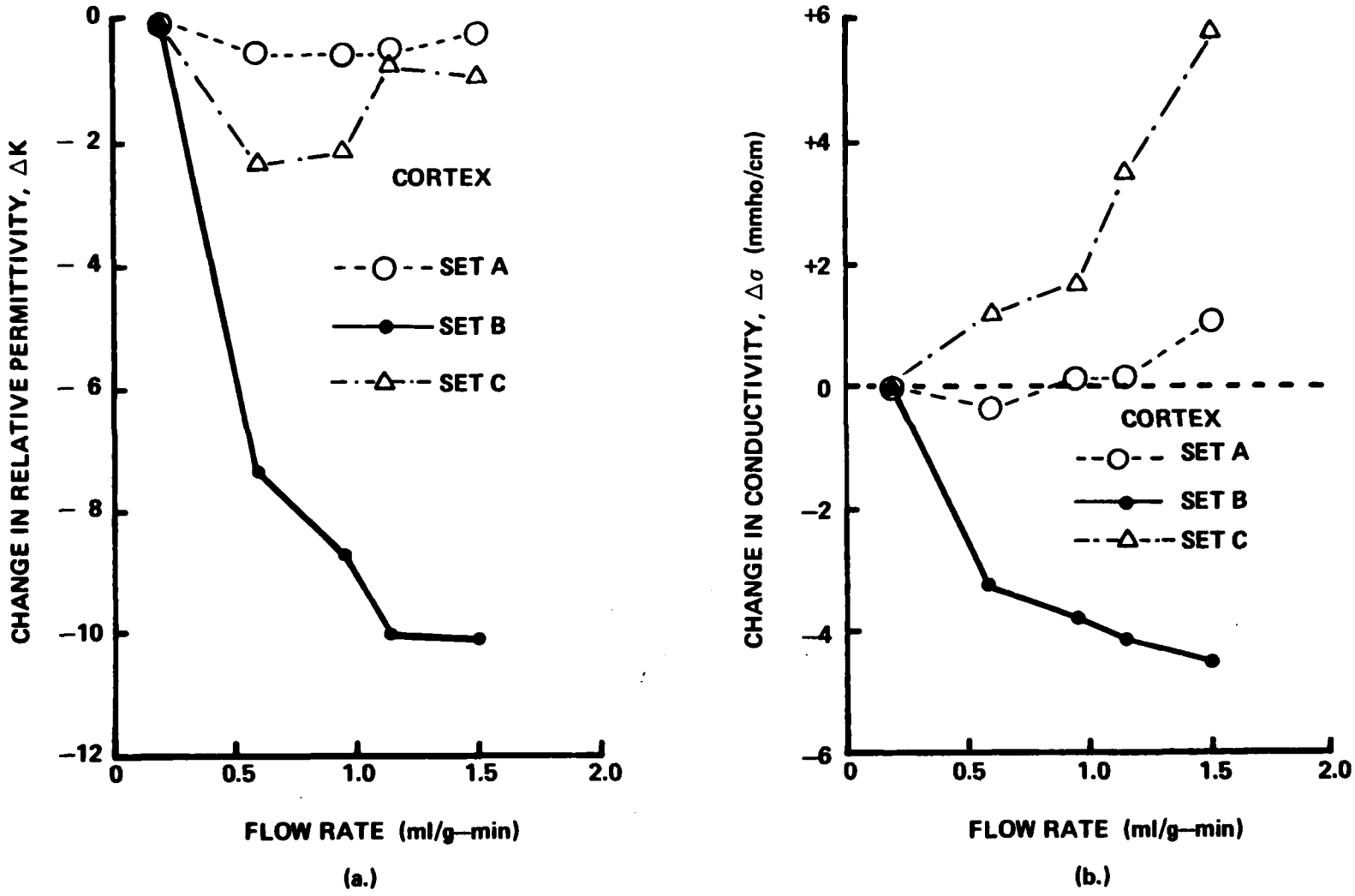

Figure 15. Baseline-subtracted dielectric properties with respect to flow rate for each of the three sets of contact force used on Kidney #8, Cortex, illustrating the effects of different probe contact forces on measured dielectric properties. Cortex, Set A represents a heavy, variable contact force. Cortex, Set B represents a light, variable contact force similar to previous experiments. Cortex, Set C represents a heavy, constant contact force.

apparently because the spring used in the spring-loaded probe holder was too stiff (spring constant too large). Therefore, as the kidney expanded, it compromised its own flow in the local region of probe contact. This was found to indeed be the case when this effect was studied as part of the radioactive tracer flow studies.

Attempts were made with kidney #8 to determine how dielectric properties would change with respect to controlled flow changes under constant probe contact force, but the contact force selected was too heavy and prevented local flow changes. Therefore, the experiment with kidney #9 was re-designed to better control contact force by keeping probe-tissue contact force both constant and light (between 5 and 10g). The measured results are shown in Figures 16-19. Figure 16(a) displays the total renal flow/pressure relationship, while Figure 16(b) shows the measured probe contact forces for the experiment, which were consistently between 5-10 grams. Unfortunately, this kidney again became hypertensive and edematous over a period of 5-6 hours on the perfusion circuit as can be seen by the increasing pressure values for decreasing flow rate at flow rates of about 2.0 ml/g-min. Because of the hypertension, we were unable to show better evidence of autoregulation. Figures 17(a) and 17(b) show the weight changes in relation to flow rate, and they also exhibit the increasing edema and peripheral shutdown occurring at flow rates of approximately 2.0 ml/g-min (seen as the break in the curve and increasing weight in spite of decreasing flow rates) after 5-6 hours perfusion. Although problems with edema and hypertension of this kidney plagued the latter portion of the experiment, the pressure/flow relationship was near normal values earlier in the experiment when the first data sets were measured. Figures 18(a) and 18(b) show the excellent correlation of relative permittivity and conductivity with flow rate. The second set of data plotted for kidney #9 shows the dielectric changes for the same kidney with increasing edema and shutdown of peripheral perfusion.

The most significant difference between the dielectric data (from the measurements prior to shutdown of peripheral perfusion) shown in Figure 18 and previous sets of dielectric data is that the relative changes in permittivity and conductivity with respect to baseline values show a strong positive correlation with renal flow rate. This same positive correlation is seen in Figures 19(a) and 19(b) where dielectric changes are examined with respect to perfusion pressure. It is probably most interesting to

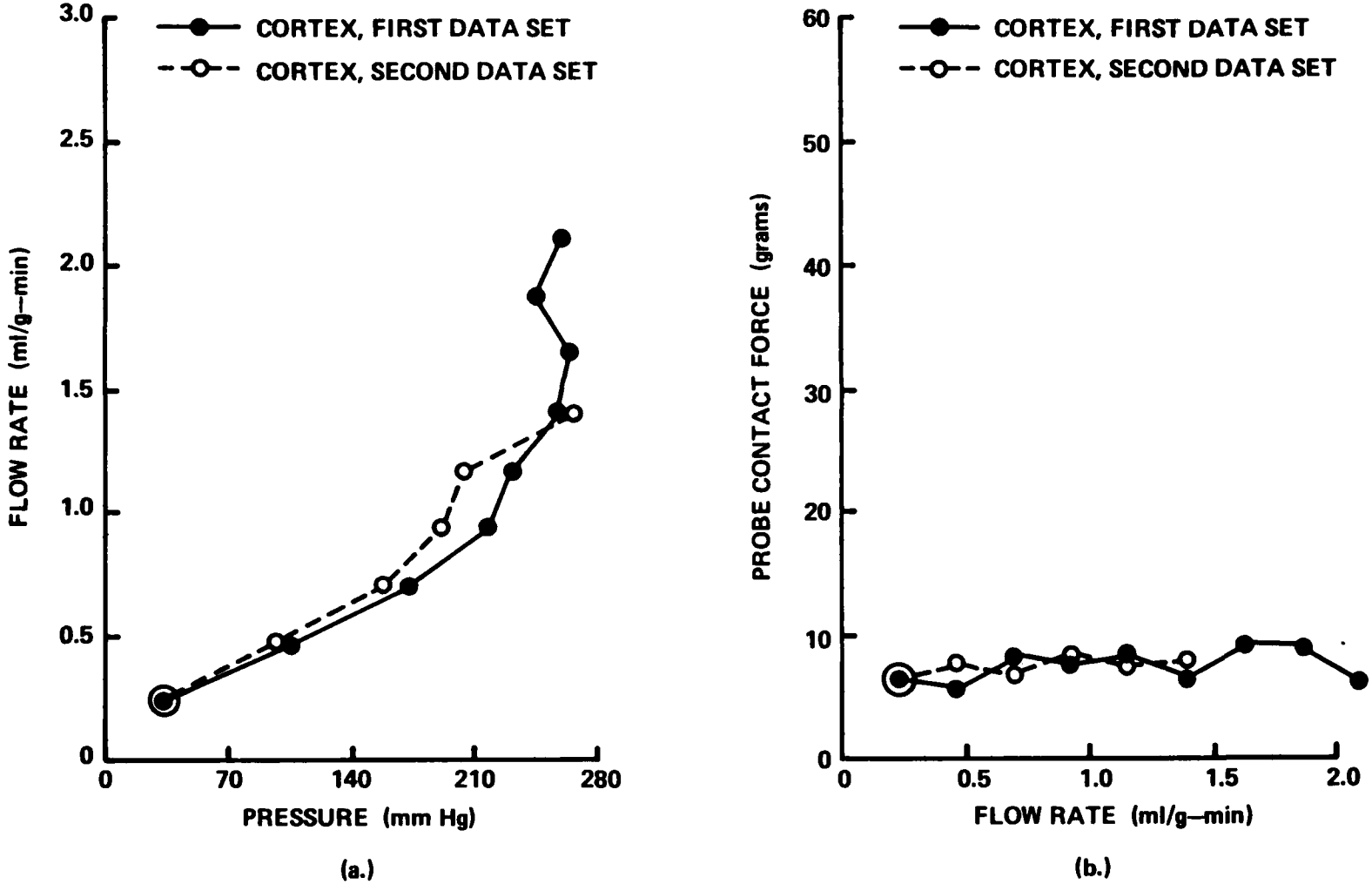

Figure 16. (a) Flow rate versus perfusion pressure for Kidney #9. (b) Probe contact force versus flow rate for Kidney #9. Note how the probe contact force has been kept light (5-10g) and approximately constant for measurements of this kidney.

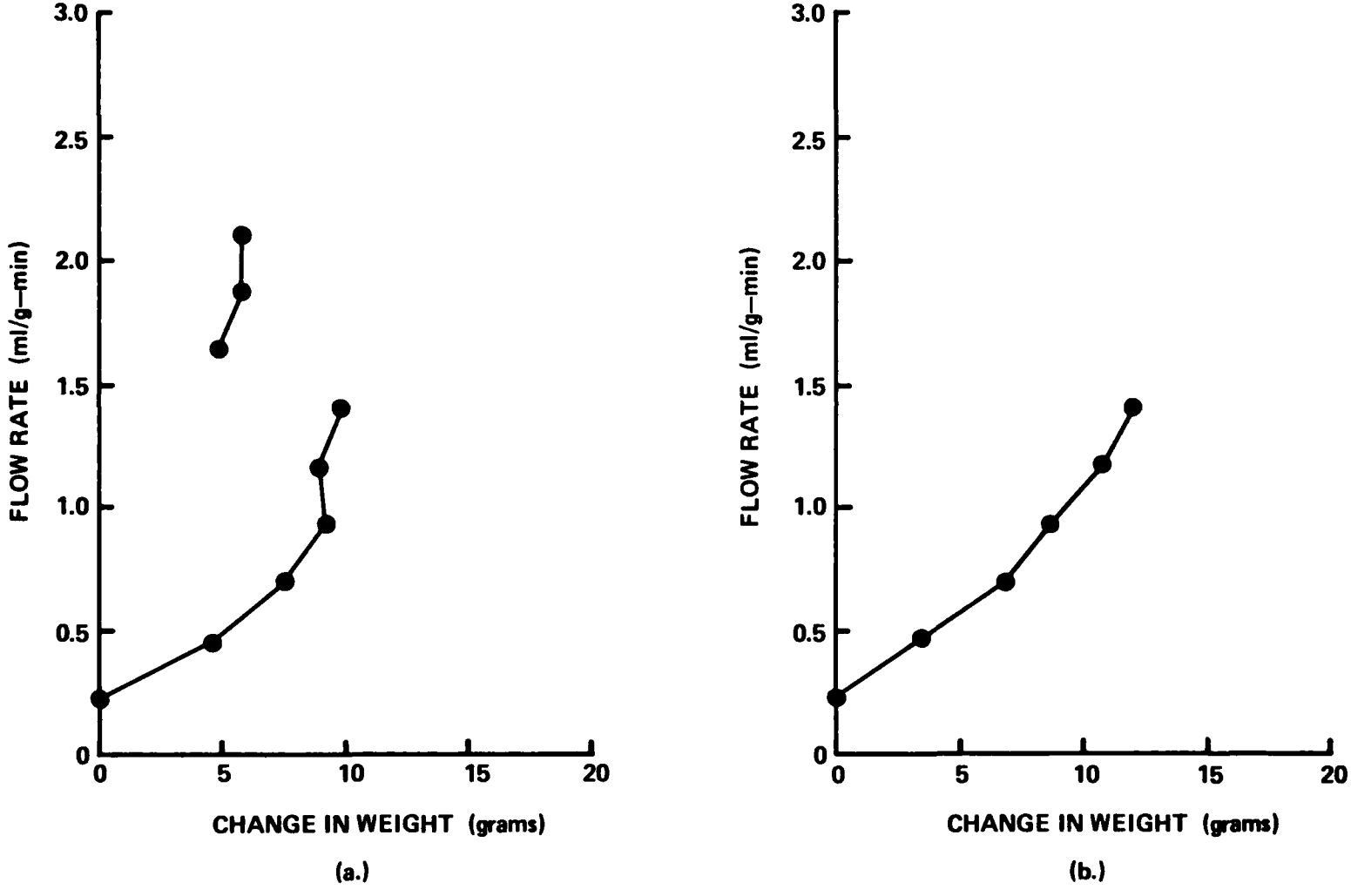

Figure 17. Relationship between changes in kidney weight and flow rate for Kidney #9. (a) Data from initial data set on Kidney #9 as kidney was becoming more hypertensive and edematous during perfusion at a high flow rate to a low flow rate. (b) Data from second data set on Kidney #9 as kidney remained hypertensive and edematous during perfusion at a low flow rate to a high flow rate.

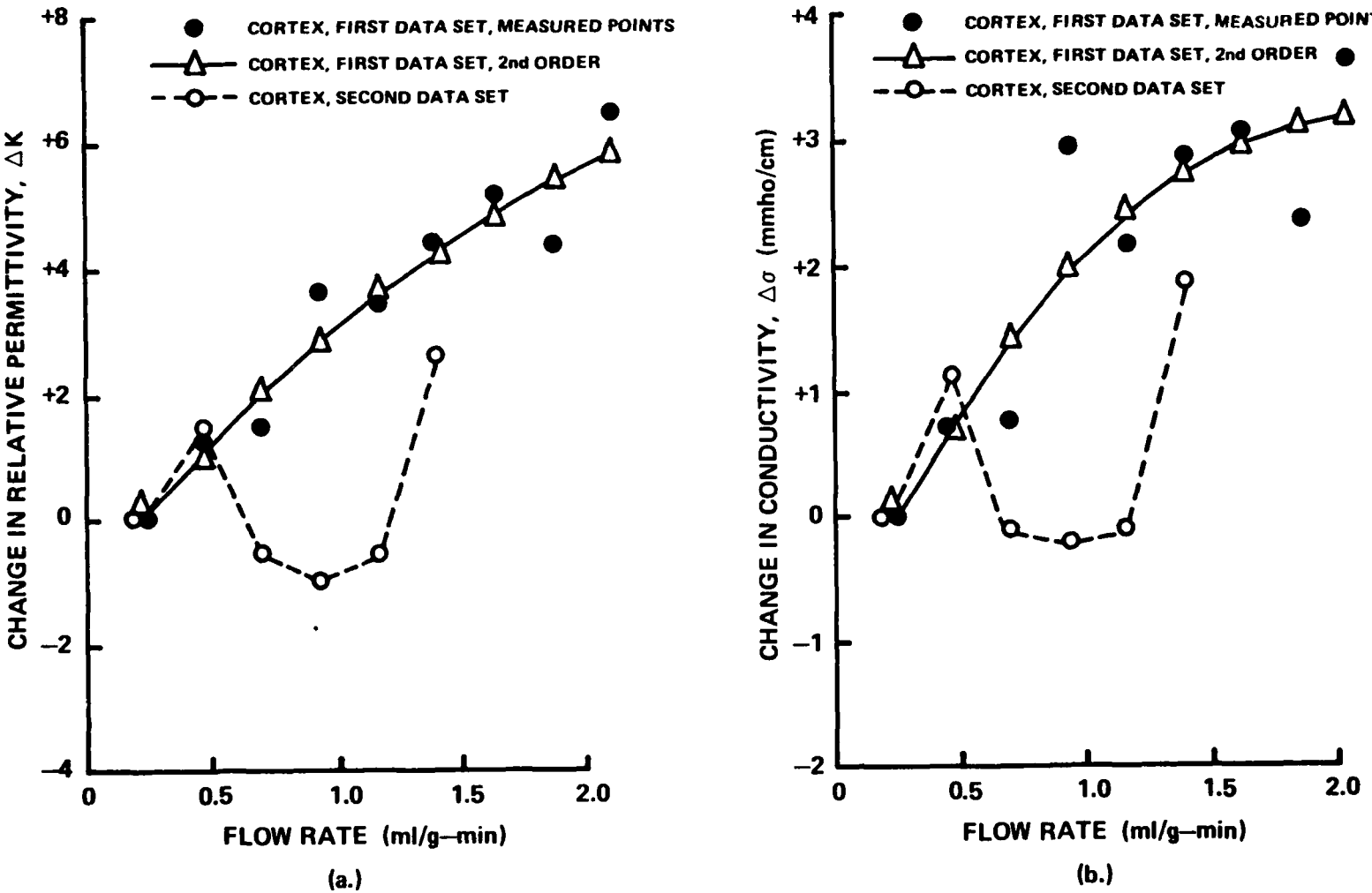

Figure 18. Baseline-subtracted dielectric properties as a function of flow rate in Kidney #9 with probe force kept light and constant. Note the positive correlation with flow rate. The solid curve connecting computed points (open triangles) represents a second order "best fit" approximation to measured data (solid circles) for the first data set. The open circles connected by a dashed line represent data collected as the kidney became increasingly edematous and hypertensive.

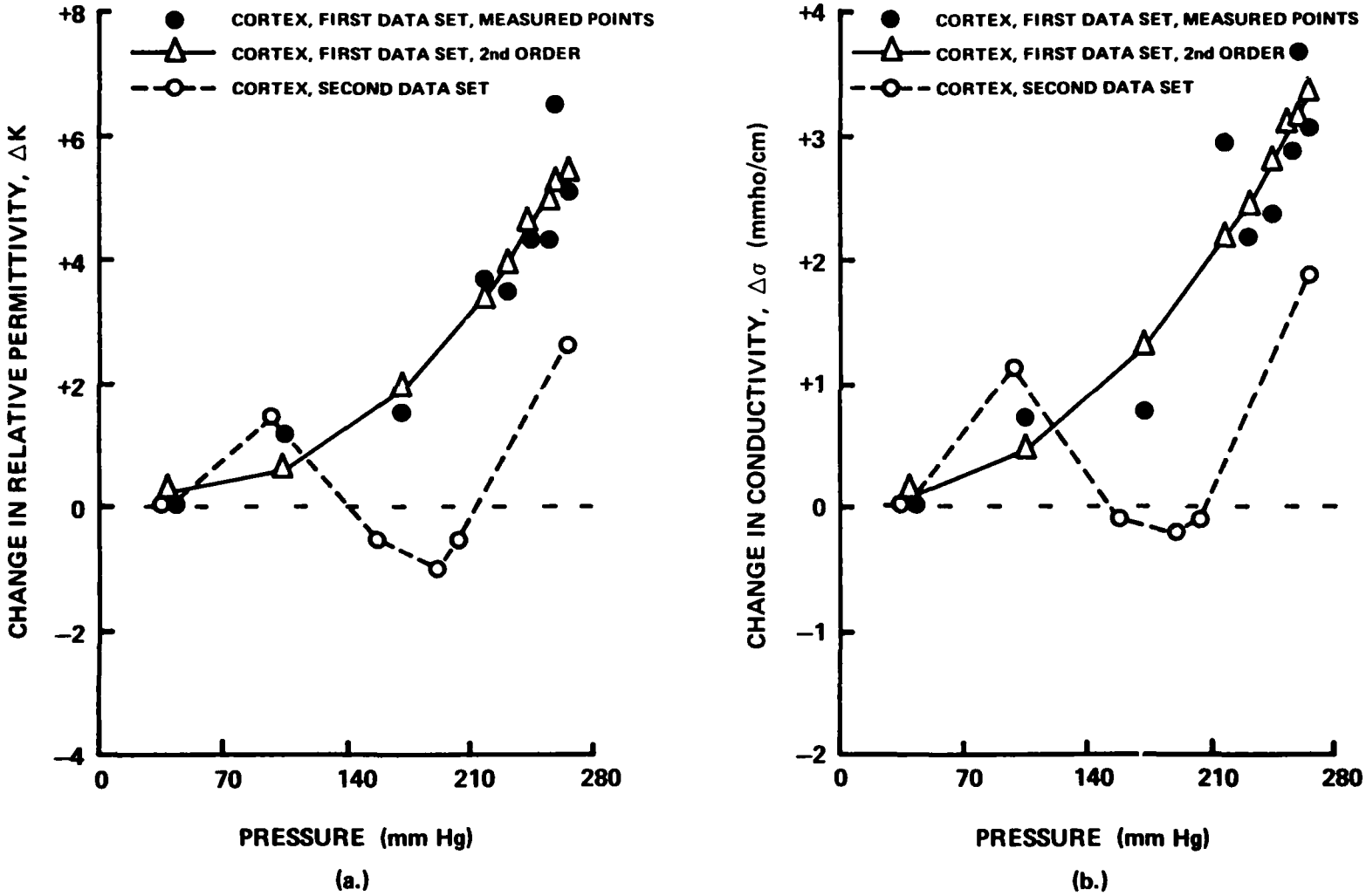

Figure 19. Baseline-subtracted dielectric properties as a function of pressure in Kidney #9 with probe force kept light and constant. Note the positive correlation with flow rate. The solid curve connecting computed points (open triangles) represents a second order "best fit" approximation to measured data (solid circles) for the first data set. The open circles connected by a dashed line represent data collected as the kidney became increasingly edematous and hypertensive.

compare Figures 18(a) and 18(b) with the flow/pressure curve in Figure 16(a) and see how closely they correspond, lending strong support to the theory that changes in dielectric properties are representative of changes in local tissue flow.

The experimental procedure used for kidney #10 was essentially the same as that used for kidney #9 described above. Figure 20(a) represents the flow vs. pressure curve for this kidney which demonstrates the decreasing flow rates as duration of perfusion increases secondary to the increased resistance induced by accumulating edema. Flow rates are much lower for the second set of data than they are for the first set. Figure 20(b) illustrates how probe contact force was kept constant and light (5-10g) throughout the experiment. The increase of edema with the duration of perfusion is again demonstrated in Figure 21 by the increase in kidney weights in the second data set relative to the first data set for the same flow rates. Figures 22(a) and 22(b) are graphs of the measured relation between flow rate and relative permittivity and between flow rate and relative conductivity which show a strong positive correlation. The relationship measured was not linear, and it is interesting to note the slight sigmoidal-type dip in the curve around a flow rate of 2 ml/g-min, which was also seen for the previous kidney. The changes in permittivity and conductivity with respect to pressure are displayed in Figures 23(a) and 23(b). As can be seen, these curves bear a strong resemblance to the pressure/flow curve in Figure 20(a) if the flow rate axis is equated to the dielectric property axis. Thus, the measured changes in relative dielectric properties appear to be most representative of the changes in flow rate.

One must be cautious in comparing the results from these two kidneys since their flow/pressure curves are so markedly different (due to the effects of edema and peripheral vascular shutdown). Yet, when the dielectric properties of these two kidneys are compared, both show a definite positive correlation with flow rate. This relationship is not linear but is instead at least curvilinear, if not sigmoidal. Also, when comparable flow rates are averaged between the two kidneys, the corresponding dielectric properties show relatively small variations between kidneys, despite differences in their respective pressure-flow curves. These results support the theory that the dielectric properties of tissues examined can be used to examine the physiological state of a tissue (i.e., whether or not being perfused

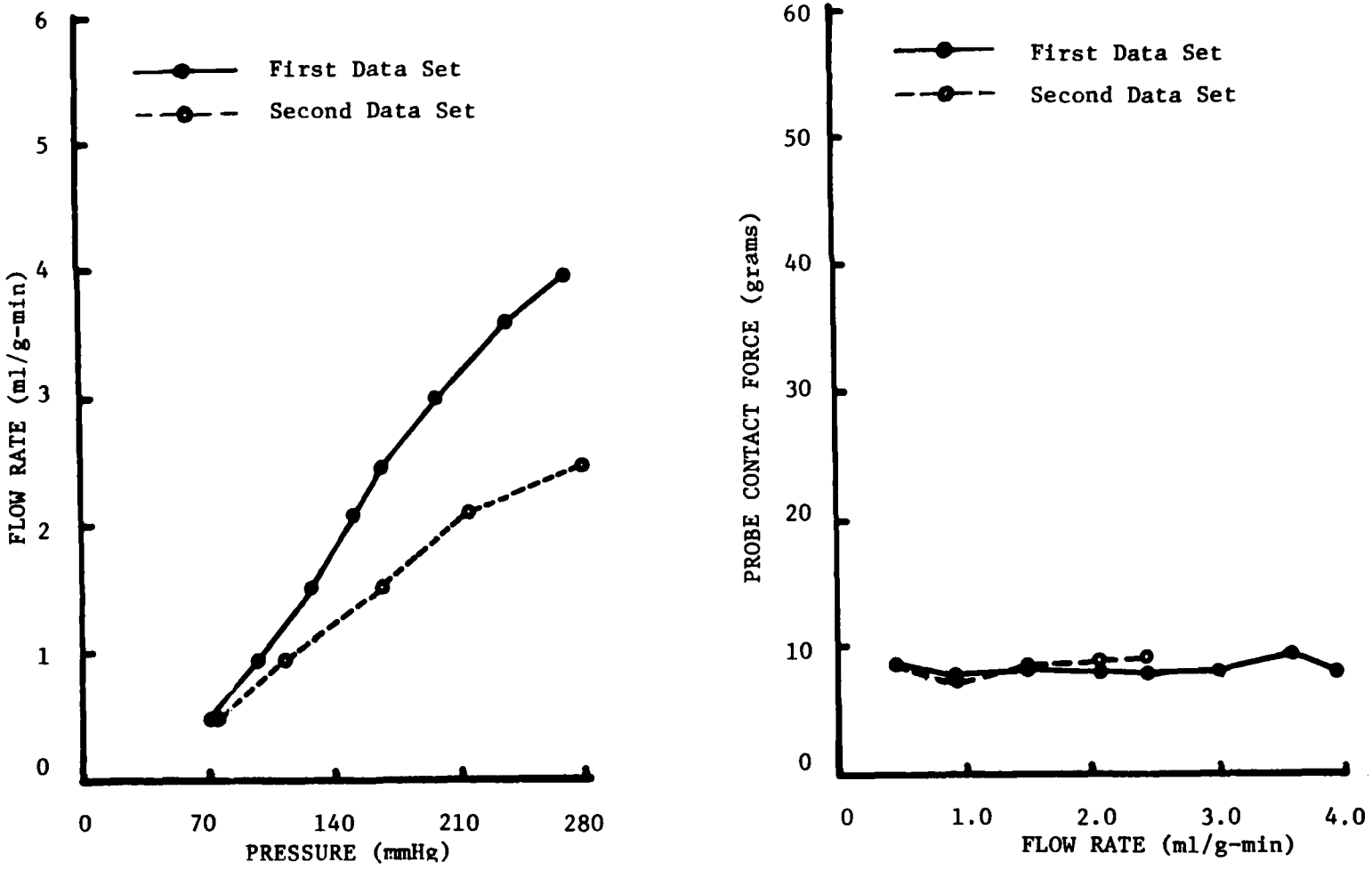

Figure 20. (a) Flow rate versus perfusion pressure for two data sets measured for the kidney #10.
(b) Probe contact force versus flow rate corresponding to the measured pressure-flow relationships in (a).

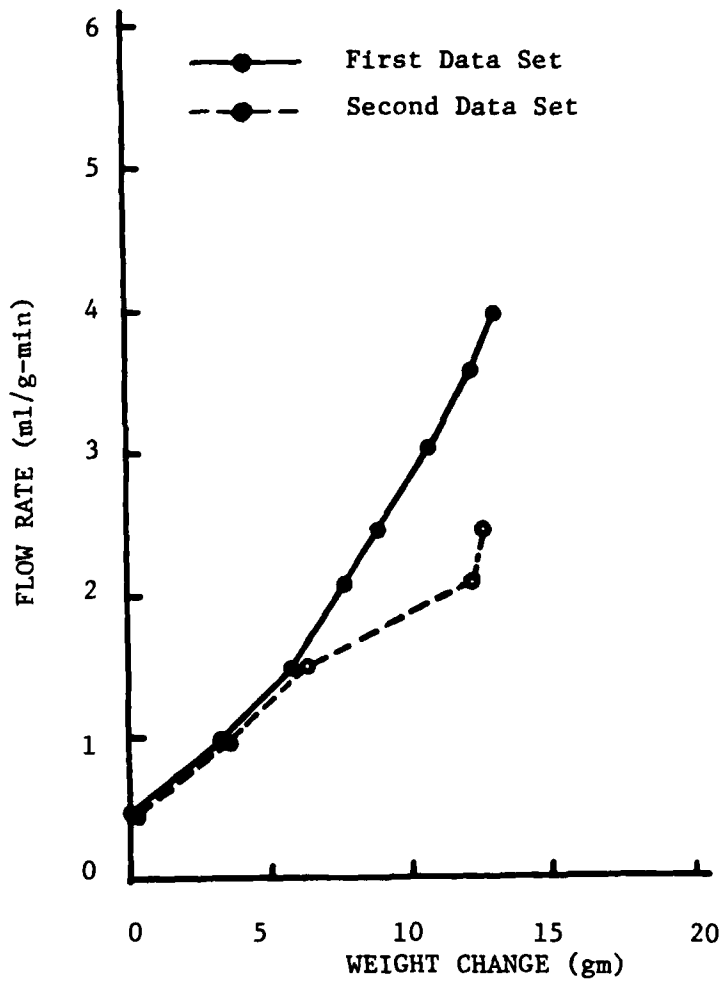

Figure 21. Relationship between changes in kidney weight and flow rate for the kidney of Figure 6.

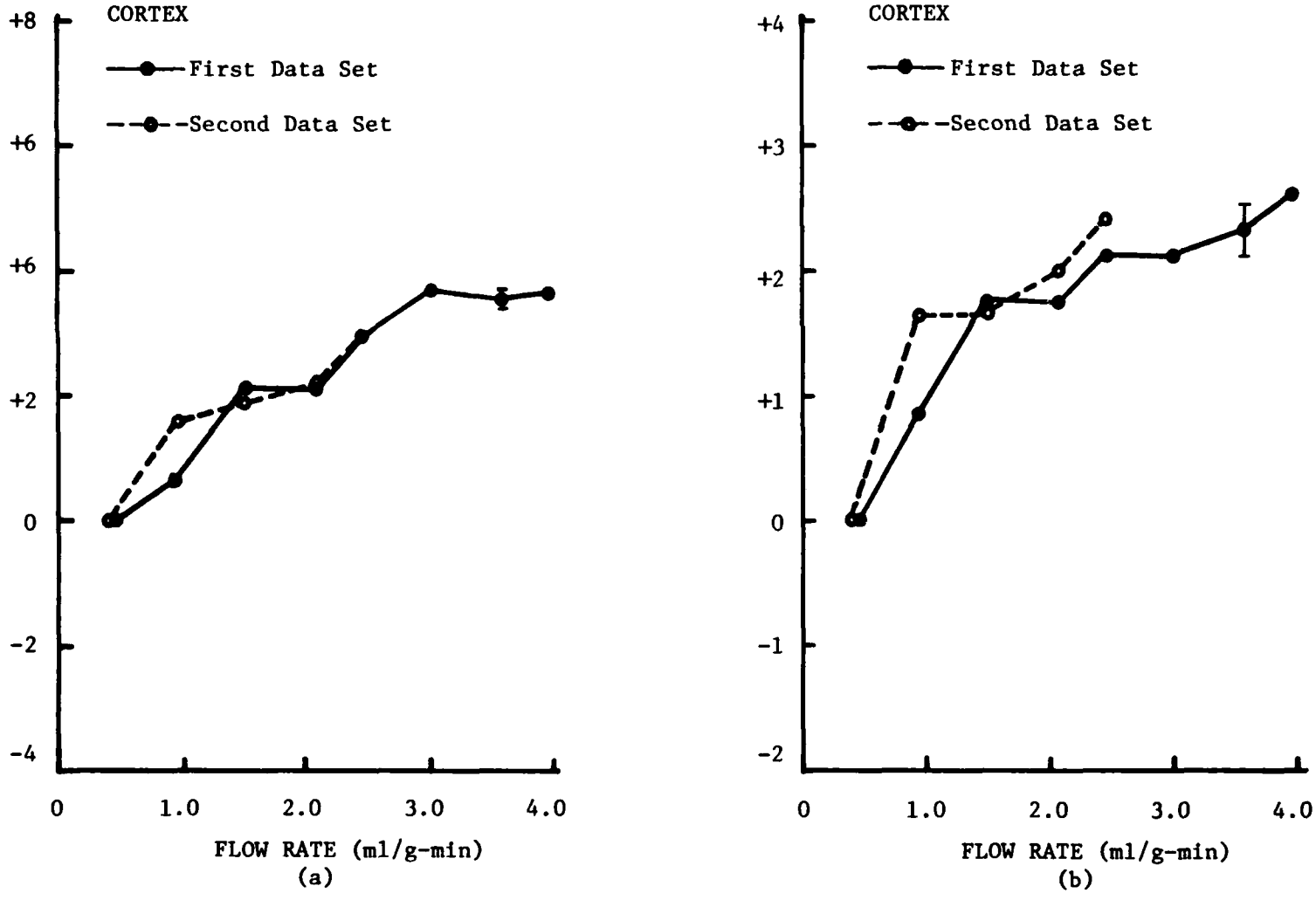

Figure 22. Baseline-subtracted dielectric properties, (a) ΔK and (b) $\Delta\sigma$, of canine kidney cortex for the kidney of Figures 6 and 7 measured as a function of flow rate.

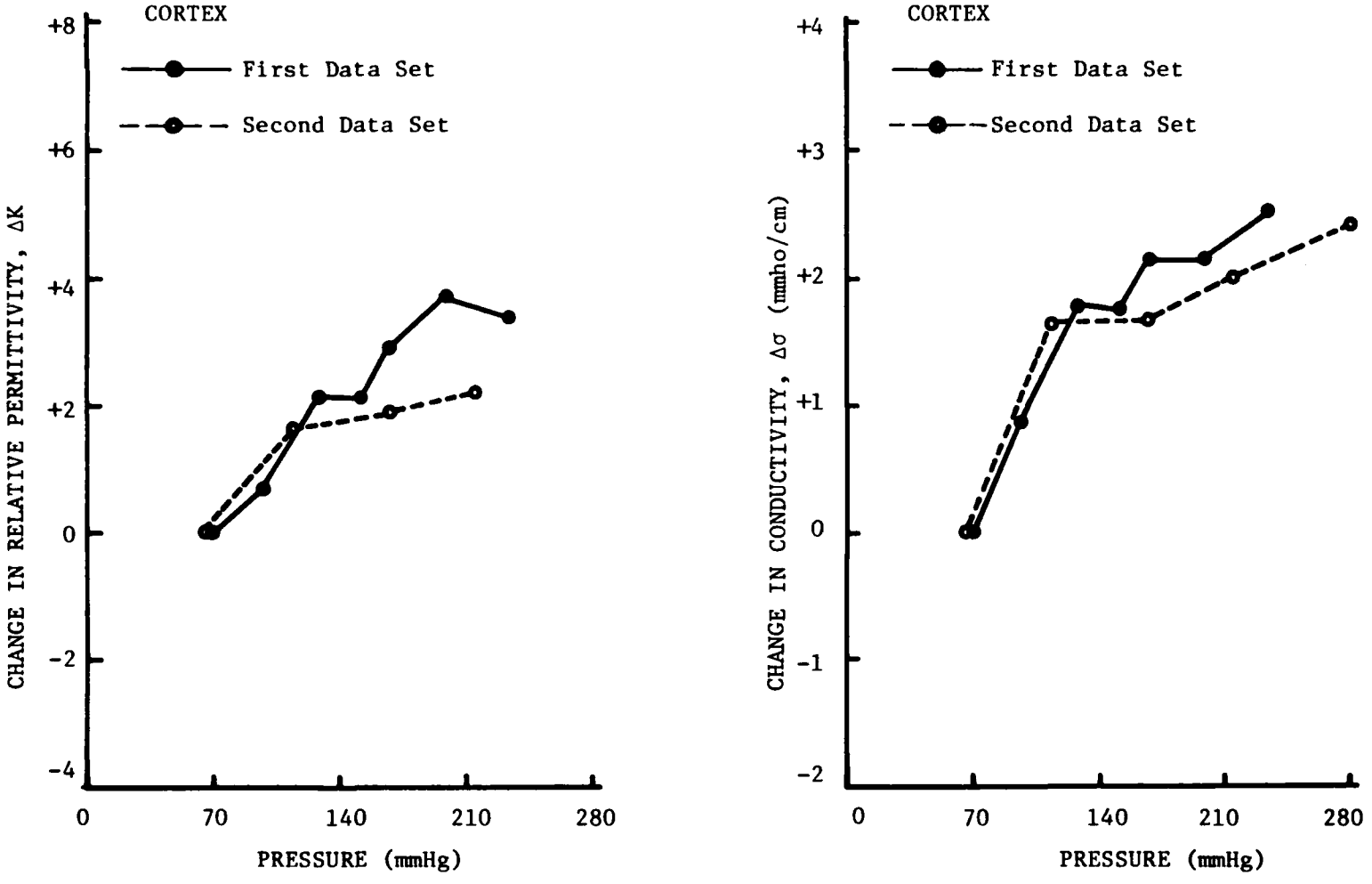

Figure 23. Baseline-subtracted dielectric properties, (a) ΔK and (b) $\Delta\sigma$, measured as a function of perfusion pressure for the kidney of Figures 6-8. Note the "flattened" curve shape between approximately 100 and 200 grams.

well) and to indicate the presence of physiologic pathology (i.e., the presence of tumors or diseased tissue).

B. Kidney Model Studies

In the renal dielectric property experiments, we have been seeking a good renal model not only of blood flow but also of blood flow autoregulation with the hope of determining what dielectric changes, if any, are associated with autoregulation. Autoregulation, of course, is the ability of the kidney to efficiently maintain renal blood flow (RBF) and glomerular filtration rate (GFR) at control levels dispite changes in arterial pressure (which, in the dog, usually ranges from 75 to 180 mm Hg) [14]. Under normal conditions, GFR and RBF are closely coupled, however, renal autoregulation is not dependent solely on arterial pressure changes. It has been shown to be also dependent on many other factors, including changes in venous pressure, ureteral pressure, and plasma colloid oncotic pressure [14]. In response to any of these changes, the bulk of the experimental evidence to date seems to indicate that the renal autoregulatory mechanism always compensates for external disturbances in such a way as to bring GFR back to a normal control level. This compensation is accomplished by means of vascular vasodilation or vasoconstriction which results in changes of RBF and appropriate changes in glomerular filtration pressure.

In an attempt to further improve our renal autoregulatory model, a review of the literature was done to see how other experimenters had investigated renal autoregulation in the fully-isolated, artificially perfused kidney. Most studies of autoregulation have been done using in-vivo catheterized kidneys perfused by the animal's own heparinized blood in the same manner as the original Shipley and Study experiment in 1951 [15]. Their experiment produced one of the first renal curves of pressure vs. flow which is still used in physiology texts today. Their individual kidney data, however, showed extremely wide variations, and at least one of their 13 dogs had a straight line plot rather than the usual sigmoid curve.

In an attempt to generate more reproducible data in a more controlled environment isolated from the effects of the multitude of biological hormones and metabolic products in the living animal, experiments turned to the isolated, in-vitro, kidney model using artificial perfusates, but without much success. In 1958 Witt Waugh was one of the first to demonstrate autoregulation in

an isolated kidney perfused with a colloidal solution containing no corpuscular bodies, thus disproving many then popular theories of the mechanism of autoregulation [16]. The perfusate was oxygenated Ringer-Locke solution with heparin and a colloidal substance being either dextran or polyvinylpyrrolidone (PVP). In his study, only three points were measured, two of which were averaged at the baseline perfusion pressure of 100 mmHg and the third of which was measured at a perfusion pressure of 150 mmHg. From these three points, the relative flow change per 50% change in arterial pressure was calculated yielding an average of 22% flow change. The kidneys were only perfused for several minutes and rapid deterioration of autoregulation was seen when total perfusion time exceeded 20-30 min or when the kidneys were without perfusion for greater than 4 min between surgical ligation and attachment to the perfusion system.

In 1960, Waugh [17] continued his autoregulation studies with approximately the same type of perfusate but this time with and without the addition of heparinized dog plasma. When perfused with colloidal solution without plasma, the kidneys again demonstrated autoregulatory behavior as well as reactivity to vasoconstrictors. However, the autoregulatory behavior rapidly deteriorated with duration of perfusion within as short as 6-7 minutes or as long as 10-20 minutes. With the addition of 20 volume percent of dog plasma, to the same colloidal solution, it was reported that loss of autoregulation was prevented and the kidney showed relative changes in flow of only 12% per 50% change in arterial pressure. The duration of time over which deterioration could be prevented was not stated, however, Waugh did state that the autoregulation seen was usually just as rapid and intense as in his blood-perfused control kidneys. Addition of 5 volume percent dog plasma only partly prevented the deterioration after 5-15 minutes. Very similar findings were reported again by Waugh in 1964 [18] along with additional findings that autoregulation was not severely impaired by anoxic perfusion for less than 20 minutes, and that autoregulation was depressed by pentobarbital anesthesia but not by α-chloralose.

Since these studies, most of the work with the isolated, artificially-perfused kidney model has been done using rat kidneys partly because of the problem of renal vasoconstriction with dog kidneys [19], but also because of the rat's convenient size, genetic uniformity, and low cost [20]. In 1977, M. Bullivant [21], using isolated rat kidneys, reported that:

1. Only linear flow-pressure changes without autoregulation were seen with perfusates of balanced ionic solutions simulating rat plasma with 3% PVP replacing the plasma proteins;
2. Autoregulation was seen when human serum (5 volume percent) or bovine serum albumin (3 g/l) was added to the same ionic pefusate; and
3. Autoregulation was not dependent on globulin or angiotensinogen.

The rats used in this study were anesthetized with pentobarbital prior to removal of the kidneys, and the kidneys were then attached to a pulsatile perfusion system. It was reported that the autoregulatory ability of the perfusion kidneys deteriorated slowly as a function of time and that after 20 minutes of perfusion autoregulation was completely absent. During autoregulation the kidneys showed a 25-26% relative flow change per 50% pressure change.

In an editorial review by B. D. Ross in 1978 [20], various aspects of rat kidney isolation and artificial perfusion were reviewed. The conclusion was reached that the ideal perfusion system (for rat kidneys) seemed to be a system that was temperature controlled at 37°C using Millipore filtered medium containing 75-80 g Fraction V Bovine Serum Albumin/liter and at least one metabolic substrate (usually glucose, 5 mmole/liter) in Krebs-Henseleit solution, gassed with O_2/CO_2 (95:5 v/v). It was stated that such a solution should be suitable for experiments lasting up to 2 hours. It was also stated that low GFR's are characteristic of isolated kidney experiments, no matter how successful the surgical removal, and that a steady decline of 10%/hour of perfusion time could be expected. Haemmaccel or dextran of high molecular weight have reportedly been successfully used previously as a substitute for Bovine Serum Albumin, as have other plasma expanders such as Pluronic (poloxalene) or hydroxyethyl starch. Another author, H. J. Schurek, in 1980 [19] reported on his work with isolated rat kidneys and stated that certain techniques were now considered standard in isolated kidney perfusates. These techniques included Bovine Serum Albumin in pure preparation with dialysis prior to use, Krebs-Henseleit ionic solution, and additional substrates depending on the study, usually including glucose, amino acids, and other fuel sources.

A more recent study by H. S. Baker, et al., (1981) [22] using isolated rat kidneys examined the effects of albumin and calcium concentrations on

autoregulation. Using Krebs-Henseleit bicarbonate solution with varying concentrations of calcium and albumin, they found:

1. Autoregulation was present in the absence of albumin providing the ionized calcium concentration was 1.82 mM;
2. Addition of 20 and 60 g/l of albumin to the same solution as above markedly increased flow but abolished autoregulation;
3. Keeping the ionized calcium level at 1.82 mM (since albumin binds ionized calcium) restored autoregulation even in media containing 20 and 60 g albumin/l (although with 60g albumin/l autoregulation occurred at a much higher flow rate); and
4. 1.82 mM ionized calcium seems to be a critical level for autoregulation to occur since no autoregulation was seen with 60 g albumin/l and only 1.80 mM ionized calcium.

The rats in this study were anesthetized with pentobarbital. The kidneys were perfused for 30-60 minutes total during which time several measurements were made to generate the pressure-flow curve. Calcium ion concentrations were measured with a calcium ion-sensitive electrode. The conclusion reached was that the smooth muscles of the afferent arterioles are probably dependent on ionized calcium for autoregulatory contractions and that raising the albumin concentration could lower the level of ionized calcium as a result of calcium-binding by the albumin.

The longest reported duration of perfusion of an isolated kidney with preserved function was documented by W. H. Waugh and T. Kubo in 1969 [23]. Using a modification of their original perfusion mechanism [16-18] and a perfusate of difibrinated heparinized dog blood, they were able to obtain renal function tests, GFR's, autoregulatory curves, and autoregulatory responses to various drugs all of which were within normal range for up to 3 to 4.5 hours. However, all the various tests of renal function still tended to deteriorate with time. Their best results were obtained using defibrinated dog blood stored less than 1-1/2 hours prior to perfusion and with the added substrates of glucose, lactate, and pyruvate as well as aldosterone.

As a result of our review of the literature, we have modified our perfusion system by inserting a variable resistance as described in the Methods section in order to provide a situation closely simulating previous autoregulation studies in the literature using isolated kidneys for better comparison of results. We next began examining the different perfusates used in the literature.

Our original perfusate, Solution A, was a high K^+-concentration perfusate used previously in kidney cryopreservation studies. Another perfusate we were interested in trying was Euro-Collins Solution [24] which has yielded good results for hypothermic kidney preservation prior to transplantation. Finally, we were interested in the wide range of perfusates used by other experimenters in the field of autoregulation. A list of these different solutions and their composition can be seen in Table 1. In order to better evaluate these various perfusates, we performed a series of experiments with isolated kidneys in which only the flow-pressure response was evaluated and various perfusates compared.

Kidney #1KE was perfused for 1-2 hours prior to measurements. Because of renal vasconstriction and low flow rates (~60 cc/min), the experiment was terminated after 40 minutes of measurements. Flow rates were so low it was difficult to measure changes accurately. The flow-pressure curve generated appeared to be a straight line; however, there was a possible very slight sigmoidal leveling between 150 and 180 mm Hg where the slope of the curve was 0.07 as compared to 0.43 and 0.31 on either side (Figure 24). This kidney was perfused only with Solution A.

Kidney #2KE was perfused with three different solutions over a total period of 4-1/2 hours; first with Solution A for 80 minutes, then flushed for 40 minutes and perfused with Euro-Collins solution for 50 minutes (total albumin concentration equal to 1.7 g/100 ml). Perfusion with Solution A for the first 80 minutes of measurements yielded low flow rates with respect to pressure but did exhibit a minimal sigmoidal dip in the slope between 125 and 200 mmHg where the slope reached a minimum of 0.348 compared to the maximum of 0.545 on either side (Figure 25). Perfusion with Euro-Collins solution for the next 90 minutes of measurement resulted in marked relaxation of the renal vasculature with the pressure-flow curve slope increasing to greater than twice (average = 1.071) that of the preceeding Solution A curve (Figure 26). As already mentioned, Euro-Collins solution is used to preserve kidneys for transplantation purposes and obviously is good for that purpose in that the high concentration of extracellular potassium reduces the trans-membrane potential of cells, thus preventing muscular contraction and vasospasm. Although Euro-Collins solution is suitable for preserving kidneys and preventing vasospasm, it is not suitable for studying renal autoregulation. For the next 45 minutes, kidney #2KE was flushed with Solution A during which time

TABLE I

DIFFERENT PERFUSATE SOLUTIONS USED IN RENAL AUTOREGULATION STUDIES

	Waugh[3,4,5] Ringer-Locke Pentobarb Anesth		Bullivant[6] Pentobarb		Baker[9] Krebs-Henseleit Bicarbonate Sol'n Pentobarb		Ross[7] Krebs-Henseleit +Gluc.+Alb.		Proposed Solution		Ringer's Lactate		Euro-Collins Solution		Burdette Solution A Pentobarb	
	g/l	mM	g/l	mM	g/l	mM	g/l	mM	g/l	mM	g/l	mM	g/l	mM	g/l	mM
NaCl	9.0 (or 8.0)	154 (or 137)	6.72	115	7.0	120	6.92	118.5	7.0	120	5.96	102	-	-	5.63	96.2
KCl	0.20	2.68	0.373	5	0.224	3.0	0.354	4.7	0.30	4.0	0.30	4.0	1.12	15.0	3.00	40.3
$NaHCO_3$	0.25	2.975	2.10	25	2.10	25.0	2.10	24.9	2.10	25.0	-	-	0.84	10.0	1.00	11.9
$CaCl_2 \cdot 2H_2O$	0.265	1.8	0.147	1	[1.05] 0.849	[7.15] 5.77	0.368	2.5	[1.05] 0.849	[7.15] 5.77	0.221	1.5	-	-	0.189	1.7
$MgSO_4 \cdot 7H_2O$	-	-	0.246	1.0	0.294	1.0	0.294	1.2	0.246	1.0	-	-	-	-	3.075	12.5
Na Lactate	-	-	0.336	3	-	-	-	-	3.14	28	3.14	28	-	-	-	-
KH_2PO_4	-	-	0.054	0.4	0.136	1.0	0.162	1.2	0.136	1.0	-	-	2.05	15.1	-	-
K_2HPO_4	-	-	-	-	-	-	-	-	-	-	-	-	7.4	42.5	-	-
Inulin	-	-	0.25	-	-	-	-	-	-	-	-	-	-	-	-	-
Urea	-	-	-	5	-	-	-	-	-	-	-	-	-	-	-	-
Glucose	1.0	5.54	2.71	15	1.81	10	0.90	5	2.71	15	-	-	35	194.3	2.0	11.1
Heparin	0.01	-	-	-	-	-	-	-	-	-	-	-	-	-	-	-
pH	7.2-7.3	-	-	-	-	-	-	-	-	-	-	-	-	-	-	-
Oxygen	Yes	-	Yes	-	Yes	-	Yes and CO_2		Yes	-	-	-	-	-	-	-
Colloid																
Dextran	60.0 or 40.0	-	-	-	-	-	-	-	-	-	-	-	-	-	-	-
PVP		-	30	-	-	-	-	-	-	-	-	-	-	-	-	-
Albumin Bovine SA	-	-	3 or 50 cc/1	0.043	[60] 20	[0.870] 0.290	75-80	1.09-1.16	[60] 20	0.725	-	-	-	-	-	-
Human Serum	-	-		-	-	-	-	-	-	-	-	-	-	-	-	-
Haemaccel	-	-	-	-	-	-	-	-	-	-	-	-	-	-	-	-

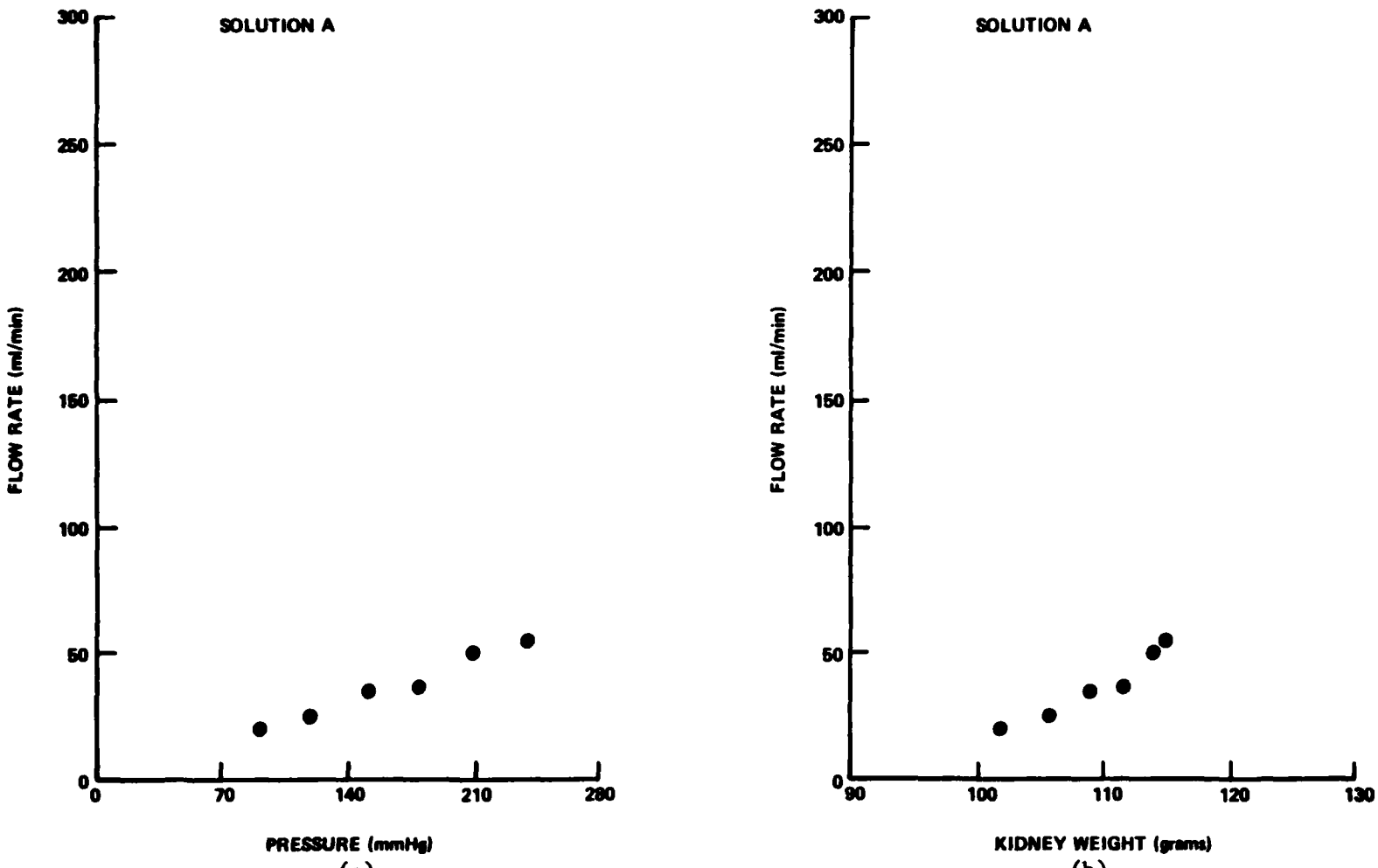

Figure 24. Flow rate versus (a) perfusion pressure and (b) kidney weight for Kidney # 1KE perfused with Solution A.

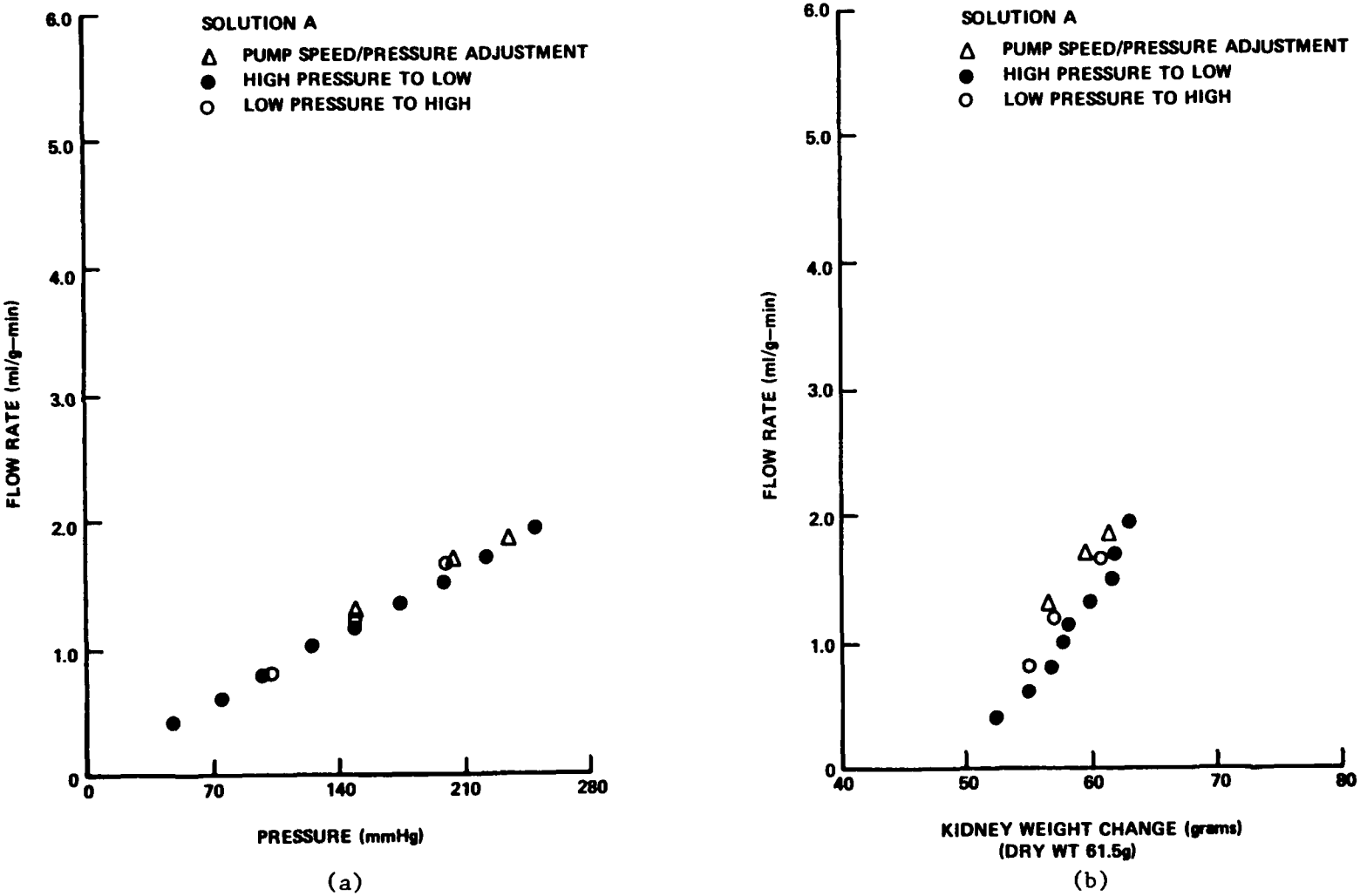

Figure 25. Flow rate versus (a) perfusion pressure and (b) kidney weight for Kidney # 2KE when perfused with Solution A.

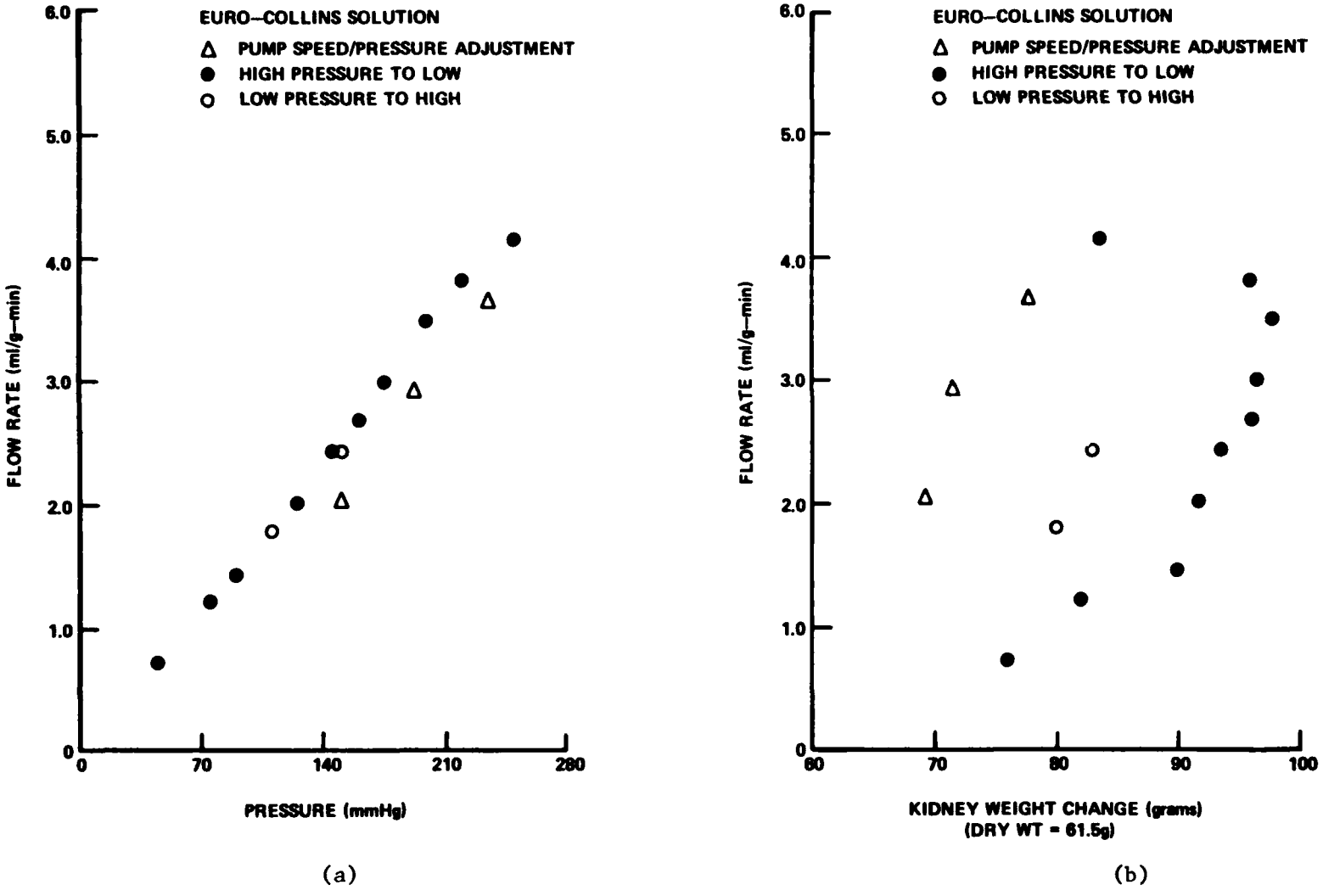

Figure 26. Flow rate versus (a) perfusion pressure and (b) kidney weight for Kidney #2KE when perfused with Euro-Collins solution. (a) Note the large change in slope from Figure 5. (b) Note large weight variation with flow rate.

the slope of the pressure-flow curve remained essentially unchanged from that of the curve for Euro-Collins solution (Average Slope 1.05), and showed virtually no evidence of autoregulation. Duration of perfusion at this point was approximately 4-1/2 hours so it is difficult to say whether the renal autoregulatory mechanism was "poisoned" by the Euro-Collins solution or whether the mechanism had merely deteriorated due to the prolonged perfusion time. When albumin was added to the perfusate (to a concentration of 1.7 g/100cc), the pressure-flow curve continued as essentially a straight line without any evidence of the sigmoidal shape of autoregulation, although the slope of the line increased despite the state of total relaxation induced by the Euro-Collins solution (Figure 27). This increase in slope (average 1.25) was most likely due to the increased intravascular plasma oncotic pressure decreasing the amount of accumulated interstitial edema and thus, decreasing the amount of extravascular interstitial pressure and the resultant externally induced resistance of the renal vasculature.

Kidney #3KE was first perfused with Solution A for 75 minutes and then with Solution A and albumin (~1.67g/100cc) for the next 90 minutes (Figures 28 and 29). On taking measurements from high to low pressures, the pressure-flow curve had initially a low slope (0.20) which gradually increased as pressure decreased (0.80). This curvilinear plot is what might be expected to result from a passive system influenced at high pressures by increased interstital edema and pressure acting externally on the renal vasculature to induce increased resistance. There was no evidence for autoregulation other than a suggestion of a dip in the slope between 110 and 85 mmHg. On measuring from low to high pressures, however, there as a more obvious sigmoidal-type dip in the pressure-flow curve between 85 and 155 mmHg with an average slope of 0.70 as compared to an average of 1.17 for the slopes on either end. Although this curve cannot be called a "normal" autoregulatory curve, it is possible that, in going from high to low perfusion pressure, whatever minimal autoregulatory ability might have been present was obscured by edema secondary to the high pressure of perfusion and the resultant edema and externally induced resistance. At low perfusion pressures, the edema would be drawn back into the intravascular space thus decreasing the externally induced resistance and allowing the minimal autoregulatory ability of the kidney to become manifest. The existence of this "ebb and flow" of edema is supported by the graphs of flow vs. weight (Figure 28 (b)) which show

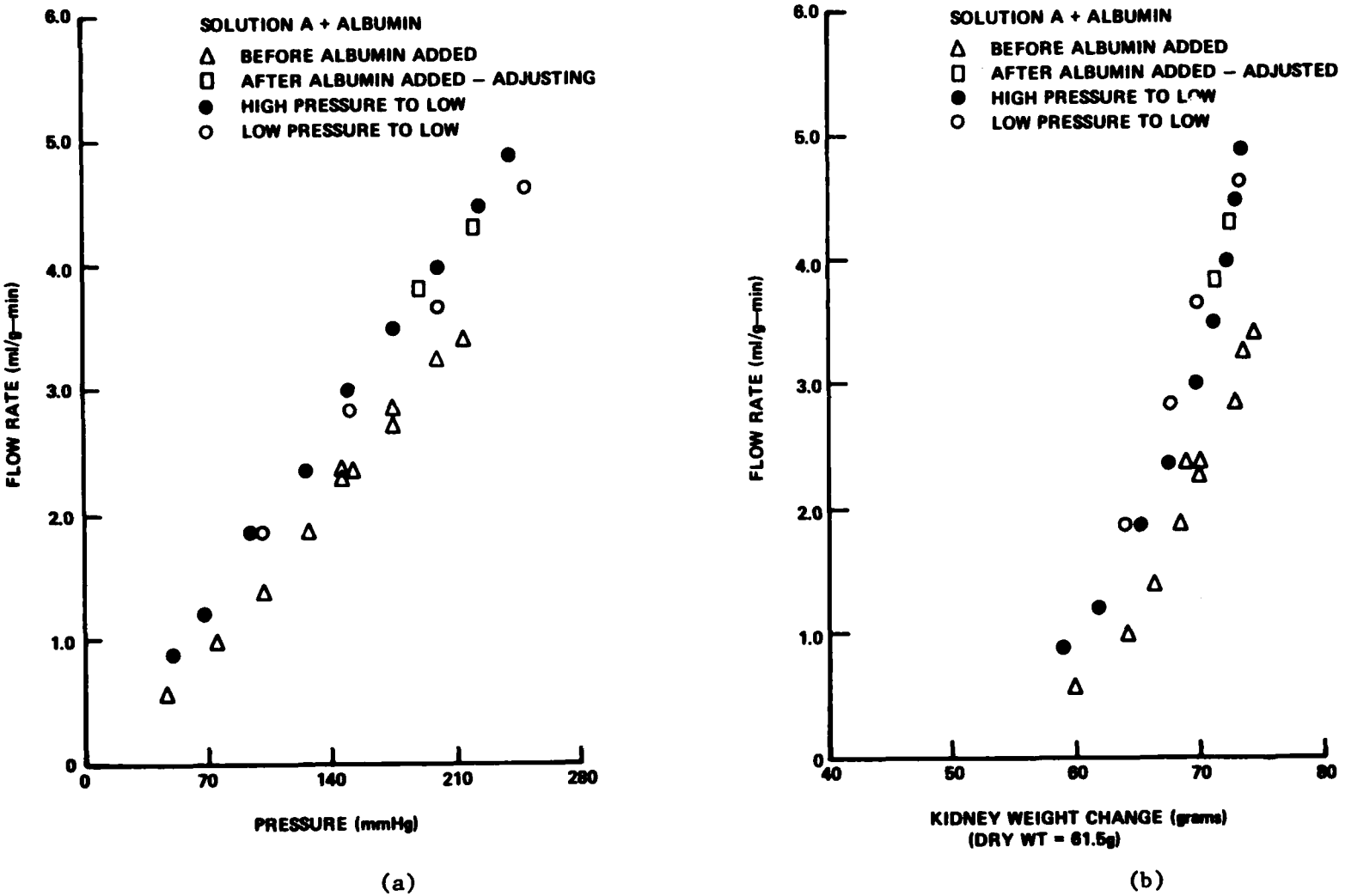

Figure 27. Flow rate versus (a) perfusion pressure and (b) kidney weight for Kidney # 2KE when perfused with Solution A before and after albumin added. Compare with Figure 5 and 6. Note changes before and after albumin added. Note the much improved control of kidney weight in (b) as compared to Figure 6 (b).

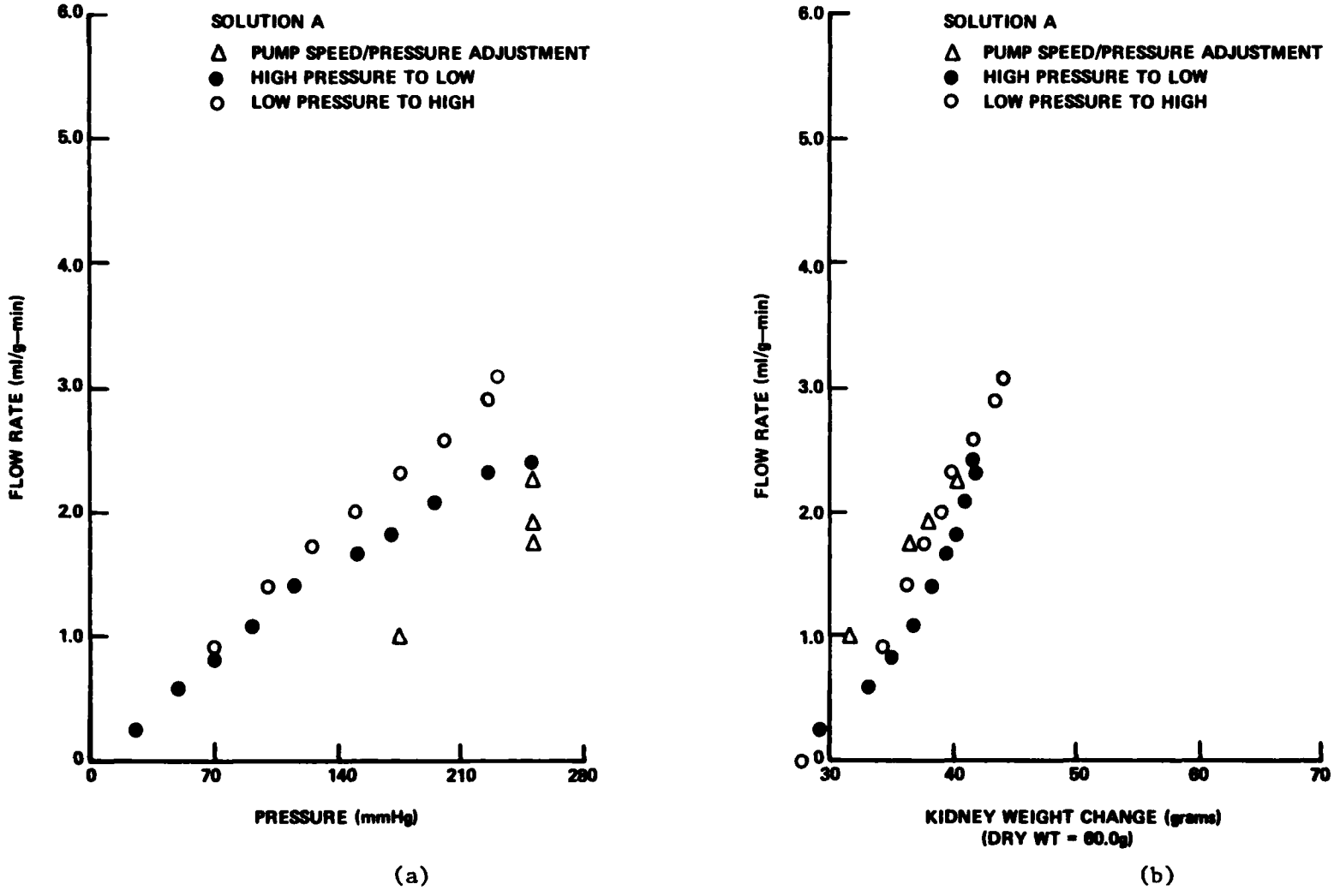

Figure 28. Flow rate versus (a) perfusion pressure and (b) kidney weight for Kidney # 3KE when perfused with Solution A.

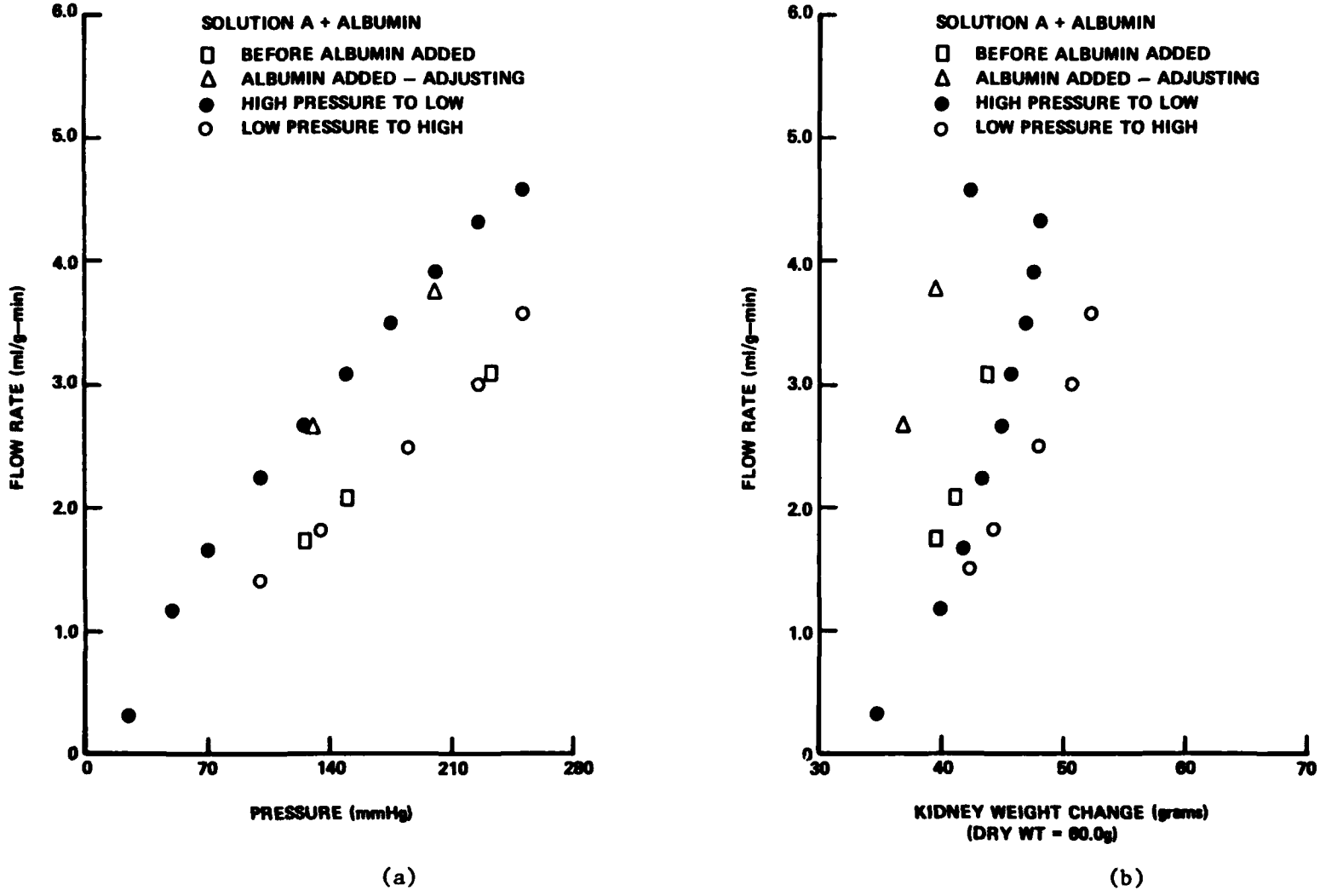

Figure 29. Flow rate versus (a) perfusion pressure and (b) kidney weight for Kidney # 3KE when perfused with Solution A plus albumin.

a hysteresis effect illustrating that prolonged high perfusion pressures (solid circles) induce an accumulating increase in weight which is greater than at similar flow rates in going from low to high perfusion pressures (open circles).

Addition of albumin to Solution A for the same kidney (#3KE) markedly increased flow, but only minimal flow autoregulation was observed as indicated by a decreased slope in the flow/pressure curve at high pressures (Figure 29(a)). It should be remembered, however, that the albumin added was only a small amount (1.7 g/100 ml which is approximately equivalent to plasma colloid oncotic pressure of 4.5 mmHg) and that the albumin was added after more than 75 minutes of perfusion without albumin. This small amount of albumin also evidently did not produce enough oncotic pressure to prevent edema from accumulating with high perfusion pressures and with prolonged duration of perfusion as can be seen from the increases of weight change vs. flow curve for kidney #3KE (Figure 29(b)). Total perfusion time was greater than 3 hours.

Kidney #4KE was from the right side of the same dog as kidney #3KE. It was perfused with Ringer's Lactate solution that was modified to resemble the Krebs-Henseleit bicarbonate solution used by Baker, et al. [22] in their perfusion of the isolated rat kidney. The solution contained no albumin and was reported by Baker, et al. to have resulted in autoregulation when used as a perfusate. Our results when perfusing this dog kidney showed minimal, if any, evidence of autoregulation with this perfusate (Figure 30(a)), but did show evidence of edema formation with high perfusion pressures (Figure 30(b)) as well as the resulting increased interstitial pressure and externally induced vascular resistance accompanying this edema. There was a very small sigmoidal-type dip in the flow-pressure curve at 100-125 mmHg perfusion pressure, but these results did not quantitatively agree with those obtained by Baker, et al. [22].

As a result of our review of the literature and our experiments to evaluate various perfusates, we have been able to define certain aspects of isolated kidney perfusion which can be improved in order to provide a better model of autoregulation. One aspect is the interval of time between ligation of the renal artery and perfusion of the kidney. Waugh was one of the first authors to recognize that interruption of perfusion for 4-10 minutes markedly depressed autoregulation [16], but anoxic perfusion for

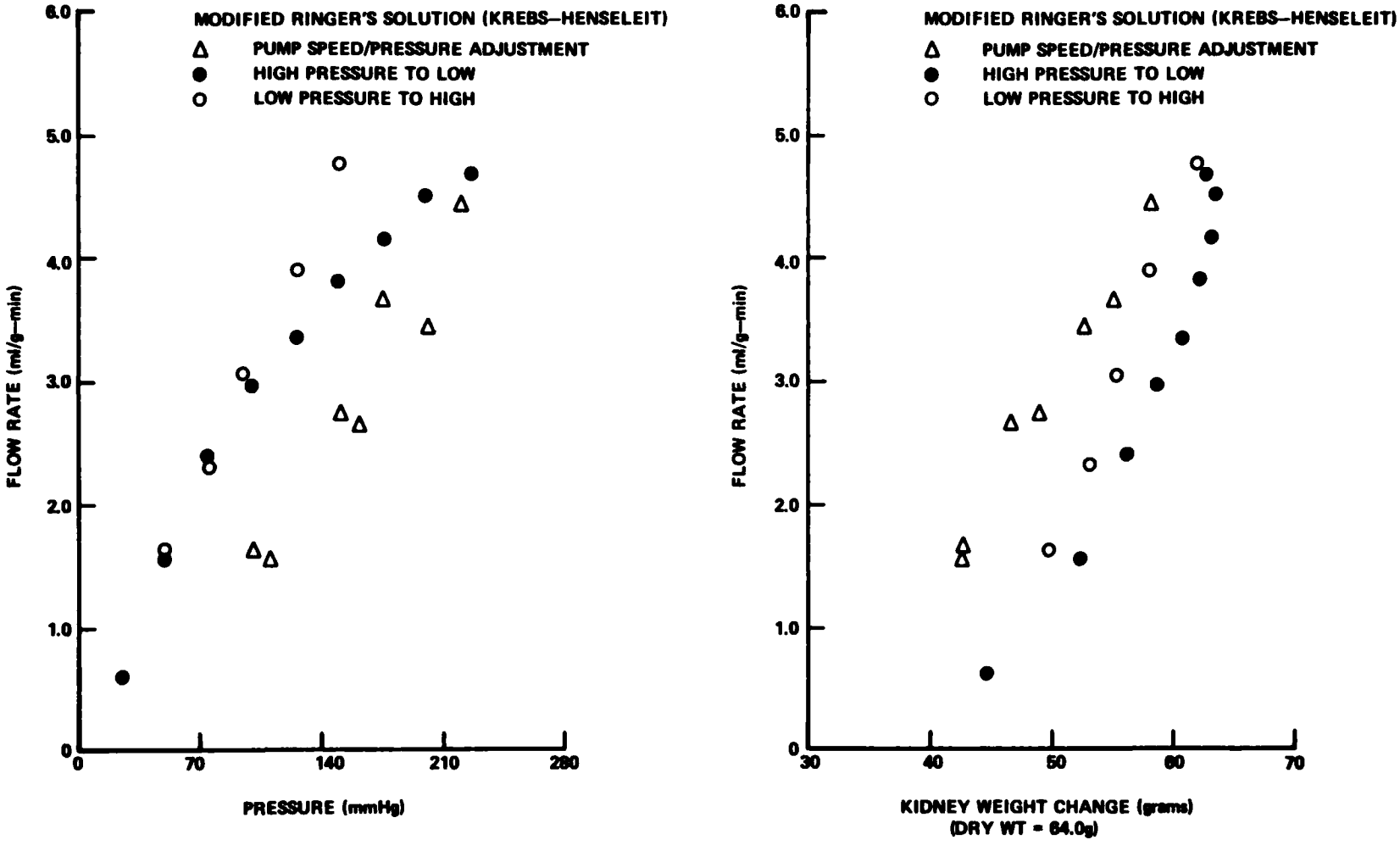

Figure 30. Flow rate versus (a) perfusion pressure and (b) kidney weight for Kidney # 4KE perfused with modified Ringer's lactate solution (Krebs-Henseleit solution).

less than 20 minutes did not. By modification and improvement of our surgical and cannulation techniques we shortened this time span of interrupted perfusion to 4 minutes.

Another parameter which we altered was the duration of perfusion. Previously, we have been allowing up to 6 or more hours of perfusion during which we would perform measurements; however, even the best reported results of kidney perfusion could only maintain kidney function within normal range for no more than 4-1/2 hours [18], and a slow deterioration with time was still present. Therefore, we modified our experimental procedure so as to limit our perfusion time to approximately 2 hours as recommended by Ross [20]. One modification was shortening the time for the kidney to "settle down" to no more than 10-15 minutes as have most other investigators. Another necessary change was to limit the time spent at any selected perfusion pressure to 2-3 minutes and no more than 5 minutes. However, even with such alterations, relatively low GFR's characteristic of isolated kidneys existed and there was a steady decline of at least 10% of renal function per hour of perfusion [20].

Another major problem we have identified during our perfusion studies is that of edema. Edema is the result of intravascular pressure being greater than interstitial fluid pressure causing fluid to leak into the interstitium. Thus, at high pressures of perfusion, edema will accumulate resulting in increased interstitial fluid pressure which will compress the vasculature and produce an externally induced resistance on the vasculature. This effect has been noted previously by Waugh [16] and others and has been described as a "fictitious and passive type of flow autoregulation...caused by the effects of abnormally high tissue pressures" [18] resulting in a curvilinear flattening of the flow rate at high perfusion pressures. This type of flattening was observed in many of the kidneys we studied, and this was accompanied by increases in weight as perfusion duration increased at these pressures. The only opposing force to this accumulating edema is the colloid oncotic pressure which, in effect, "draws" the fluid from the interstitium into the vascular space.

To combat this problem of edema, in the radioactive tracer studies conducted during this reporting period, we permitted "settling down" of the kidney to occur at a near physiologic perfusion pressure approximately halfway between the high and low pressure limits studied. From this point,

we decreased resistance (increased perfusion pressure) or increased resistance (decreased perfusion pressure) from a central point to generate the flow-pressure curve, thus limiting the amount of time spent at abnormally high or abnormally low perfusion pressures. We also added Bovine Serum Albumin, Fraction V to our perfusate, so as to increase plasma oncotic pressure to near-physiologic values (16-22 mmHg which would correspond to 50-60 g albumin/l).

There are other possible advantages to adding albumin to the perfusate. Waugh in 1960 [17] and 1964 [18] reported that he was able to prevent the usual rapid deterioration of autoregulation in his isolated kidneys by the addition of 5 volume percent dog plasma to his perfusates and he attributed these results to the presence of plasma proteins and substrates in the dog plasma. Bullivant in 1977 [21] found that isolated rat kidneys showed no evidence of autoregulation unless 5 volume percent human serum or 3g Bovine Serum Albumin/l were added to the perfusates. Ross in 1978 [20] advocated the use of 75-80g of Bovine Serume Albumin, Fraction V per liter of perfusate in isolated kidneys, while Schurek (1980) [19] stated that the use of Bovine Serum Albumin or a suitable oncotic substitute was now a standard technique. While Baker (1981) [22] disputed the dependence of autoregulation on the presence of albumin and related autoregulation more to the presence of ionized calcium, there can be no disputing of the fact that albumin in physiologic concentrations producing a physiologic oncotic pressure should prevent edema and preserve kidney function. One must be careful with the use of albumin, however, since autoregulation does vary with increases of plasma oncotic pressure and with increases to 28-30 mmHg will approach a passive type of system dependent only on tissue interstitial pressure. Also, as pointed out by Baker, albumin will bind calcium, so more calcium must be added to the perfusate to balance the amount bound by the albumin and keep the level of ionized calcium approximately normal.

Finally, we changed the perfusate used from Solution A to a solution resembling Krebs-Henseleit solution, which more closely approximates the physiologic ionic composition of plasma. This type of solution has been advocated by most authors in the field of isolated kidney perfusion (see Table 1) and seems to give the best results. We have simulated this solution by using Ringer's lactate solution and adding certain constituents so as to most closely approximate the best aspects of each of the suggested solutions in Table 1. The major difference between Solution A and the other solutions

is in the concentration of potassium, and we have already shown that a solution high in potassium concentration is not useful in studying autoregulation. The lactate in the final solution we used should cause no problem since Waugh in 1969 [23] showed that the addition of lactate or pyruvate as a metabolic substrate in addition to glucose helps to prolong normal renal function. The new solution was used in all radioactive tracer experiments conducted during this quarter. The significant improvement in autoregulation by the isolated perfused dog kidney when using this perfusate solution is evident.

After determining the best perfusate for use in the renal investigations, flow/pressure studies were performed on six more isolated canine kidneys using our modified Krebs-Henseleit solution with albumin in order to improve our technique and to better characterize the flow/pressure relationship of kidneys using the modified techniques. It was during these studies, in conjunction with the Radioactive Tracer Studies, that we developed a new protocol to monitor the baseline deterioration of our kidneys in order to provide a more accurate interpretation and normalization of our data. The data from the last 6 kidneys in the kidney model study are not included here since data resulting from those experiments very closely approximates that obtained in the Radioactive Tracer Study results which are summarized in the next sub-section (Figures 33, 36-38, 40, 42, 44). The new protocol and normalization analysis are also presented in the next sub-section.

C. Radioactive Tracer Studies

Because of differences between the measured dielectric property changes in kidney medulla and cortex and reported differences in the autoregulatory activity of these two regions [25,26], Anger gamma camera flow studies were conducted. In these studies, Technetium Tc 99m was the radioactive tracer used and the renal flow studies were conducted as described above in Experimental Methods. Separate 4mCi injections of Tc 99m were used for each perfusion condition. Total renal radioactivity and regional activity as a function of time were measured using the gamma camera with subsequent digital image processing. Dr. Rauf Sarper, a physicist in the Nuclear Medicine Research Laboratory at Emory University, served as a consultant and made available the necessary equipment and supplies for these studies.

Time/activity curves for each of six renal pressure-flow perfusion conditions are shown in Figure 31. These results represent total uptake

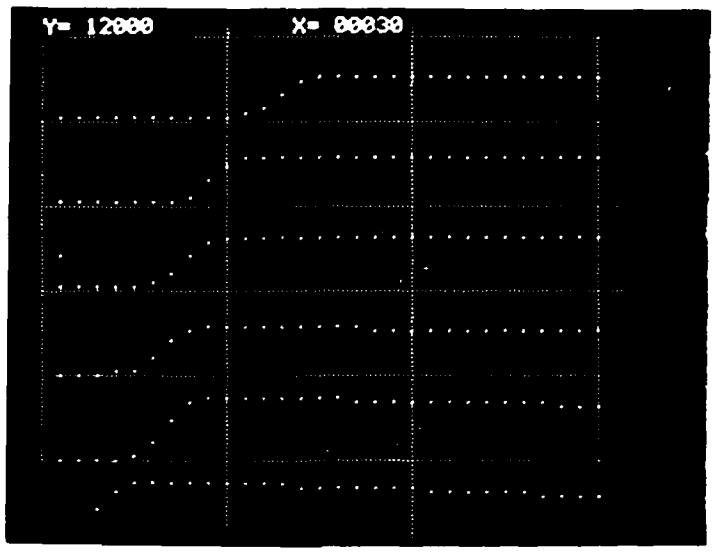

Figure 31. Technetium time/activity curves for six renal pressure-flow perfusion conditions. Pressure/flow rates increasing from uppermost to lowermost curve.

of free ^{Tc} 99m by a single kidney as a function of time following injection. Results at the lowest perfusion pressure (and lowest flow rate) are shown by the uppermost curve in the figure and the greatest renal flow condition is displayed by the bottom curve.

For each perfusion condition, the total renal flow is proportional to the rate of uptake of free Technetium by the kidney. In Figure 31, this rate of uptake is simply the slope of each curve during the period Technetium is entering the kidney through the arterial circulation until a steady-state condition between arterial and venous flow of the free Technitium is reached. Figure 32(a) shows the digital image of an isolated perfused kidney at the time of maximum uptake of free Technetium. Maximum radioactivity is indicated by the brightest area, which for this case, was the entire kidney. The dim, circular region of radioactivity represents the background radiation. In Figure 32(b), the activity of the cortex and medulla are outlined separately. The image was formed from activity data recorded during initial uptake of free Technetium at one flow condition.

The digital data processing algorithms available made it possible to analyze renal flow not only for the entire kidney, but for various selected regions of the kidney as well. For each selected region, separate time/activity curves were generated and the slope of free Technetium uptake computed. The slopes, representing the renal perfusion for the studied region of the kidney, were normalized to the greatest flow rate, and relative flow rates were computed using a hand-held calculator. In the study reported herein, cortical and medullary regional divisions were studied. In future efforts, we plan to measure the activity in very small regions which correspond to the position of each of the five dielectric measurement probes. In this manner, the renal flow data and dielectric property data can be correlated to each probe position in the renal anatomy. Two data sets for one of the renal flow studies using the Anger gamma camera are shown in Figure 33. Figure 33(a) is the pressure-flow curve for two data sets measured in a single kidney. In this case, flow was measured by an in-line flowmeter and pressure was the independent variable controlled by resistance changes. Figure 33(b) shows total kidney weight measured at each total renal flow rate. In Figure 34, the relative normalized renal flow determined from free Technitium time/activity curves is shown as a function of pressure for cortex, medulla, and total kidney. Figure 34(a) shows the computed

(a) Renal perfusion with free Technetium tracer under steady-state conditions (maximal uptake of T_c 99m for preset perfusion conditions).

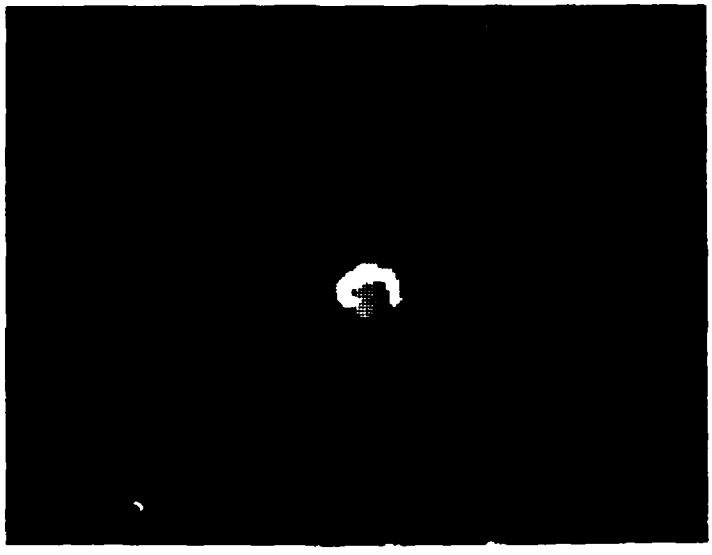

(b) Activity of cortex and medulla outlined separately during initial uptake of T_c 99m at preset flow condition.

Figure 32. Digital images of isolated perfusion kidney using free Technetium tracer.

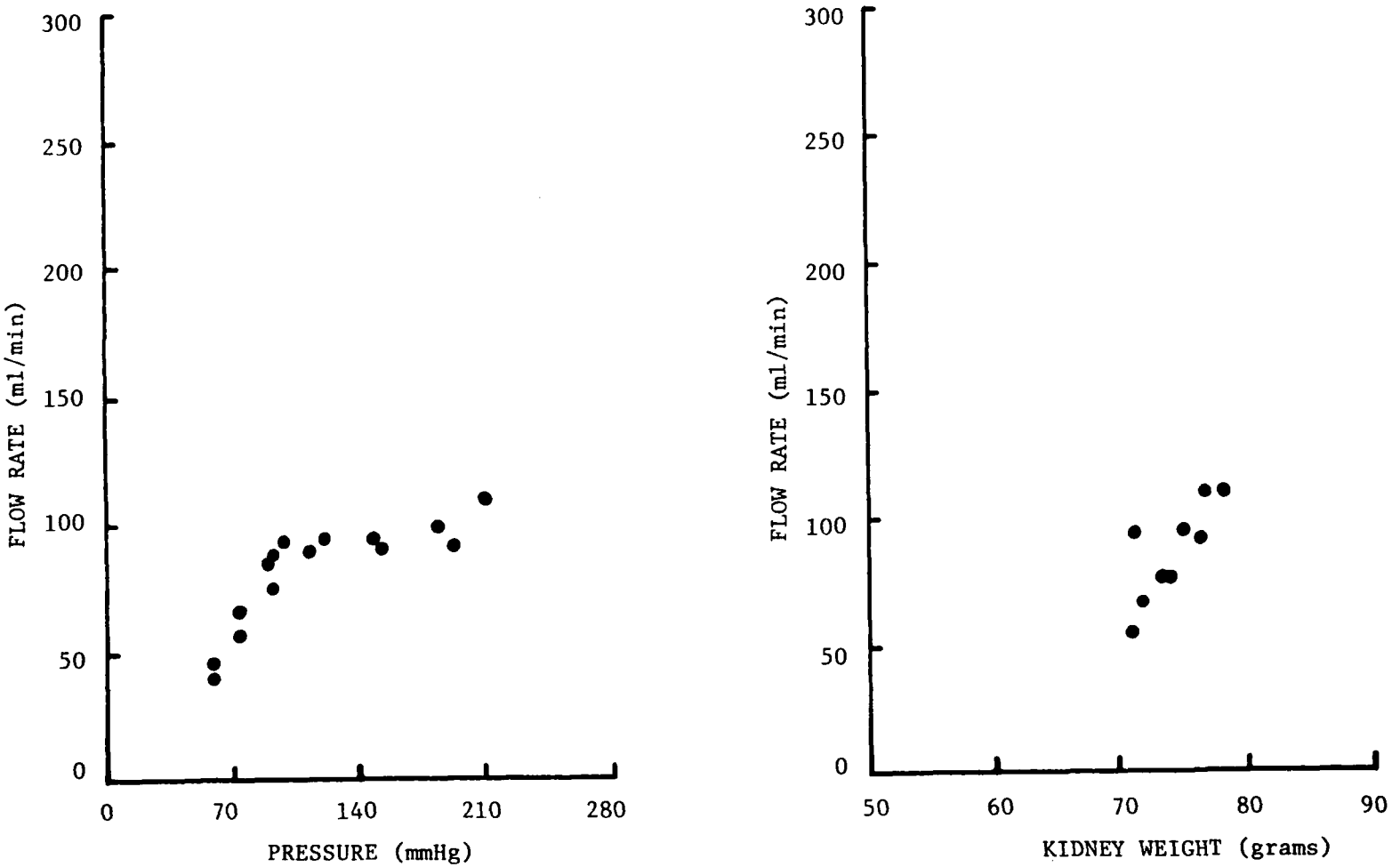

Figure 33. (a) Total renal flow rate measured as a function of perfusion pressure from in-line flowmeter measurements. (b) Relationship between kidney weight and flow rate for the kidney in (a).

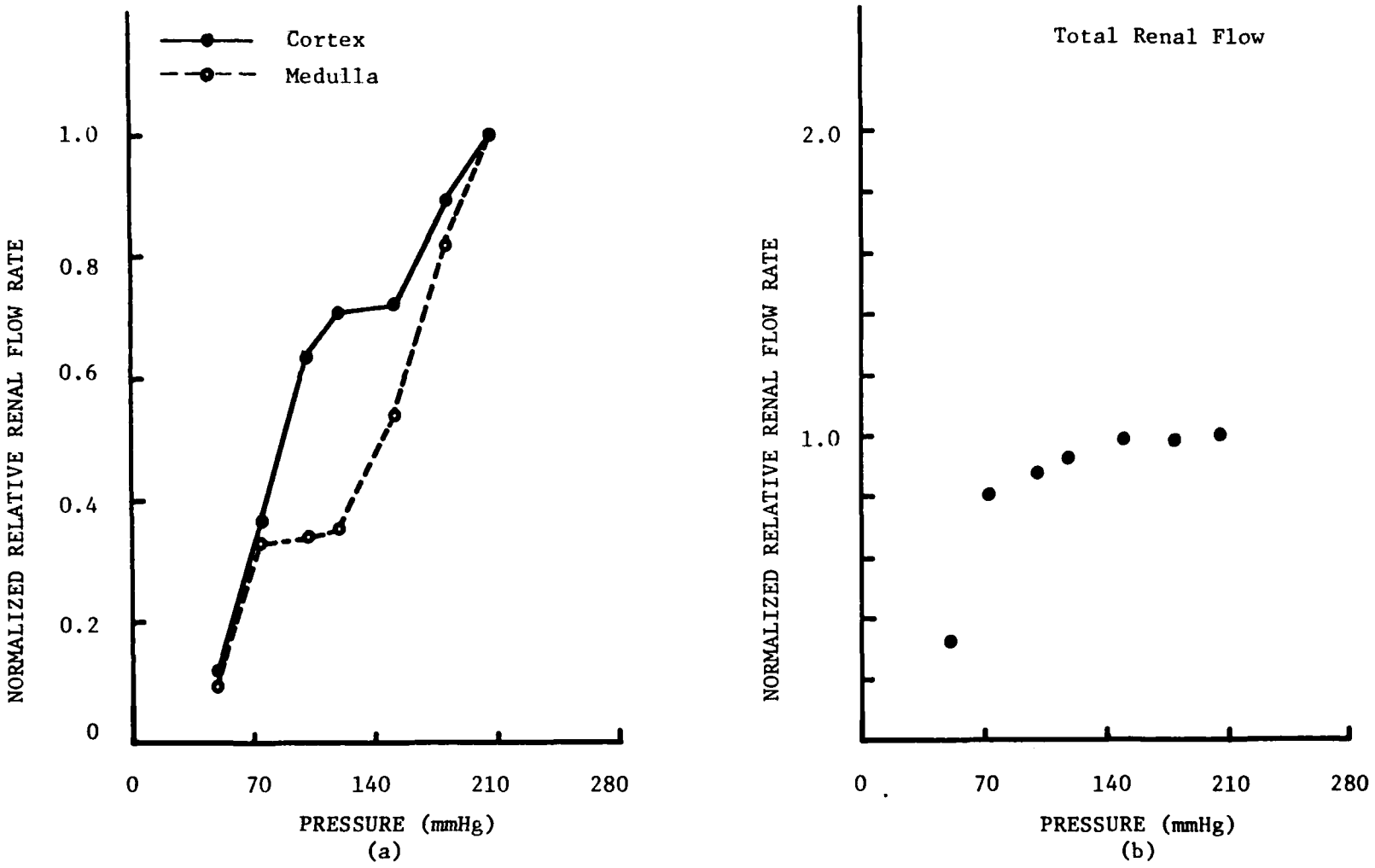

Figure 34. Normalized relative renal flow results from radioactive tracer study. (a) Pressure-flow curves determined separately for cortex and medulla. (b) Normalized total renal flow as a function of perfusion pressure for the same kidney determined from whole kidney Technetium time/activity curves (Figure 31).

normalized relative flow as a function of perfusion pressure for the cortex and medulla. Note that both regions exhibit autoregulatory activity; however, the pressure-flow relationships at which autoregulation occurs are markedly different for the two regions. This is of interest because of the controversy existing in the literature concerning the level of autoregulatory activity in the medulla versus cortex. Thurau [25] reported no medullary autoregulation in the dog kidney, whereas Aukland [26] has reported that medullary autoregulation in the dog kidney exists, but not to the same degree as in cortical tissue. Gulskov and Niseen [27] have reported that, in the cat, medullary autoregulation is equal to autoregulation in the cortex. Different measurement techniques were used in each of the above studies. Use of the needle dielectric measurement probe and/or radioactive tracer regional flow studies may be better methods for resolution of the above discrepancy concerning cortical and medullary renal autoregulation. Figure 34(b) displays total normalized renal flow as a function of pressure determined from the whole kidney free Technetium time/activity curves. Comparing Figure 34(b) to Figure 33(a) reveals excellent correlation between the curve shapes as determined from in-line flowmeter measurements and Technetium renal uptake computations.

During these renal experiments, we have noted that various renal parameters vary with duration of perfusion. As noted previously in this report, B. D. Ross [20] stated that, no matter how successful the surgical removal in isolated kidney experiments, one could still expect a steady decline of 10% per hour of perfusion time. As a result of our experiments, we have concluded this steady decline in renal function withtime following surgical removal is present, but is complicated by variations in perfusion pressure and by presence or absence of edema, which also show individual variations with time. As a result of these findings, we altered our experimental protocol somewhat in an attempt to better account for these variations.

During an experiment, an initial pressure of either 100 or 150 mm Hg was established as the baseline perfusion pressure and various kidney functions were monitored intermittently at this baseline pressure throughout the duration of the experiment. These functions were then charted as a function of experiment duration in order to better characterize a kidney's time-dependent changes. In Figure 35, the solid lines connect the baseline points for flow and weight at 100 mmHg, while the dotted lines connect the other measured points. These plots of the time course of the kidney function can then

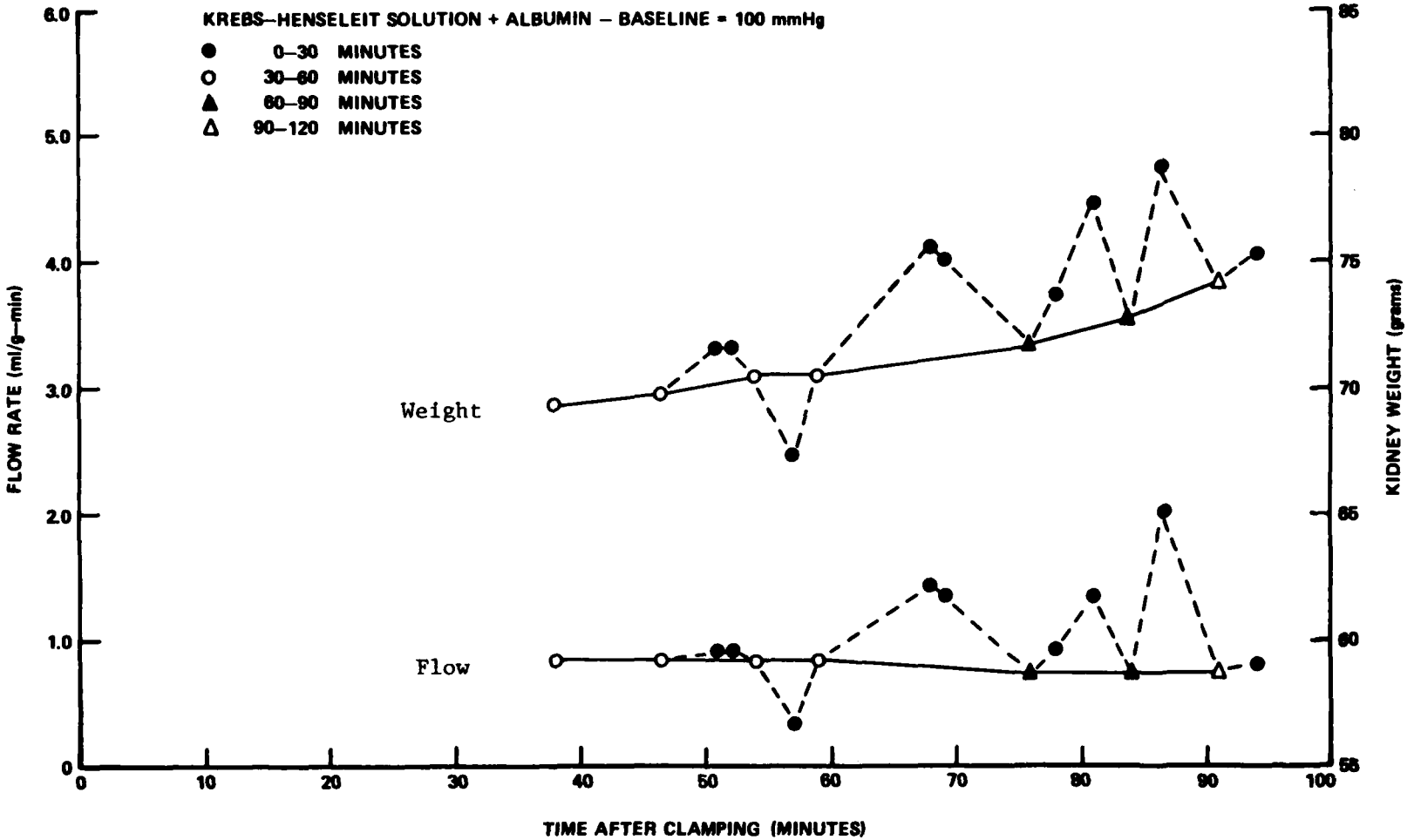

Figure 35. Flow rate and kidney weight as functions of time course of the experiment for Kidney # 3GT (Radioactive Tracer Study). The upper curve represents kidney weight and the lower curve represents flow rate. The solid lines connect the flow rate and kidney weight measurements made at the baseline pressure of 100 mm Hg, while the dashed lines connect measurement values at other pressures.

illustrate the deterioration of renal function with time. For example, in Figure 35 the baseline flow at 100 mmHg drops 10% over the course of 100 minutes while the weight increases 7% as a result of accumulating edema. One can also see how the rate of accumulating edma (illustrated by the rate of increase of the baseline weight) increases as the controlled perfusion pressure being measured increases.

Once the time course of the baseline variation has been charted, the baseline data can then be used to normalize the rest of the collected data so that the values of renal function are expressed as percentages of the baseline value. Since the baseline values are varying with time, the measured values are actually calculated as a time-weighted percentage of the average of the baseline values before and after the measurement. Renal flow data were normalized in terms of percentage change in flow relative to the time-weighted average baseline flow (where baseline flow is the flow at the preselected baseline pressure). The total percent flow relative to baseline flow is given by:

$$\text{PERCENT TOTAL FLOW (at baseline pressure)} = \frac{F_m\,(100)}{F_{B1} + \dfrac{t_m - t_1}{t_2 - t_1}\left(F_{B2} - F_{B1}\right)}, \qquad (1)$$

where

F_m is the measured flow at pressure of interest,
F_{B1} is the baseline flow at time t_1 prior to measurement time t_m,
F_{B2} is the baseline flow at time t_2 subsequent to measurement time t_m,
t_1 is the time at which F_{B1} is measured (prior to t_m),
t_2 is the time at which F_{B2} is measured (subsequent to t_m), and
t_m is the time at which F_m is measured.

Equation (1) assumes a linear time-weighted relationship between the baseline flow values at times t_1 and t_2. Based on our experience and reports in the literature [15,16,18], this assumption is not unreasonable. Use of this relation results in a significantly more meaningful display of renal pressure-flow data because first-order time-dependent variations are normalized. Thus, the mean renal pressure-flow relationship for the overall period studied can be displayed by a single graph. This same procedure was used to develop

a relation for normalizing kidney weight (changes) with respect to time averaged baseline values. Kidney weight gain and loss data plotted following normalization are much more consistent with respect to expected changes with increasing or decreasing flow.

Figure 36 is a plot of the actual measured values for one kidney used in a radioactive tracer study. In this case (Figure 36), no accounting was made for the time dependency of the baseline flow rates. Although it is evident that some type of flow regulation with pressure was occurring, the exact nature of that relationship is not clear. When the normalization procedure outlined above (Equation 1) was used to account for the time-dependent baseline flow, the pressure-flow relation clearly exhibited a normal renal autoregulatory curve. This result is shown in Figure 37. Also shown in Figure 37 is the relative normalized total renal flow determined from free Technetium time/activity curves. Note that agreement between total renal flow as a function of perfusion pressure obtained using the in-line flowmeter and using free Technetium radioactive tracer was excellent. Figure 38 shows the computed normalized relative flow as a function of perfusion pressure for the cortex and medulla of the same kidney. Note that both regions exhibit autoregulatory activity; however, as reported previously [28], the pressure-flow relationship for the two regions is different. The reasons for particular interest in this result were discussed in our last quarterly technical report [28]. The results of radioactive tracer studies performed in two additional kidneys are presented in Figures 39 and 40. Again, excellent agreement in total renal flow rate is obtained for the two methods used (free Technetium tracer and in-line flow meter). Unfortunately, in both of these studies (Figures 39 and 40) free Technetium time/activity curves were obtained at only three perfusion pressures due to technical difficulties with the gamma camera. Results from two additional experiments are presented in Figures 41 through 44. In these experiments, excellent agreement between renal flow measurement methods was observed over perfusion pressures ranging from 50 mmHg to 250 mmHg.

D. Combined Radioactive Tracer/Dielectric Property Studies

As part of an effort to draw together all of the techniques developed and results obtained from this year's efforts, we performed experiments on two separate isolated canine kidneys in which dielectric measurements

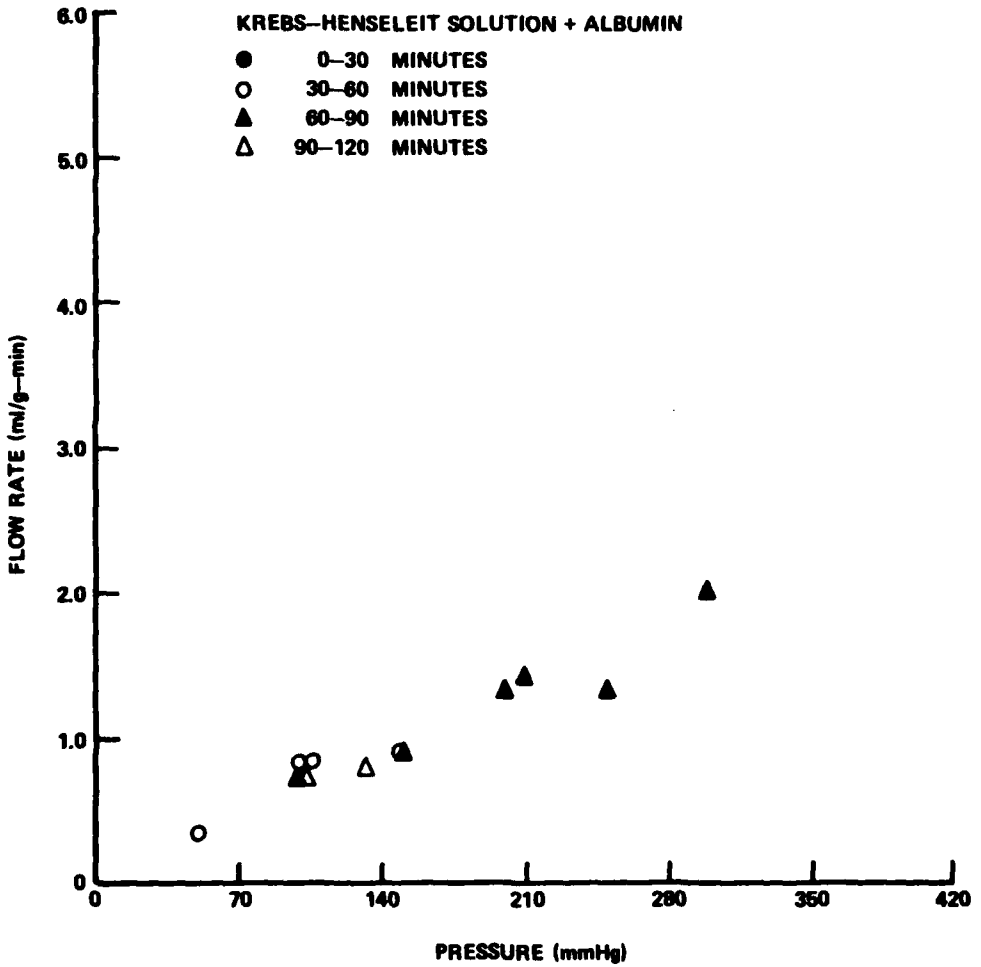

Figure 36. Flow rate plotted as a function of perfusion pressure for Kidney # 3GT (Radioactive Tracer Study) which is the same kidney as for Figure 35. These are the plotted actual measured points.

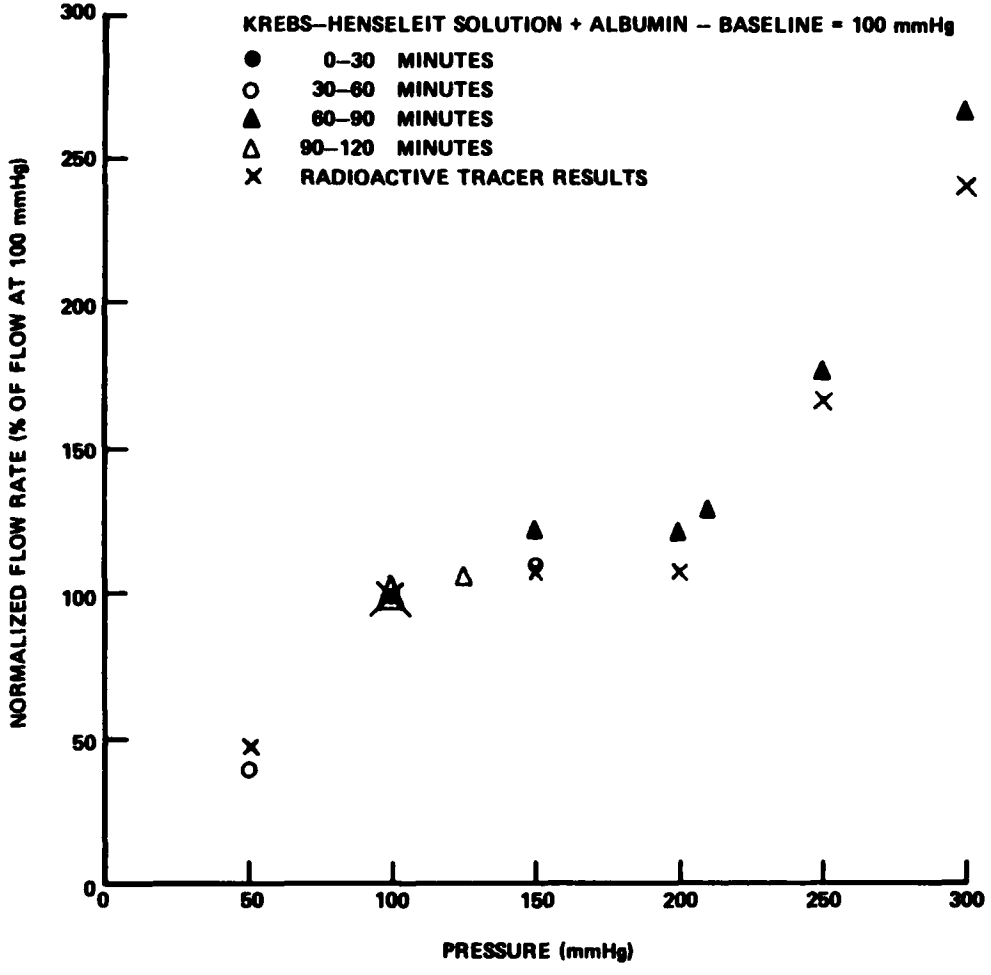

Figure 37. Normalized flow rate as a function of perfusion pressure for Kidney # 3GT (Radioactive Tracer Study) using equation (1) to normalize the points plotted in Figure 36. Also plotted are the normalized tracer study flow rate measurements for comparison.

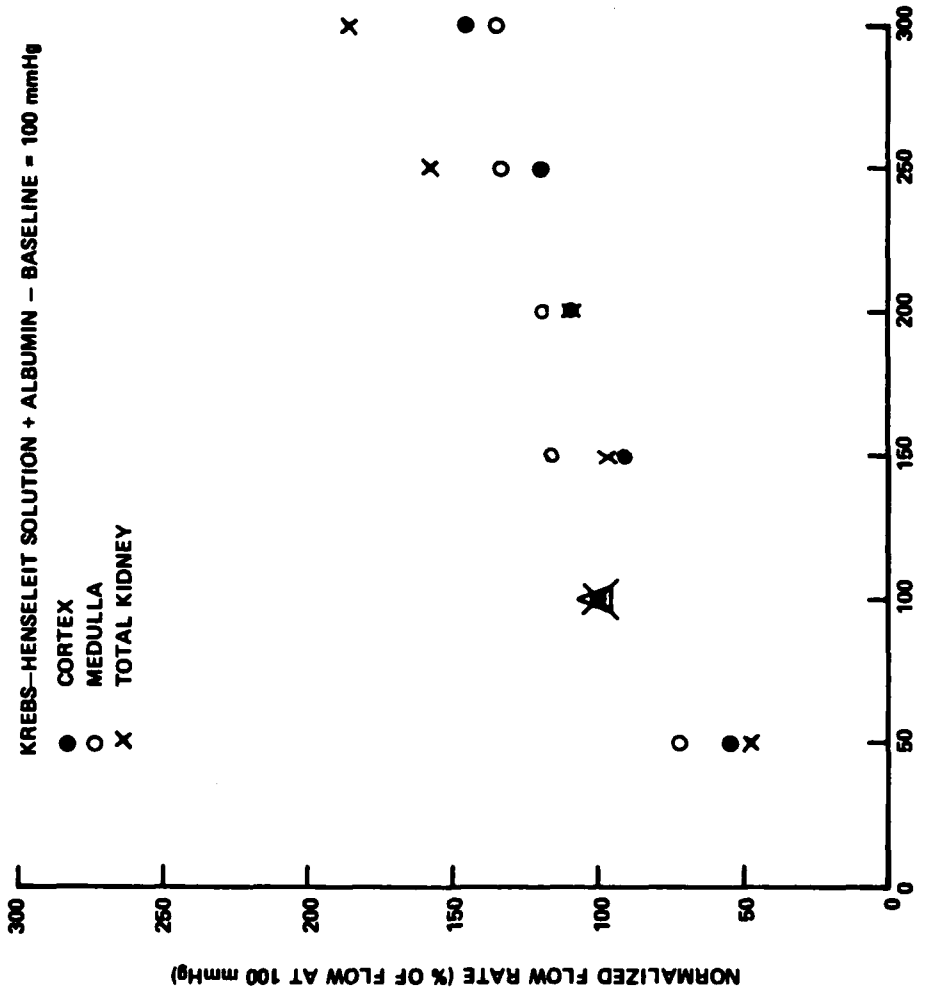

Figure 38. Radioactive Tracer Study results showing the computed normalized relative flow rate as a function of perfusion pressure for cortex, medulla and total kidney for Kidney # 3GT (Figures 35-37).

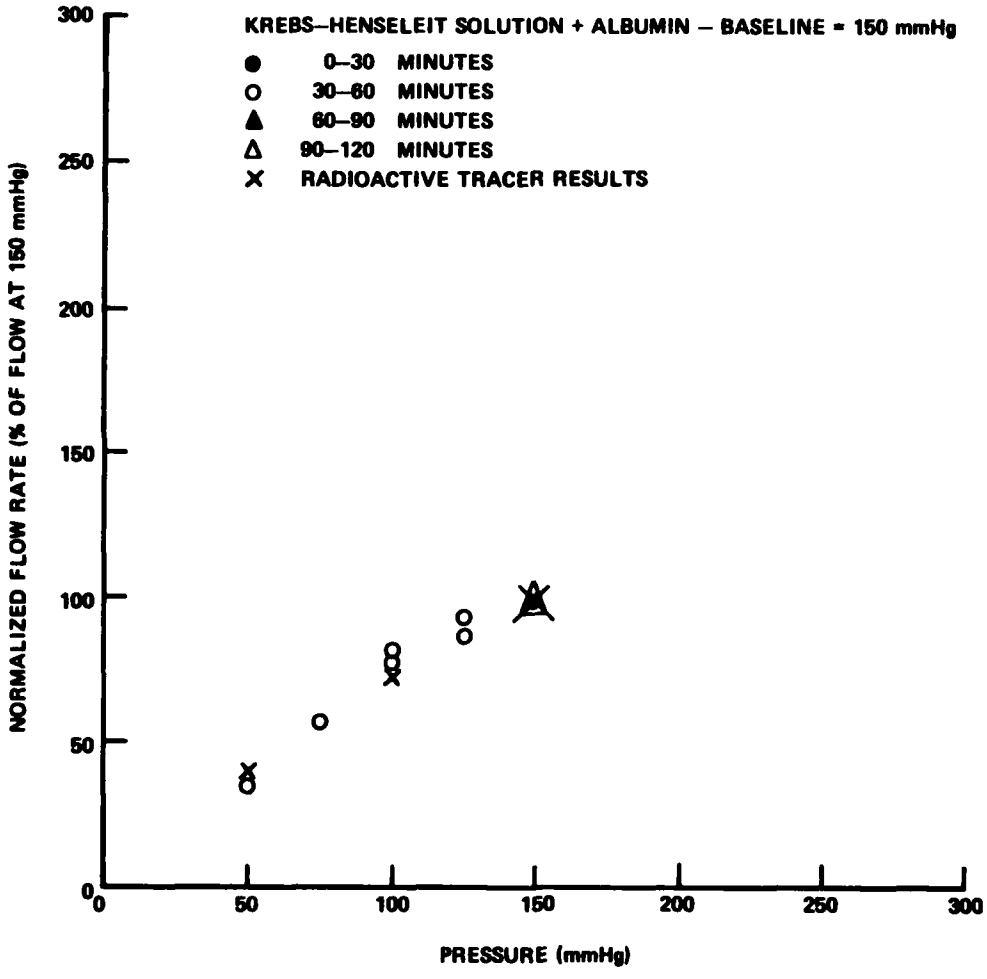

Figure 39. Normalized measured flow rate and normalized Radioactive Tracer flow rate as functions of perfusion pressure for Kidney # 4GT (Radioactive Tracer Study).

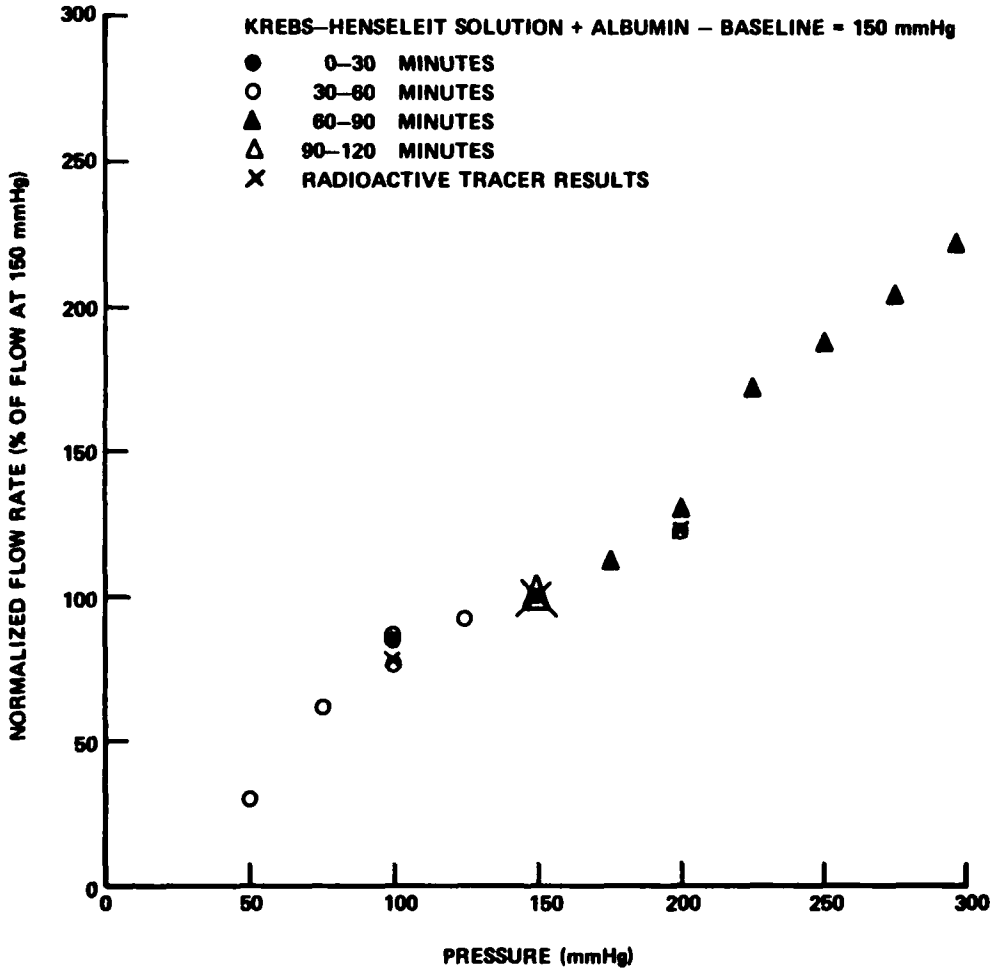

Figure 40. Normalized measured flow rate and normalized Radioactive Tracer flow rate as functions of perfusion pressure for Kidney # 5GT (Radioactive Tracer Study).

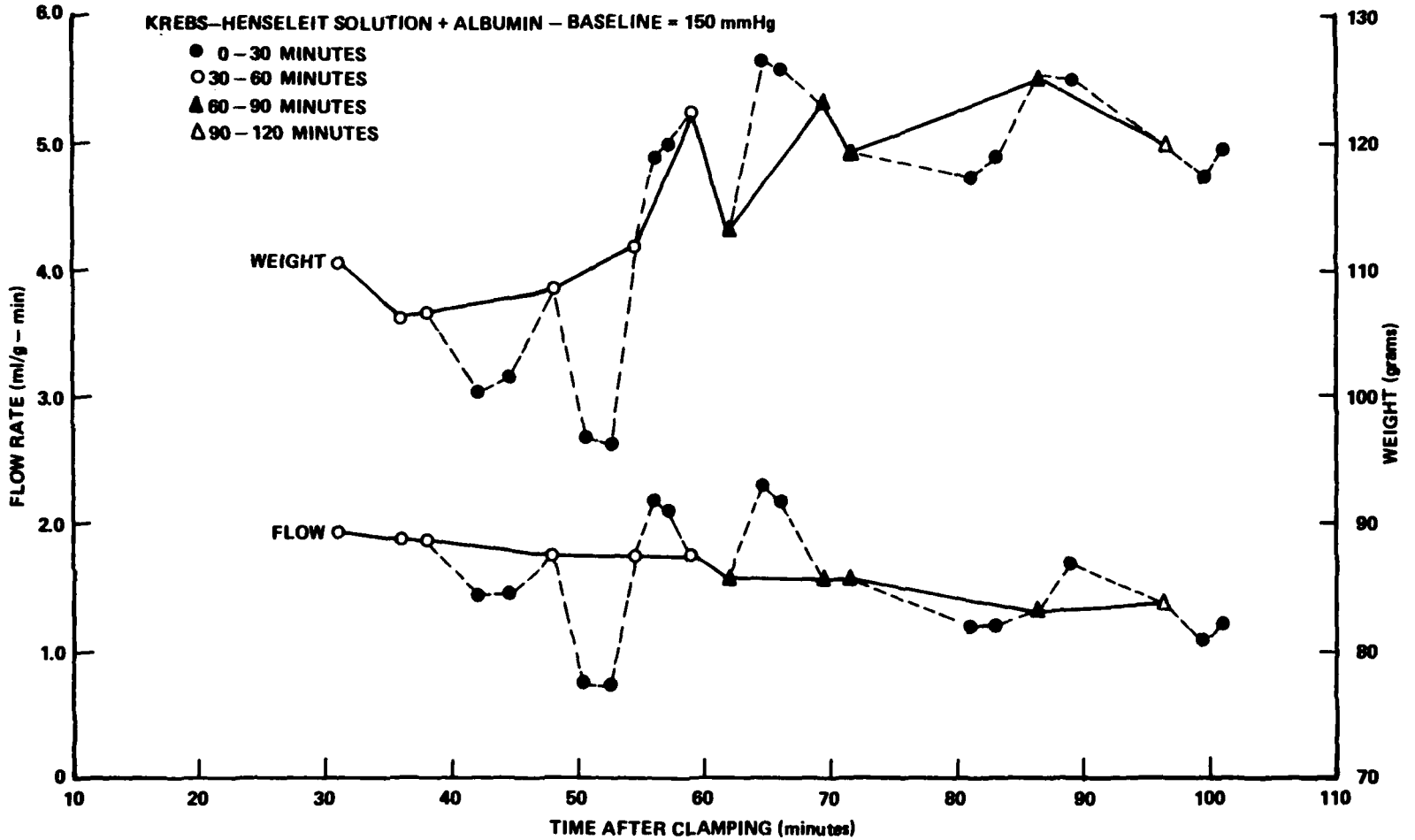

Figure 41. Flow rate and kidney weight as functions of time course of the experiment for Kidney # 6GT (Radioactive Tracer Study). The upper curve represents kidney weight and the lower curve represents flow rate. The solid lines connect the flow rate and kidney weight measurements made at the baseline pressure at 150 mm Hg, while the dashed lines connect measurement values at other pressures.

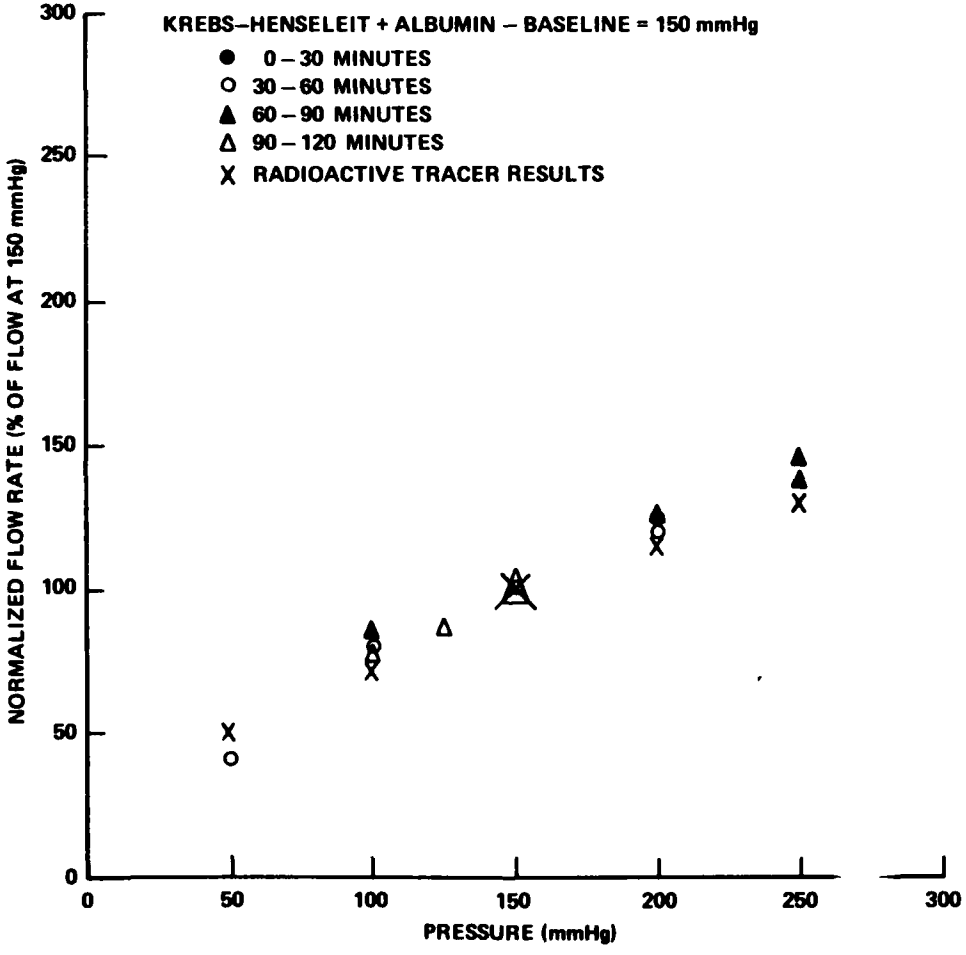

Figure 42. Normalized measured flow rate and normalized Radioactive Tracer flow rate as functions of perfusion pressure for Kidney # 6GT (Radioactive Tracer Study).

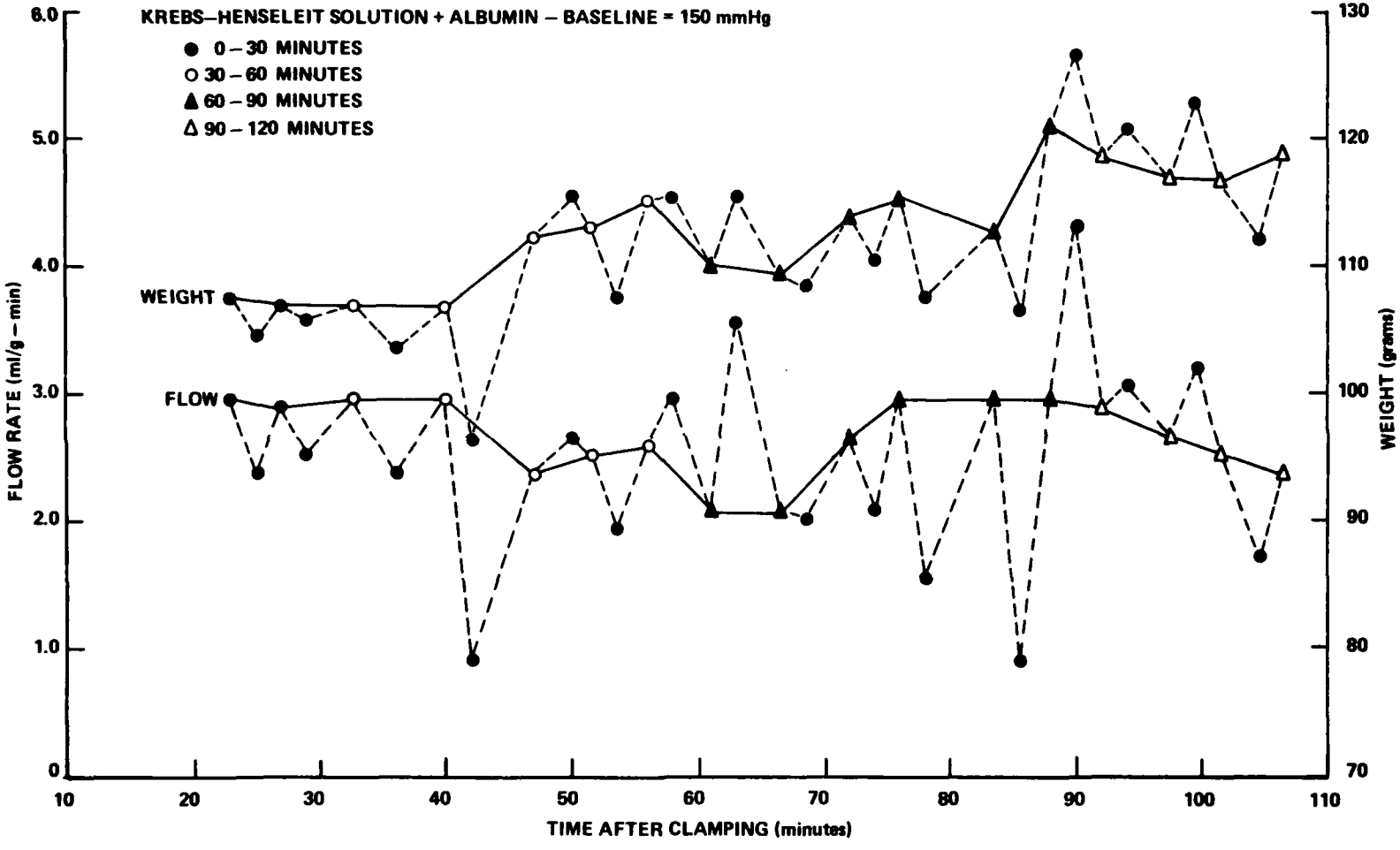

Figure 43. Flow rate and kidney weight as functions of time course of the experiment for Kidney #7GT (Radioactive Tracer Study). The upper curve represents kidney weight and the lower curve represents flow rate. The solid lines connect the flow rate and kidney weight measurements made at the baseline pressure of 150 mm Hg, while the dashed lines connect measurement values at other pressures.

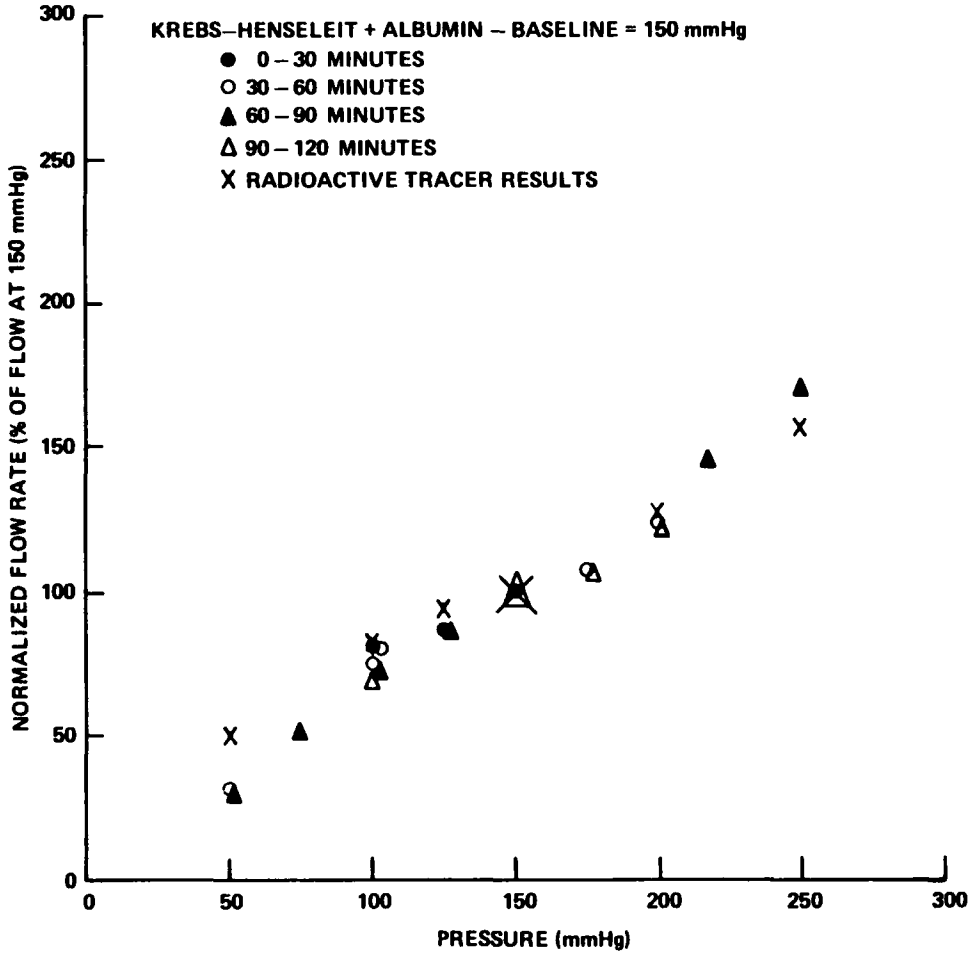

Figure 44. Normalized measured flow rate and normalized Radioactive Tracer flow rate as functions of perfusion pressure for Kidney #7GT (Radioactive Tracer Study).

AD-A154 107 PHYSIOLOGICAL INFLUENCES ON TISSUE ELECTRICAL PROPERTIES IN SITU(U) GEORGIA INST OF TECH ATLANTA E C BURDETTE ET AL. SEP 82 DAMD17-78-C-8044 2/2

UNCLASSIFIED F/G 6/16 NL

END

FILMED

DTIC

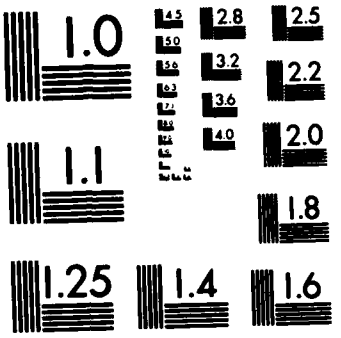

MICROCOPY RESOLUTION TEST CHART
NATIONAL BUREAU OF STANDARDS-1963-A

and radioactive tracer measurements were performed simultaneously. The objective of these experiments was to provide not only a comparison of each technique with the measured flow/pressure data for an functioning autoregulating kidney, but also to provide direct comparison of the dielectric property probe measurement results and the radioactive tracer flow rate and distribution results with each other. The results of these experiments are exhibited in Figures 41-47. Radioactive tracer results are compared to in-line flowmeter measurements in Figures 41 through 44. In Figures 45 and 46, changes in relative dielectric constant and conductivity are plotted as a function of pressure and flow, respectively. Note that the complex permittivity versus perfusion pressure results have the same sigmoidal relationship observed for flow/pressure in the normal autoregulating kidney. If indeed the changes in complex permittivity versus pressure (expressed as percentage changes from values at baseline pressure) are indicative of flow changes within the kidney, then the complex permittivity changes plotted as a function of flow rate should exhibit a linear or nearly linear relationship. This is evidenced by the results shown in Figure 46, where changes in relative dielectric constant and conductivity, expressed as a percentage change from baseline values, vary approximately linearly with flow. Total renal flow changes measured using free Tc 99m tracer are plotted versus changes in the same parameter measured by the in-line flowmeter in Figure 47(a). Note that excellent overall agreement exists, with some exception at very low and very high flow rates. At very low flow rates, this is thought to be due to in-line flowmeter inaccuracy which appears to increase at flow rates below 40-50 ml/min. At very high flow rates, the disagreement between the two methods is most likely due to "smearing" of the injected tracer bolus because of the high flow rate and the finite time required for injection of the tracer into the renal artery. Figures 47(b) and 47(c) are similar correlation plots for cortical flow changes measured by the tracer method with corresponding changes in relative dielectric constant (Figure 47(b)) and conductivity (Figure 47(c)). Good correlation between the independent measurement methods is observed, thus strongly supporting the measurement of complex permittivity changes as an indirect means of measuring regional flow.

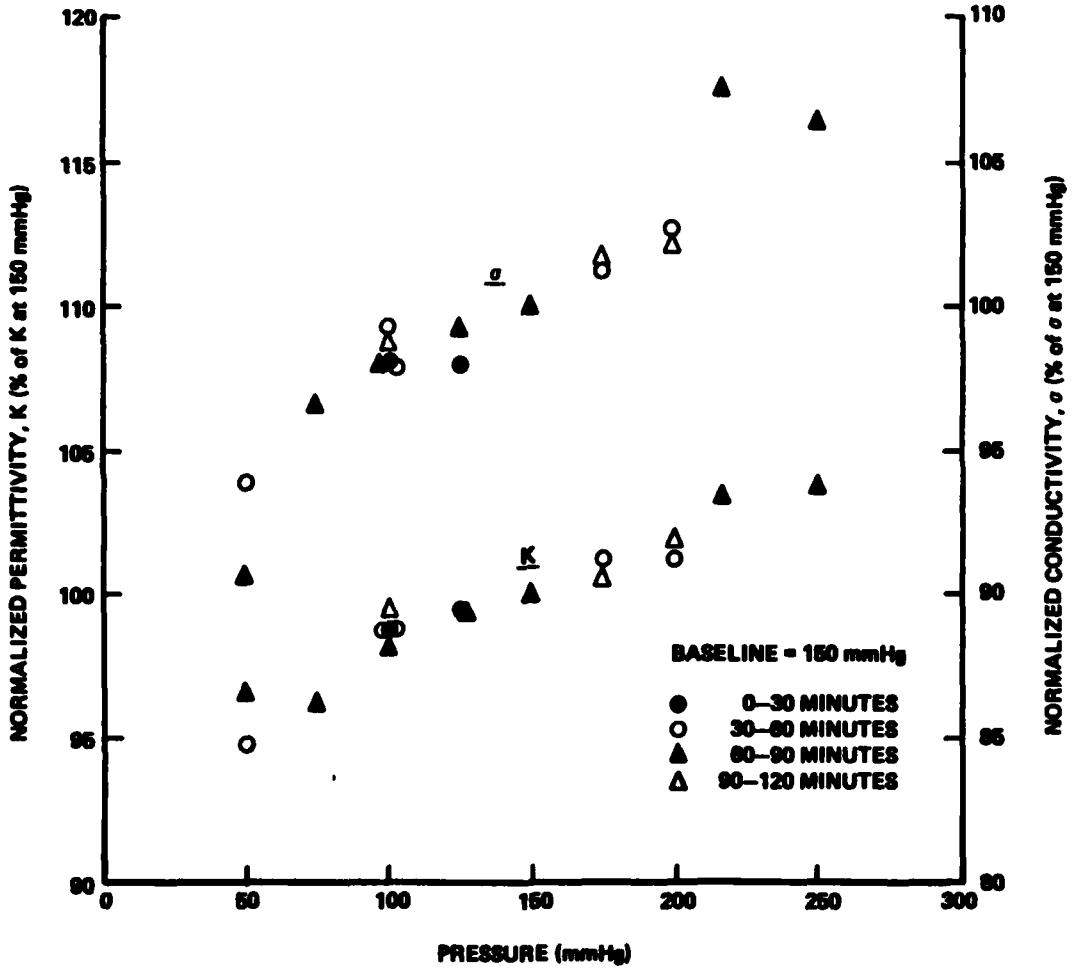

Figure 45. Normalized dielectric properties, K and σ, as functions of pressure for kidney #7GT.

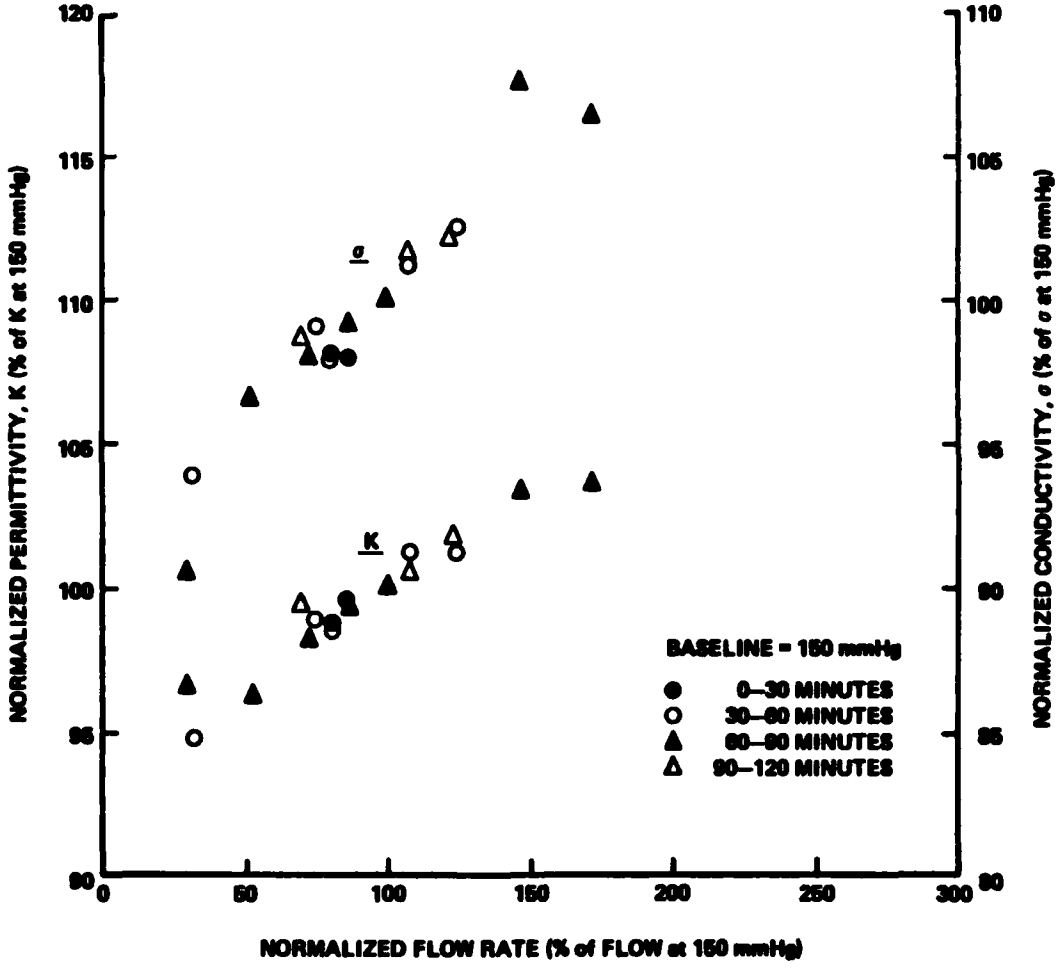

Figure 46. Normalized dielectric properties, K and σ, as functions of normalized flow rate for kidney #7GT.

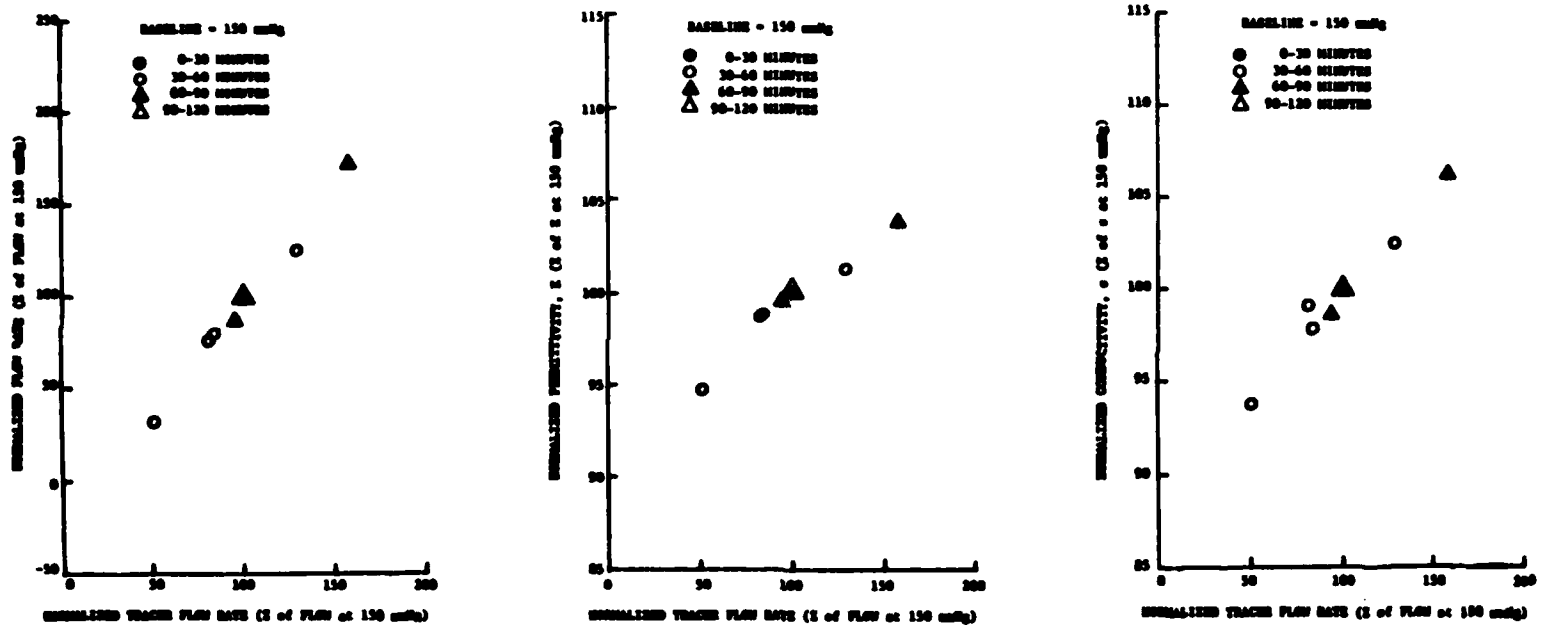

(a) (b) (c)

Figure 47. (a) Normalized measured flow rate versus normalized Radioactive Tracer flow rate for kidney #7GT (Radioactive Tracer study).
(b) Normalized permittivity, K, versus normalized Radioactive Tracer flow rate for kidney #7GT.
(c) Normalized conductivity, σ, versus normalized Radioactive Tracer flow rate for kidney #7GT.

SECTION V

CONCLUSIONS AND RECOMMENDATIONS

The objectives for the fourth year of this research program were successfully achieved. The primary fourth-year objectives were (1) to complete software for the automated data acquisition system including multiplexing for up to five dielectric measurement probes, (2) to develop a 1 mm-diameter needle-like probe for measurement of renal medulla dielectric properties during perfusion/flow changes, (3) to develop improved methods for controlling probe/tissue contact force during renal tissue dielectric measurements, (4) to evaluate different perfusate solutions and develop a solution which best preserved renal autoregulatory function, (5) to characterize renal pressure/flow relationships using both direct flow measurement and radiographic methods, and (6) to compare renal dielectric property changes with radioactive tracer results during isolated kidney perfusion conditions. In this section, conclusions based on results of the fourth year's efforts are discussed, followed by recommendations for the fifth-year efforts. Three different emphasis areas for continuation of the ongoing research efforts are outlined in the recommendations.

A. Conclusions From Results

The most important conclusion which can be stated based on the results of this year's efforts is that normal physiological changes of clinical significance are reflected by changes in tissue complex permittivity at microwave frequencies. The specific model system studied where such was found to be the case was the canine kidney. The kidney model was selected for study for several reasons. First, it was relatively straightforward to determine an overall input/output relationship for the kidney because of the single arterial supply and venous return. Thus, total renal flow and perfusion pressure could be readily measured. Second, isolation and controlled perfusion of the kidney was easily achieved. Third, the kidney was well-suited for local/regional complex permittivity measurements using the probe dielectric measurement technique. Fourth, renal regional flow distribution could be assessed using radiographic methods and those results compared to regional complex permittivity changes. Intrarenal flow and

flow distribution over a wide range of perfusion pressures are complex; however, measurement of tissues having reasonably complex flow distributions are a good test of the ability of tissue complex permittivity to reflect physiologically relevant flow changes. This ability is exemplified by the results shown in Figures 41-46. These results indicate that (1) the total renal flow rates measured by the in-line flowmeter and by the radioactive tracer method (free Tc 99m) correlate well over perfusion pressures in the physiological range (Figure 47(a)) and (2) the renal cortical flow measured using free Tc 99m correlates very well with changes in renal permittivity and conductivity (Figures 47(b) and 47(c)). Thus, local dielectric property changes at microwave frequencies do indeed reflect changes in regional perfusion which are within normal physiological bounds. Further, it can be implicated that drugs which affect regional flow would also influence complex permittivity and thus their effects/concentration could be indirectly measured by measuring changes in the local/regional complex permittivity. Since the reported measurements were made in the microwave frequency range (2.45 GHz), it is reasonable to expect the potential for microwave imaging of such changes to be possible, and perhaps practical, depending upon the degree of complex permittivity change occurring.

Other important achievements during this year include the development of the flow measurement method using bolus injection of free Technetium in conjunction with an Anger camera and the development of an artifical perfusate which maintains autoregulatory function in the isolated kidney preparation. The radioactive tracer method using Tc 99m permits measurement of fluid movement through the kidney and, just as important, the distribution of flow for each pressure/flow condition studied. This permits direct comparison of local/regional flow changes in the kidney at different perfusion pressures with local dielectric constant and conductivity changes measured using the probe technique. Thus, it was possible to confirm the use of complex permittivity measurements as an indirect flow measurement method. The importance of having an autoregulating kidney within the normal physiological range is obvious. For probe-measured complex permittivity changes to be of physiological significance, those changes must be measured under normal and/or reasonable physiological conditions. The development of the modified Krebs-Henseleit solution (refer to Table I and Section IV.B) permitted us to work with the isolated perfused kidney model under normal flow-regulating physiological conditions.

B. Recommended Future Efforts

Although major advancements in the realm of dielectric measurements were accomplished during the fourth year of this program, a number of questions of physiological significance remain. Further, the results raise additional questions that should be investigated to provide significant information to the Army in terms of EM field interaction with living tissues. Continuation of the ongoing research effort could naturally follow any of three primary directions. A first alternative would be to continue the studies of renal permittivity and flow changes under varying physiological conditions. Second, further studies of in-situ brain complex permittivity and blood flow under conditions of hypercapnia and during external sensory stimulation could be conducted, making use of radiolabeled tracers as a confirmatory method of flow measurement. Third, emphasis could be placed in a direction leading toward non-invasive measurement of renal flow changes through the development of a non-contacting "probe" for measuring fields scattered from renal tissue.

The first alternative would be a direct continuation of present efforts. Additional complex permittivity/flow studies of the in-vitro isolated perfused kidney would be performed and the effects on both flow distribution and complex permittivity of several pharmacological agents examined. Once these studies are completed for the artifically perfused kidney, they would be repeated for the isolated perfused kidney in the intact animal. Thus, regional complex permittivity/blood flow relationships could be evaluated in-vivo under controlled perfusion conditions. Cardiovascular/complex permittivity changes during renal nerve stimulation could also be evaluated.

A second alternative would be to proceed with further studies of physiological effects on canine brain in-situ dielectric properties. Because of the emphasis on resolving problems which had rendered the results of our early renal experiments unusable (requiring considerable additional effort), studies of brain complex permittivity were not performed during this past year. A logical option would be to resume those studies to investigate effects of hypercapnia and anoxia on brain dielectric properties and to investigate complex permittivity and blood flow changes which may occur during sensory stimulation. Specifically, effects on the properties of the auditory cortex during acoustical stimulation would be investigated. Variations in regional brain blood flow and changes in regional flow during hypercapnia and anoxia could also be evaluated using multiplexed multiple needle probes combined with radioactive tracer studies.

These studies would provide basic information relevant to the use of diagnostic EM imaging for patho-physiological changes in brain blood flow.

The third alternative suggested would be the development of a non-contacting "probe" for measuring blood flow changes in the renal model system we have developed. Essentially, the monopole or coaxial probe would be replaced by a newly developed antenna which would not necessarily be in direct contact with the renal cortex or medulla, but would instead couple to the kidney through a dielectric bolus. Such a bolus could then serve as an "impedance transformer" between the kidney and the new antenna. The exact nature of the new antenna design is as yet undefined. Two possibilities are a very small aperture guide loaded with a high dielectric constant material or a "long" monopole antenna inserted into the bolus material. A third possibility would be the use of a dual-waveguide coupled probe for non-invasive measurement of complex permittivity. The ability to assess changes in dielectric properties (and flow) using a non-contacting probe would provide an important link to the use of diagnostic EM imagery for non-invasive detection/monitoring of regional flow changes in organs through the intact skin. We believe that results which demonstrate this feasibility can be obtained in our renal model system using such a device.

From the three alternatives described above, it is recommended that the follow-on effort consist of either a mix of the first and third alternatives or the second alternative alone. Selecting the first alternative above is a viable option which will result in the generation of new information and data, but by concentrating immediately on the isolated perfused kidney in the intact animal and limiting the number of drug-induced effects which are studied, it would be possible to work on the third alternative also during the coming year's efforts. Essentially, by combining the major portions of the first and third alternatives, it should be possible to accomplish the most significant aspects of the in-vivo renal complex permittivity/blood flow investigations in approximately six months and then development of a non-contacting "probe" during the second six months. The same model system can be used for both studies and results obtained using the new probe configuration could be directly compared with results obtained using the present multiple contacting-probe configuration. Development of the new non-contacting probe will require longer than six months; however, initial design, fabrication, and feasibility assessment should be possible during the latter half of

the coming year's follow-on effort. An equally viable alternative would be the second one outlined above (in-situ brain complex permittivity studies). That effort (second alternative) would require approximately a 12-month period to perform, when done thoroughly.

SECTION VI
REFERENCES

1. L. E. Larsen and J. H. Jacobi, "Microwave interrogation of dielectric targets. Part I: By scattering parameters", Med. Phys., Vol. 5, No. 6, 500-508, 1978.

2. J. H. Jacobi and L. E. Larsen, "Microwave interrogation of dielectric targets. Part II: By microwave time delay spectroscopy:, Med. Phys., Vol. 5, No. 6, 509-513, 1978.

3. L. E. Larsen and J. H. Jacobi, "Microwave scattering parameter imagery of an isolated canine kidney", Med. Phys., Vol. 6, No. 5, 394-403, 1979.

4. J. H. Jacobi and L. E. Larsen, "Microwave time delay spectroscopic imagery of isolated canine kidney", Med. Phys., Vol. 7, No. 1, 1-7, 1980.

5. C. H. Durney, "Electromagnetic Dosimetry for Models of Humans and Animals: A Review of Theoretical and Numerical Techniques", Proc. IEEE, Vol. 68, No. 1, 33-40, 1980.

6. E. C. Burdette, "Electromagnetic and Acoustic Properties of Tissues," in PHYSICAL ASPECTS OF HYPERTHRMIA, Ed. G. N. Nussbaum (presented at American Assoc. Phys. Med. Summer School, Dartmouth College, Hanover, NH, August 1981).

7. J. Seals and E. C. Burdette, "Comparison of the Dielectric Properties of In-Vivo Rat Brain, Muscle, and Tumor," Digest of 1981 Microwave Power Symposium, 176-178, Toronto, 9-12 June 1981.

8. E. C. Burdette, R. L. Seaman, J. Seals, and F. L. Cain, "In-Vivo Techniques for Measuring Electrical Properties of Tissues", Annual Technical Report No. 1, Project A-2171, U.S. Army Medical Research and Development Command, Contract No. DAMD17-78-C-8044, July 1979.

9. E. C. Burdette, P. G. Friederich, and F. L. Cain, "In-Vivo Techniques for Measuring Electrical Properties of Tissues", Annual Technical Report No. 2, Project A-2171, U.S. Army Medical Research and Development Command, Contract No. DAMD17-78-C-8044, September, 1980.

10. E. C. Burdette, P. G. Friederich, and A. M. Moser, "In-Vivo Techniques for Measuring Electrical Properties of Tissues", Annual Technical Report No. 3, Project A-2171, U.S. Army Medical Research and Development Command, Contract No. DAMD17-78-C-8044, September 1981.

11. E. C. Burdette, F. L. Cain, and J. Seals, "In-Vivo Determination of Energy Absorption of Biological Tissue", Final Technical Report, Project A-1755, U.S. Army Research Office Grant No. DAAG29-75-G-0182, January 1979.

12. E. C. Burdette, F. L. Cain, and J. Seals, "In-Vivo Probe Measurement Technique for Determining Dielectric Properties at VHF Through Microwave Frequencies", IEEE Trans. Microwave Theory Tech., Vol. 28, No. 4, 414-428, 1980.

13. Semi-Automated Measurements Using the 8410B Microwave Network Analyzer and the 9825A Desk-Top Computer, Hewlett-Packard Application Note 221, March 1977.

14. Navar, Lois Gabriel, "Renal Autoregulation: Perspections from Whole Kidney and Single Nephron Studies", Am. J. Physiol. 234(5):F357-F370, 1978.

15. Shipley, R. E. and R. S. Study, "Changes in Renal Blood Flow, Extraction of Inulin, Glomerular Filtration Rate, Tissue Pressure and Urine Flow with Acute Alterations of Renal Artery Blood Pressure", Am. J. Physiol. 167:676-688, 1951.

16. Waugh, W. H. "Myogenic Nature of Autoregulation of Renal Flow in the Absence of Blood Corpuscles", Circ. Res. 6:363-372, May 1958.

17. Waugh, W. H. and R. G. Shanks, "Cause of Genuine Autoregulation of the Renal Circulation", Circ. Res. 8:871-888, July, 1960.

18. Waugh, W. H., "Circulatory Autoregulation in the Fully Isolated Kidney and in the Humorally Supported, Isolated Kidney", Circ. Res., Vols. 14 and 15, Suppl. 1:I-156-I-169, August 1964.

19. Schurenk H. J., "Application of the Isolated Perfused Rat Kidney in Nephrology", Contr. Nephrol. 19:176-190, 1980.

20. Ross, B. D., "The Isolated Perfused Rat Kidney" (Editorial Review), Clin Sci & Molecular Medicine (1978) 55(b) 513-21, December 1978.

21. Bullivant, M., "Autoregulation of Plasma Flow in the Isolated Perfused Rat Kidney", J. Physiol. 280:141-53, July 1978.

22. Baker, S. and A. J. Cohen, "Role of Calcium and Albumin in the Autoregulation of Renal Perfusate Flow", J. Physiol. 311:1-9, 1981.

23. Waugh, W. H. and T. Kubo, "Development of an Isolated Perfused Dog Kidney with Improved Function", Am. J. Physiology 217(1):277-290, July 1969.

24. Kreis, H. "Renal Preservation", Renal Transplantation - Theory and Practice, ed. by J. Hamburger, J. Crosnier, J.-F. Bach, H. Kucis. Williams and Wilkins, Inc., Baltimore, Md., 1981.

25. Thurau, K., P. Deetjen, and K. Kramer: Hamodynamik des Nierenmarks: II. Mitteilung. Wechselbeziehung zwischen vascularem and tubularem Gegenstromsystem bei arteriellen Druckssteigerungen, Wasserdiurese and osmotischer Diurese. Pfluegers Arch 270:270-285, 1960.

26. K. Aukland: Study of the renal circulation with inert gas measurements in tissue, Proc. 3rd. Int Congr Nephrol 1:188-200, 1967.

27. Galskov, A. and O. I. Nissen, "Autoregulation of Directly Measured Blood Flow in the Superficial and Deep Venous Drainage Areas of the Cat Kidney", Circulation Research 30:97-103 (1972).

28. Burdette, E. C., S. R. Crowgey, and P. G. Friederich, "Physiological Influences on Tissue Electrical Properties Measured In-Situ", Quarterly Technical Report No. 15, Project A-2171, U.S. Army Medical Research and Development Command, Contract No. DAMD17-78-C-8044, May 1982.

END

FILMED

7-85

DTIC